Dynamics of Essentially Unstable Nonlinear Waves

Connor Smith

B.S. in Mathematics with Minor in Chemistry, Oregon State University

Submitted to the graduate degree program in Department of Mathematics and the Graduate Faculty of the University of Kansas in partial fulfillment of the requirements for the degree of Doctor of Philosophy.

Committee members

Mathew Johnson, Chair

Milena Stanislavova

Weishi Liu

Dionyssios Mantzavinos

Jonathan P. Lamb, External Reviewer

Date defended: May 06, 2019

The Thesis Committee for Connor Smith certifies
that this is the approved version of the following thesis :

Dynamics of Essentially Unstable Nonlinear Waves

Mathew Johnson, Chair

Date approved: May 13, 2019

Abstract

In this thesis we primarily consider the stability of traveling wave solutions to a modified Kuramoto-Sivashinsky Equation equation modeling nanoscale pattern formation and the St. Venant equations modeling shallow water flow down an inclined plane. Numerical evidence suggests that these equations have no unstable spectrum other than $\lambda = 0$, however they both have unstable essential spectrum. This unstable essential spectrum manifests as a convecting, oscillating perturbation which grows to a certain size independent on the initial perturbation — precluding stability in the regular $L^2(\mathbb{R})$ space. Exponentially weighted spaces are typically used to handle such instabilities, and in Theorem 5.7 we prove asymptotic orbital linear stability in such an exponentially weighted space. We also discuss difficulties with extending this to a nonlinear stability result. In Section 5.5 we discuss another way of obtaining stability, through ad-hoc periodic wave trains.

Chapter 6 concerns the general problem of creating a spectral projection to project away unstable essential spectrum. We consider this problem in the context of spatially periodic-coefficient PDE by proposing a candidate spectral projection defined via the Bloch transform and showing that initial perturbations which activate a sufficiently unstable part of the essential spectrum lead to solutions which are not Lyapunov stable. We also extend these results to dissipative systems of conservation laws.

Additional chapters of interest are Chapter 3 where we address finding the spectrum and Chapter 4 where we discuss the numerics which lead to many of the figures in this thesis.

Acknowledgements

I would like to thank my advisor, Mathew Johnson. Initially it was for providing a problem whose statement is simple enough to illustrate with pictures, but is rich enough mathematically to confound to this very day. But also for the mentorship, opportunities, and patience while working on said problem. In particular I would like to thank him for going out of his way to teach me what it would mean to be a professor, both in terms of day to day duties, but also in terms of their duty to society.

I would also like to thank the members of my oral exam and thesis defense committee — Milena Stanislavova, Weishi Liu, Geng Chen, Dionyssios Mantzavinos, and Jonathan P. Lamb — for their time, comments, constructive criticism, and questions.

I would like to thank everyone who either invited me to give a talk, helped with a paper, or wrote a letter of recommendation: Blake Barker, Margaret Beck, Stephane Lafortune, Greg Lyng, Melissa Shabazz, and Kevin Zumbrun.

I would like to thank the office support — Kerrie Brecheisen, Debbie Garcia, Gloria Prothe, Lori Springs — for everything they've organized, forgiving me for all the deadlines I may have missed, and for providing cookies every Tuesday and Thursday without fail.

I would like to thank every professor who taught a class I took for making KU an enriching experience. I would like to thank all of the math graduate students for making KU a fun experience.

And finally I would like to thank you, the reader. For without you this thesis would have little reason to exist.

Contents

List of Figures

Chapter 1

Introduction

Before starting with stability of traveling waves for PDE, we first start by recalling stability theory for ODEs. Stability theory of ODEs serves as an "elementary example" with its main theorem providing the idealized template for translating spectral information to stability. We consider the following time evolution ODE system

$$x'(t) = \mathscr{F}(x(t)), \qquad x \in \mathbb{R}^n,\ t \in \mathbb{R}. \tag{1.1}$$

We begin by searching for stationary points x_0 with $\mathscr{F}(x_0) = 0$: this also means that the solution with initial condition x_0 is constant in time. This leads to the definition of Lyapunov stability,

Definition 1.1. Lyapunov Stability, Asymptotic Stability, Instability

[10, Definition 1.20, p. 18, Definition 1.22, p. 19] A stationary point x_0 of the differential equation (1.1) is (Lyapunov) stable if for each $\varepsilon > 0$ there is a number $\delta > 0$ such that requiring $|x(0) - x_0| < \delta$ ensures that $|x(t) - x_0| < \varepsilon$ for all $t \geq 0$.

If in addition $\lim_{t\to\infty} |x(t) - x_0| = 0$, then x_0 is said to be asymptotically stable.

If x_0 is not stable, then it is unstable.

When attempting to characterize stability/instability, a useful technical trick is to define a "perturbation to the solution" v via

$$x(t) = x_0 + v(t), \tag{1.2}$$

where characterizing stability is equivalent to showing that v remains small for all time. Before discussing any results characterizing when stability occurs, we use Taylor's theorem and linearize (1.1) about x_0: that is, by rewriting it as

$$x'(t) = \mathscr{F}'(x_0)(x - x_0) + \mathscr{N}(x), \qquad x \in \mathbb{R}^n,\ t \in \mathbb{R}.$$

Note that we used the fact that $\mathscr{F}(x_0) = 0$, and also that $\mathscr{F}'(x_0)$ is a linear operator in $\mathbb{R}^n$ and hence a matrix. Substituting in the perturbation v as in 1.2, we have an evolution equation for the perturbation v,

$$v'(t) = \mathscr{F}'(x_0)\, v + \tilde{\mathscr{N}}(v). \tag{1.3}$$

Both terms $\mathscr{N}(x)$ and $\tilde{\mathscr{N}}(v)$ are nonlinear and $\tilde{\mathscr{N}}(0) = 0$: hence when the solution $x(t)$ is close in value to x_0, then the evolution is expected to be primarily governed by the linear operator $\mathscr{F}'(x)$. Following this line of reasoning we define "linear stability" to be showing that a perturbation satisfying the linearized equation $v'(t) = \mathscr{F}'(x_0)\, v$ becomes small, rather than a perturbation satisfying the full nonlinear equation (1.3); to distinguish the two, showing that a perturbation satisfying (1.3) becomes small will be referred to as "nonlinear stability." We then expect that linear stability is a necessary but not sufficient condition for nonlinear stability. We can then state the following well-known stability theorem which uses the operator $\mathscr{F}'(x)$ to characterize stability.

Theorem 1.2. Stability of ODEs

[10, Theorem 1.25, p. 21] If x_0 is a stationary point for (1.1) and all the eigenvalues of the matrix $\mathscr{F}'(x_0)$ have negative real part, then x_0 is asymptotically stable.

In Theorem 1.2 we used the term "eigenvalue": recall that the eigenvalues $\lambda \in \mathbb{C}$ of a linear operator L with domain $\mathscr{D}(L)$ are those values of $\lambda \in \mathbb{C}$ for which there exists some nontrivial $\phi \in \mathscr{D}(L)$ with

$$L\phi = \lambda \phi \,. \tag{1.4}$$

In this context — where L is a matrix — the ϕ are called eigenvectors, and the collection of all the eigenvalues is called the spectrum of L, denoted by$\sigma(L)$. The proof of Theorem 1.2 hinges on the observation that, for ϕ an eigenvector of $\mathscr{F}'(x_0)$, choosing $x(0) = \phi$ reduces the linear evolution to $x'(t) = \lambda x(t)$ with a solution of

$$x(t) = e^{\lambda t}\phi \,. \tag{1.5}$$

Consider the special case when $\mathscr{F}'(x_0)$ has a basis of eigenvectors, with their eigenpairs denoted by (λ_i, ϕ_i). Then any initial condition $x(0)$ can be written as a linear combination of eigenvectors $\sum_{j=1}^{n} a_j \phi_j$, and the linear evolution is

$$x(t) = e^{\lambda_1}\phi_1 + e^{\lambda_2}\phi_2 + \cdots + e^{\lambda_n}\phi_n \,.$$

Note that this leads to the simple characterization of the linear behavior given in Theorem 1.2: if for all the eigenvalues $\operatorname{Re}\lambda_j < 0$, then the linear solution decays exponentially to zero. Although note that while we have just discussed the linear behavior, Theorem 1.2 concludes full nonlinear stability.

This is a recurring theme, that the linearization's spectral information determines nonlinear stability. Specifically, that spectrum with negative real part leads to stability and spectrum with positive real part leads to instability. With this intuition in mind, we define a linearization L to be spectrally stable if $\sigma(L)$ is entirely in the right half-plane.

The reason why the stability of ODEs is so simple is because everything can be decomposed in terms of eigenvalues

and eigenvectors, whose time evolution is completely understood. In contrast, the stability theory of traveling waves of PDEs is complicated by the fact that eigenvalues no longer describe everything about the linear dynamics: one has to account for an additional component to the spectrum in the form of the essential spectrum (defined in Section 3.1), where it is defined non-explicitly as a "dimension mismatch" rather than an explicit equation such as in (1.4), in turn losing the explicit time evolution equation (1.5).

We now give the setup for the stability theory for traveling waves of PDEs. In analogue to (1.1), we consider the following time evolution initial value problem,

$$\begin{cases} u_t(x,t) &= \mathscr{F}(u(x,t)) \qquad x \in \mathbb{R}^n,\ t > 0 \\ u(x,0) &= u_0(x) \qquad\qquad u \in \mathbb{R}^d \end{cases} \tag{1.6}$$

posed on $X = H^m(\mathbb{R}^n)$, an appropriate Sobolev subspace of $L^2(\mathbb{R}^n)$. While initially (1.6) might resemble (1.1), this $\mathscr{F}$ is allowed to include terms involving the x-partial derivatives of u such as u_x, $-u_{xx}$, or $(u_x)^2$.

Choosing an analogue of the stationary solution x_0 of (1.1) is less straightforward. In [26] it was conjectured that for any solution of the Korteweg-de Vries equation which vanishes at infinity the long time behavior can be described in terms of traveling wave solutions — sometimes referred to as solitons — with solutions of the form $u(x,t) = q(x-ct)$. From this there has emerged a general sense that all longtime dynamics can be described somehow in terms of solitons, and hence one typically focuses on the stability or instability of the solitons.

One may search for a traveling wave solution $u(x,t) = q(x-ct)$ by setting its time evolution to zero, leading to the ODE

$$\mathscr{F}(q(x-ct)) = 0. \tag{1.7}$$

To simplify this analysis one usually changes to the traveling wave coordinate $\tilde{x} = x - ct$, where q can be viewed as an equilibrium solution in the vein of the stationary solution x_0 of (1.1). From the chain rule applied to u_t, the one noticeable effect this has is introducing a cu_x term. Hence in the following we will add in this cu_x term and otherwise ignore this change of coordinates, writing $\tilde{x}$ as x.

Following the intuition behind (1.2), for a solution u to be stable we expect that in its decomposition

$$u(x,t) = q(x) + v(x,t) \tag{1.8}$$

the perturbation term $v(x,t)$ remains small for all time. (Technically, due to the the translation invariance of the problem — discussed prior to Definition 5.11 — we must allow for translation in our ansatz, so we actually expect the decomposition $u(x,t) = q(x+\gamma(t)) + v(x,t)$ and to prove asymptotic orbital stability — discussed following Theorem

5.8 — rather than the usual Lyapunov stability of Definition 1.1. This need to account for translation can be seen in Figure 1.1, where as the perturbation travels through the traveling front solution it pushes the traveling front solution to the left. We save this technicality for Section 5.4.1, where we prove a general nonlinear stability argument.)

Substituting (1.8) into (1.6) allows one to obtain an evolution equation for the perturbation itself, which may be written as

$$v_t(x,t) = Lv(x,t) + \mathcal{N}(v(x,t)) \tag{1.9}$$

where L is the linearized differential operator about q and $\mathcal{N}(v)$ is some sort of nonlinear term. The time evolution is given by Duhamel's equation,

$$v(x,t) = e^{Lt}v_0(x) + \int_0^t e^{L(t-s)}\mathcal{N}(v(x,s))\ ds$$

which decomposes the time evolution of v into a linear part $e^{Lt}v_0$ (the notation e^{Lt} is defined following Definition 5.4) and a nonlinear part. In the same way that in Theorem 1.2 allowed us to translate spectral stability to (at least) linear stability, the Gearhart Pruss theorem (Theorem 5.6) will allow us to translate spectral stability of L from (1.9) to linear stability, i.e. for the linear term $e^{Lt}v_0$.

One of the earliest works in this framework was [34] where it was shown that a family of solitons of the Korteweg-de Vries equation were asymptotically stable in an exponentially weighted space (introduced in Section 5.1): in this work the essential spectrum is confined to the imaginary axis. More recently much work has been done for general "reaction diffusion" equations [16, 6, 15] where the essential spectrum slightly enters the right half plane — where the word "slightly" has been used as how far the essential spectrum enters can be controlled with a parameter.

We briefly introduce the equations of interest. (They are fully introduced in Chapter 2). Firstly we have an equation modeling arising in the context of nanoscale pattern formation (for the details, see Section 2.1), the modified Kuramoto-Sivashinsky equation

$$u_t = -u_{xx} - u_{xxxx} + \left(u^3\right)_x.$$

The negative fourth-order term is spectrally stabilizing in the context of the essential spectrum (See Lemma 3.17) and beneficial for containing the point spectrum as in Lemma 3.20, while the negative second order term is spectrally destabilizing for the essential spectrum. The nonlinear term is also differentiated, which in a nonlinear argument can be handled with a nonlinear damping estimate such as in Lemma 6.9. This system (numerically) admits traveling front and back solutions: traveling wave solutions which can be viewed as heteroclinic orbits connecting two different asymptotic values.

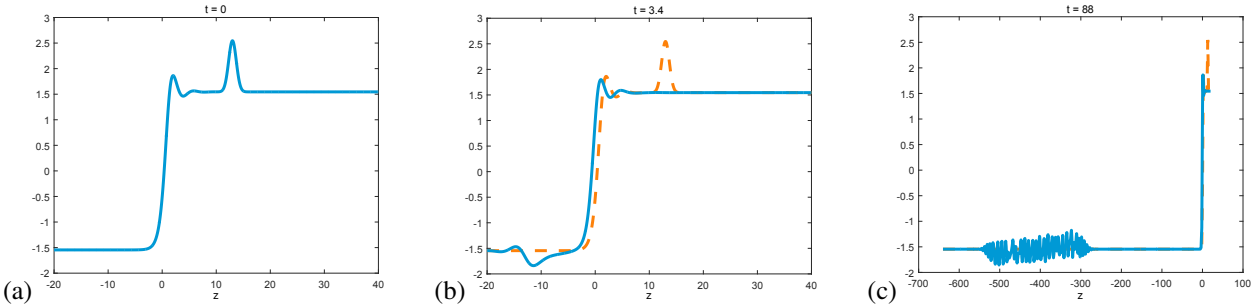

(a) (b) (c)

Figure 1.1: *(Reproduction of Figure 5.1)* Time evolution of a perturbation to a solitary wave for the modified Kuramoto-Sivashinsky equation (2.2). In (a) we show the initial condition, in (b) we show the result after a small amount of time, and in (c) we change the scale to show the result after a long amount of time.

The second are the St. Venant equations, modeling viscous shallow water flow down an inclined plane,

$$\begin{aligned} \tau_t &= u_x + c\tau_x \\ u_t &= cu_x - \left(\frac{1}{2F\tau}\right)_x + 1 - \tau u^2 + \nu\left(\frac{u_x}{\tau^2}\right)_x . \end{aligned}$$

While this is a system of equations, which introduces its own share of complications, we have a similar situation where the highest even order term — now a positive second-order term — is spectrally stabilizing for the essential spectrum (See Lemma 3.18) and beneficial for containing the point spectrum as in Lemma 3.23. This system admits traveling pulse solutions: traveling wave solutions which can be viewed as homoclinic orbits for a set of asymptotic values.

The primary difference between these two equations and those considered in [16, 6, 15] is that for these two equations the essential spectrum will be firmly in the right half-plane. In particular, there is no parameter to be manipulated that varies the degree to which the essential spectrum enters the right half-plane.

One commonality between these two equations is that seemingly in exchange for the unstable essential spectrum the only point spectrum with Re $\lambda \geq 0$ is a simple eigenvalue at $\lambda = 0$ arising from translation invariance (for the reason why $\lambda = 0$ is the only one see Section 3.5, for why $\lambda = 0$ is point spectrum see Definition 5.11 and the following discussion). Unstable essential spectrum typically leads to oscillatory instabilities. In Figure 1.1 we show the time evolution of a perturbation to a traveling wave solution of the modified Kuramoto-Sivashinsky equation (2.2). In Figure 1.1 (a) we show the initial condition. In Figure 1.1 (b) the perturbation has moved leftward, and continues to move leftward. In Figure 1.1 (c) the perturbation has saturated, become highly oscillatory, and continues to convect leftward.

As a result of the difference from [16, 6, 15], the oscillatory perturbation in Figure 1.1 (c) saturates to the same size regardless of initial perturbation v_0. In [16, 6, 15] one could control the size of the resulting essential instability by keeping the initial perturbation arbitrary small. This difference raises immediate and obvious complications for a nonlinear instability argument.

In this thesis we attempt to handle this essential instability and obtain stability of the traveling waves. In Section 5.3 we obtain our main linear stability result. In Section 5.4 we discuss the main obstacles to extending this to a nonlinear instability result. In Section 5.5 we discuss an alternative to showing that individual traveling wave solutions of (2.2) and (2.5) are stable, by considering the stability ad-hoc periodic wave trains created by repeating the traveling waves.

In Chapter 2 we introduce the main equations of interest. In Chapter 3 we define and show how to find the spectrum — the latter being vital because our mail tool for linear stability requires the spectrum to be in the left half-plane. In Chapter 4 we discuss some supplementary numerical methods, in particular those used to obtain the time evolution shown in Figure 1.1. In Chapter 5 we introduce exponential weights in Section 5.1 and in later sections give the main results of this thesis.

Chapter 6 is a secondary project inspired by the results of the previous chapters. Namely that if the unstable essential spectrum is causing so much trouble, can one create a spectral projection to eliminate it? In the chapter we consider this problem in the simplifying case of periodic PDE (as one obtains a characterization of the essential spectrum in terms of eigenvalues, recovering (1.5)), create a candidate projection, and in Theorem 6.7 use this projection to show that initial perturbations that activate a sufficiently unstable part of the essential spectrum are unstable. We also extend these results to dissipative systems of conservation laws.

Chapter 2

The Equations

In chapter we introduce the primary equations studied in this thesis and discuss their respective traveling wave equilibrium solutions.

2.1 The modified Kuramoto-Sivashinsky Equation

In introducing the modified Kuramoto-Sivashinsky equation we follow the presentation as in [33, Section 2]. The physical setting starts with the surprising observation that when an initially flat elemental surface is bombarded with ion beams the surface erodes down in a seemingly periodic pattern. When viewed along the direction of the beam, the surface appears to switch between two linear rates $m_{\pm}$, one positive and one negative. See Figure 2.1 for a physical schematic of these patterns. The main mathematical problem is to somehow justify the existence of this pattern by showing it is stable.

The following equation was derived in [33] for the equation of motion,

$$h_t = -v_0 - h_{xx} - h_{xxxx} + \frac{1}{2}(h_x)^2 + \frac{\gamma}{6}(h_x)^3 \tag{2.1}$$

where h is the surface height, $\gamma > 0$ is the constant that depends on the angle of incidence of the ion beam, and v_0 is the downward drift speed. To simplify this equation, first the downward drift was removed by decomposing the height

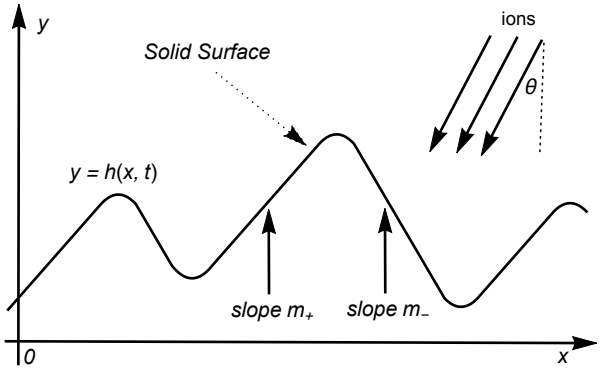

Figure 2.1: A physical schematic for the modified Kuramoto-Sivashinsky height equation (2.1). Note that the pattern chooses the characteristic slopes $m_{\pm}$. From [22].

as $h(x,t) = -v_0 t + p(x,t)$. This then gives the equation

$$p_t = -p_{xx} - p_{xxxx} - \frac{1}{2}(p_x)^2 + \frac{\gamma}{6}(p_x)^3 .$$

The quadratic nonlinearity can be removed by making the linear transformation $P(x,t) = \sqrt{\frac{\gamma}{6}}\left[p(x,t) - \frac{x}{\gamma} + \frac{t}{3\gamma^2}\right]$,

$$P_t = -P_{xx} - P_{xxxx} + (P_x)^3 - \frac{1}{2\gamma}P_x .$$

Finally by changing to the moving frame $\tilde{x} = x - \frac{1}{2\gamma}t$ and using the differentiated variable $u(x,t) = P_x(x,t)$, we find that the transformed slope u satisfies a modified Kuramoto-Sivashinsky equation

$$u_t = -u_{xx} - u_{xxxx} + \left(u^3\right)_x . \tag{2.2}$$

Due to the differentiated variable, the characteristic slopes $m_\pm$ of (2.1) are now two constant values of (2.2). They also no longer have the specific values $m_\pm$ due to the other transformations: the relationship is given by

$$u(x,t) = \sqrt{\frac{\gamma}{6}}\left(h_x(x,t) - \frac{1}{\gamma}\right) .$$

The main physical problem would then be to show that equation (2.2) admits structures such as in Figure 2.1 in its longtime dynamics. From a mathematical perspective we are interested in the stability of traveling waves. One could then interpret the structure in Figure 2.1 as a succession of traveling waves, where each individual traveling wave models the transition from the slope m_+ to the slope m_- and vice versa. Hence one possible solution to resolving the physical problem would be the mathematical problem of showing that these traveling waves obtained from the slope transitions are stable.

We then model the transitions as traveling waves: the ODE (1.7) then becomes the explicit equation

$$q_{xxxx} = -q_{xx} + \left(q^3\right)_x + sq_x$$

where s is the speed of the traveling wave. Since each term is differentiated, then we may integrate this equation. Introducing the integration constant μ, this equation becomes

$$q_{xxx} = -q_x + q^3 + sq + \mu . \tag{2.3}$$

We can view this as a system of ODEs: defining the variables $u_1 = q, u_2 = q_x, u_3 = q_{xx}$,

$$\begin{aligned} \partial_x u_1 &= u_2 \\ \partial_x u_2 &= u_3 \\ \partial_x u_3 &= -u_2 + u_1^3 + s u_1 + \mu \,. \end{aligned} \tag{2.4}$$

This system of ODEs allows for certain fixed points by setting $u_2 = 0, u_3 = 0, u_1^3 + s u_1 + \mu = 0$. Interpreting the latter equation, if r is a root of $r^3 + sr + \mu$ then it is a candidate for an asymptotic value of the traveling wave q. When $\mu = 0$, there is a positive root, a negative root, and $r = 0$: we can then view the positive root $r_+(\mu)$ and the negative root $r_-(\mu)$ as functions of μ. Then to match the physical scenario where we wanted to transition from a positive slope m_+ to a negative slope m_-, we focus on traveling waves obtained as heteroclinic orbits from the positive root to the negative root.

With this setup, we now consider the eigenspaces of the roots $r_+(\mu)$ and $r_-(\mu)$ to see if such a heteroclinic connection is possible. Returning to (2.4), we can calculate the linearization about a root r. Note that a general root r depends on s in addition to μ.

$$\nabla \mathscr{F}(u) = \begin{pmatrix} 0 & 1 & 0 \\ 0 & 0 & 1 \\ \left(3r^2 + s\right), & -1, & 0, \end{pmatrix}$$

with a characteristic polynomial of

$$\lambda^3 + \lambda - \left(3r^2 + s\right).$$

Since this real-coefficient cubic polynomial in λ has a strictly positive derivative, then it is monotone increasing and there is one and only one real root $\lambda = a$. The remaining roots form a complex conjugate pair, $\lambda = b$ and $\lambda = \overline{b}$. We may then decompose the above polynomial as

$$(\lambda - a)(\lambda - b)\left(\lambda - \overline{b}\right) = \lambda^3 - (a + 2\mathrm{Re}\, b)\lambda^2 + \left(ab + a\overline{b} + |b|^2\right)\lambda - a|b| \,.$$

Comparing coefficients, we see that

$$a + 2\mathrm{Re}\, b = 0, \qquad a|b| = 3r^2 + s \,.$$

In particular, the real root and the complex pair of roots will always have opposite signed real parts, and that the sign of the real root is given by the sign of $3r^2 + s$, which is positive when $\mu = 0$ (where the value of s was numerically determined). Thus generically we would expect a one-dimensional unstable unstable subspace and a two-dimensional stable subspace for the fixed points $r_\pm$, and it may be possible to construct a heteroclinic connection by leaving through

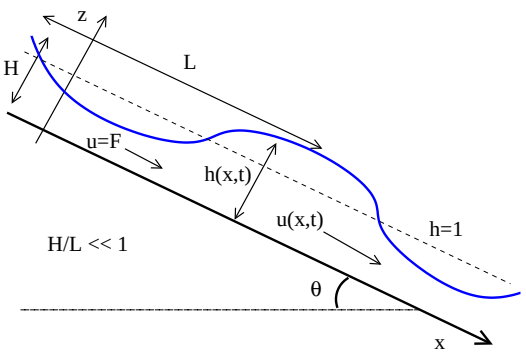

Figure 2.2: A physical schematic for the St. Venant equations.

the unstable subspace of either r_+ or r_- and entering the stable subspace of the other root.

We reiterate that our goal is to consider the stability of this traveling wave solution — formed as a heteroclinic connection corresponding to the transition from one positive slope to a negative slope, or vice versa. Unfortunately in Section 3.3 we show that its essential spectrum (defined in Section 3.1) enters the right half plane and consequently q is spectrally unstable in the standard space $L^2(\mathbb{R})$. Numerical time evolution in Section 5.1 confirms that this spectral instability translates to regular instability. We attempt instead to show that q is stable in an exponentially weighted space $L^2_a(\mathbb{R})$ (defined in Section 5.1). We are able to do this at the linear level, as concluded in Section 5.3, however we are unable to do so at the nonlinear level, with the associated technical issues described in Section 5.4.2. In Section 5.5 we also discuss repeating q periodically in an ad-hoc manner which results in a structure that is stable and perhaps more in line with the structure seen in Figure 2.1.

2.2 The St. Venant Equations

In introducing the Roll Waves equation we follow the same presentation as in [5, Section 2.1][1]. The one-dimensional viscous St. Venant equations approximating shallow water flow down an inclined ramp are

$$\begin{aligned} h_t + (hu)_x &= 0 \\ (ht)_t + \left(\frac{h^2}{2F} + hu^2\right)_x &= h - u|u| + \nu (hu_x)_x \end{aligned}$$

where h represents the height of the fluid, u is the velocity average with respect to height, F is the Froude number and ν is the inverse of the Reynolds number, both of which are non-dimensional quantities characterizing the flow inertia and the turbulence respectively. See Figure 2.2 for a physical schematic. If one restricts to positive velocities $u > 0$

[1] In the original paper there are two additional parameters r and s. However here we take $r = 2$ and $s = 0$, leading to this particular system.

and changes to Lagrangian coordinates, then has the system

$$\begin{aligned} \tau_t - u_x &= 0 \\ u_t + \left(\frac{1}{2F\tau^2}\right)_x &= 1 - \tau u^2 + \nu\left(\frac{u_x}{\tau^2}\right)_x \end{aligned}$$

where $\tau = h^{-1}$ and x is now a Lagrangian marker rather than a spatial position.

We consider traveling waves of the form $U(x-ct)$. Switching to the traveling wave coordinate, our equations become

$$\begin{aligned} \tau_t = &\quad u_x + c\tau_x \\ u_t = &\quad cu_x - \left(\frac{1}{2F\tau}\right)_x + 1 - \tau u^2 + \nu\left(\frac{u_x}{\tau^2}\right)_x \end{aligned} \tag{2.5}$$

Numerical experiments of [32, 3] indicate that when $F > 4$ there is a smooth family of periodic waves parametrized by period, and that such families appear to approach a homoclinic orbit as the period goes to infinity. Our goal is to treat this homoclinic orbit as a traveling wave $q = (\bar{\tau}, \bar{u})^T$ — here a pulse — and consider its stability. Using the methods of Section 4.1 we are able to numerically approximate this pulse solution. Much of dynamics will resemble that of the modified Kuramoto-Sivashinsky equation: in Section 3.3 we show that its essential spectrum is in the right half-plane, numerical time evolution in Section 5.1 confirms this instability, we are able to show all the prerequisites for a linear stability result in an exponentially weighted space, and finally in Section 5.5 we discuss the dynamics of ad-hoc periodic solutions created by repeating the pulse.

Chapter 3

Finding the Spectrum

In this chapter we consider the several aspects of finding the spectrum of the linearization L about a traveling wave.

- In Section 3.1 we define the spectrum of the linearized operator L, in particular dividing it into the essential spectrum and the point spectrum.
- Briefly in Section 3.2 we discuss how to find the linear differential operator L — the linearization about a traveling wave q — itself.
- In Section 3.3 we handle finding the essential spectrum (for both scalar equations and systems of equations), which will be given as the graph of a complex polynomial.
- Sections 3.4 and 3.5 discuss finding the point spectrum. In Section 3.4 we prove bounds that show that eigenvalues λ can only occur in a cone in the complex plane. In Section 3.5 the main tool for finding point spectrum is the Evan's function, an analytic function whose zeros correspond to eigenvalues. One can then search for zeros using contour integrals and the argument principle, with the bound from Section 3.4 restricting the area of search. These Evan's function calculations can be implemented numerically (which requires a numerical approximation of the equilibrium solution as obtained in Section 4.1) which requires quantitative version of the bounds from Section 3.4. In particular the calculations for a quantitative version of Lemma 3.23 are particularly lengthy and are relegated to Section 3.6.

The spectral information found in this chapter will be directly applied to the Gearhart-Pruss Theorem (Theorem 5.6) — the PDE equivalent of the ODE stability result Theorem 1.2 — which forms the basis of the Linear Stability result Theorem 5.7. As Gearhart-Pruss requires the spectrum to be in the left half-plane, one should also note Section 5.1 which uses exponential weights to move the essential spectrum to the left half-plane.

3.1 The Spectrum

In the ODE case we could define the spectrum solely as the eigenvalues through (1.4), but in the PDE case we need a broader definition. To see why this is the case, start from the eigenvalue equation (1.4) and introduce a new technical object, the resolvent

$$R(L,\lambda) = (\lambda I - L)^{-1}$$

where I is the identity operator. In this formalism λ is an eigenvalue if $\lambda I - L$ has nontrivial kernel, hence causing the resolvent to not be well defined. In the ODE case $\lambda I - L$ is an operator over the finite dimensional space $\mathbb{R}^n$, so the rank-nullity theorem applies and as a result the resolvent fails to be defined if and only if λ is an eigenvalue. When $\lambda I - L$ is an operator over an infinite dimensional vectorspace then the rank-nullity theorem notable does not apply — for an example, see Example 3.3.

Definition 3.1. Spectrum, Resolvent, Essential Spectrum, Point Spectrum

[24, Section 2.2.4] [25, Subsection 4.5.1, p. 230] The resolvent set of L, denoted by $\rho(L)$, is the set of complex numbers $\lambda \in \mathbb{C}$ such that

1. $\lambda I - L$ is invertible, and
2. $(\lambda I - L)^{-1}$ is a bounded linear operator.

The spectrum, denoted by $\sigma(L)$, is the complement of the resolvent set.

For an operator L whose range is closed, we define the Fredholm index to be

$$\begin{aligned} \text{ind}(L) &= \dim[\ker L] - \text{codim}[\text{range}(L)] \\ &= \dim[\ker L] - \dim\left[\text{range}(L)^{\perp}\right] \end{aligned}$$

The operator L is Fredholm if this index is finite.

The point spectrum of a an operator L is the set of values $\lambda \in \sigma(L)$ for which $\ker(\lambda I - L) \neq \{0\}$. If L is a Fredholm operator, then this can be characterized as

1. $\lambda I - L$ is not injective, and
2. $\lambda I - L$ is Fredholm with index 0.

Note that $\text{ind}(L) = 0$ and $\text{range}(L)$ closed are sufficient conditions for the rank-nullity theorem to apply.

The essential spectrum of an operator L are the values of $\lambda \in \sigma(L)$ when either

1. $\lambda I - L$ is not Fredholm, or
2. $\lambda I - L$ is Fredholm with non-zero index.

Example 3.2. Fredholm Index of Over/Under-determined Systems

The most intuitive way of thinking about the Fredholm index is in terms of over/under-determined systems. Consider

the following three matrices $A : \mathbb{R}^2 \to \mathbb{R}^3$, $B : \mathbb{R}^2 \to \mathbb{R}^2$, $C : \mathbb{R}^3 \to \mathbb{R}^2$, and their corresponding linear systems $A\vec{x} = \vec{y}$, $B\vec{x} = \vec{y}$, $C\vec{x} = \vec{y}$. Since the range of A, B, C is each a subspace, then it is closed.

$$\begin{bmatrix} a_{11} & a_{12} \\ a_{21} & a_{22} \\ a_{31} & a_{32} \end{bmatrix} \begin{bmatrix} x_1 \\ x_2 \end{bmatrix} = \begin{bmatrix} y_1 \\ y_2 \\ y_3 \end{bmatrix}, \qquad \begin{bmatrix} b_{11} & b_{12} \\ b_{21} & b_{22} \end{bmatrix} \begin{bmatrix} x_1 \\ x_2 \end{bmatrix} = \begin{bmatrix} y_1 \\ y_2 \end{bmatrix}, \qquad \begin{bmatrix} c_{11} & c_{12} & c_{13} \\ c_{21} & c_{22} & c_{23} \end{bmatrix} \begin{bmatrix} x_1 \\ x_2 \\ x_3 \end{bmatrix} = \begin{bmatrix} y_1 \\ y_2 \end{bmatrix}$$

Overdetermined, ind(A)=-1 | Just right, ind$(A) = 0$ | Underdetermined, ind$(C) > 0$

The matrix A results in three equations for two unknowns, and is overdetermined (so long as we assume that no equations are equivalent). One of the y_i depends on the other two, so it has codimension 1 and Fredholm index -1.

The matrix B results in two equations for two unknowns, so assuming that B is of full rank, then it has Fredholm index 0. This assumption results in a simplified scenario however as both $\dim[\ker B]$ and the codimension of B were 0: one would also have a Fredholm operator of index 0 if they were both non-zero and equal.

The matrix C results in two equations for three unknowns, and is under-determined. For simplicity we assume that no equations are equivalent (although it would still be under-determined). There are multiple choices of $\vec{x}$ to obtain a particular $\vec{y}$, hence the dimension of the kernel is 1 and it has Fredholm index 1.

Example 3.3. Fredholm Index and Left/Right Shift Operators

Consider the left shift operator acting on ℓ^∞, i.e. the operator taking $(a_1, a_2, a_3, \dots) \mapsto (a_2, a_3, \dots)$. The left shift operator takes all elements of the form $(a_1, 0, \dots)$ to zero, and hence has a kernel of dimension 1. In contrast, the range is still ℓ^∞ as any element $(a_1, a_2, \dots)$ is the left shift of $(0, a_1, a_2, \dots)$. Thus the left shift operator has a Fredholm index of 1.

The right shift operator on ℓ^∞, i.e. the operator taking $(a_1, a_2, \dots) \mapsto (0, a_1, a_2, \dots)$ has nothing in the kernel and codimension 1 as elements of the form $(a_1, \dots)$ for $a_1 \neq 0$ cannot be formed. Thus the right shift operator has a Fredholm index of -1.

Now consider applying the left shift then the right shift, i.e. $(a_1, a_2, a_3, \dots) \mapsto (0, a_2, a_3, \dots)$. This has both a kernel of dimension 1 and codimension 1, hence has Fredholm index 0.

In a Hilbert space we have the Fredholm alternative, which gives an alternate characterization for the range of L that is sometimes easier to calculate.

Theorem 3.4. Fredholm Alternative

[24, Theorem 2.2.1, p. 28] Suppose that X is a Hilbert space with inner product $\langle \cdot, \cdot \rangle$ and $L : D(L) \subset X \to X$ is a closed Fredholm operator with domain $D(L) \subset X$ dense in X. Then

$$Range\,(L) = \ker(L^*)^\perp$$

where L^* is the adjoint operator.

When $L = \sum_{j=0}^{\ell} a_j \partial_x^j$ is an ℓ-th order constant coefficient differential operator, finding elements in $\ker(L)$ is equivalent to solving the ODE $Lv = 0$. From elementary ODE theory, such as [8, Section 4.2], this is at most an ℓ-dimensional subspace.

Note that the adjoint operator L^* is, through integration by parts, $L^* = \sum_{j=0}^{\ell} (-1)^j a_j \partial_x^j$ and that similarly $\ker(L^*)$ is also at most an ℓ-dimensional subspace. Let $f \in \text{Range}(L)^{\perp}$. Then for all v in the domain of L we have

$$\langle f, Lv \rangle = 0 .$$

Using the adjoint,

$$\langle L^* f, v \rangle = 0 .$$

As the domain is dense, then $L^* f = 0$ and so $f \in \ker(L^*)$. Then

$$\dim(\ker(L^*)) \leq \ell .$$

Then if Range L is closed, L would be Fredholm. Thus the intuition is for differential operators it's whether or not the range of L is closed that's the main concern, not if the Fredholm index is finite. We also mention Lemmas 3.1.7 and 3.1.8 from [24] — which arise in the context of characterizing the essential spectrum — which gives an if and only if condition for the range of a particular operator to be closed, thereby classifying the essential spectrum.

3.2 Linearizing the PDE

Before mentioning how to find the spectrum of the linearized operator L in (1.9), we should mention how to actually find the operator L. As implied via analogue to (1.3), L is "the derivative of $\mathscr{F}$," although such terminology is a bit ambiguous in the Banach space setting.

Definition 3.5. Linearized Operator

For the evolution equation $u_t = \mathscr{F}(u)$ posed on $L^2(\mathbb{R}^n)$, the linearized operator is defined to be the Gateaux derivative of $\mathscr{F}$ at the equilibrium solution q in the u-direction;

$$Lu = \lim_{\varepsilon \to 0} \frac{\mathscr{F}(q + \varepsilon u) - \mathscr{F}(q)}{\varepsilon} . \tag{3.1}$$

Equivalently,

$$Lu = \frac{d}{d\varepsilon} \mathscr{F}(q + \varepsilon u) \Big|_{\varepsilon = 0}$$

In the context of this dissertation L will be a differential operator, so the domain of L is taken to be an appropriate Sobolev subspace $H^m(\mathbb{R}^n)$ so that the limit in (3.1) makes sense.

Example 3.6. The linearization of u^p about the equilibrium solution q is $Lu = pq^{p-1}u$.

To verify this, one can compute that

$$\frac{d}{d\varepsilon}\mathscr{F}(q+\varepsilon u) = pu(q+\varepsilon u)^{p-1}$$

and substitute in $\varepsilon = 0$.

Example 3.7. The linearization of $(u^p)_x$ about the equilibrium solution q is $Lu = pq^{p-2}((p-1)q'u + qu_x)$.

To verify this, note that $(u^p)_x = pu^{p-1}u_x$, then proceed as in the previous example computing the ε-derivative using the product rule.

Lemma 3.8. Linearization of the modified Kuramoto-Sivashinsky Equation

The linearization of the modified Kuramoto-Sivashinsky equation (2.2) about the traveling wave q is

$$Lu = -u_{xx} - u_{xxxx} + su_x + 3\left(q^2u\right)_x. \tag{3.2}$$

Lemma 3.9. Linearization of the St. Venant Equations

The linearization of the St. Venant equations (2.5) about the traveling wave $q = (\bar{\tau}, \bar{u})^T$ is

$$L\begin{pmatrix} \tau \\ u \end{pmatrix} = \begin{pmatrix} c\tau_x + u_x \\ cu_x - \dfrac{\tau}{F\bar{\tau}^3} + \dfrac{\nu u_x}{\bar{\tau}^2} - 2\bar{\tau}\bar{u}u - \bar{u}^2\tau \end{pmatrix}. \tag{3.3}$$

3.3 Finding the Essential Spectrum

To find the essential spectrum of L, we first start with a special case.

Theorem 3.10. Essential Spectrum of a Constant Coefficient Differential Operator

Let $p(x) = \sum_{j=0}^{\ell} a_j x^j$ be a real-coefficient ℓ-th degree non-constant polynomial. Then the essential spectrum of the operator

$$L = p(\partial_x) : H^{\ell}(\mathbb{R}^n) \subset L^2(\mathbb{R}^n) \to L^2(\mathbb{R}^n)$$

is $p(i\mathbb{R})$: i.e., the graph of the polynomial $p(ik)$ as k varies over $\mathbb{R}$.

Proof. To find the spectrum, it is equivalent to consider the resolvent equation and where it fails to be defined. Starting with $(L-\lambda I)$ applied to the resolvent equation,

$$(L-\lambda I)v = f \qquad \text{or} \qquad \sum_{j=0}^{\ell} a_j \partial_x^j v - \lambda v = f\,. \tag{3.4}$$

Taking the Fourier transform and recalling that the Fourier transform converts derivatives (in space x) to polynomials (in frequency ξ), this is equivalent to

$$\sum_{j=0}^{\ell} a_j (i\xi)^j \hat{v}(\xi) - \lambda \hat{v}(\xi) = \hat{f}(\xi) \qquad \text{or} \qquad (p(i\xi)-\lambda)\hat{v}(\xi) = \hat{f}(\xi)\,. \tag{3.5}$$

Finding the resolvent is equivalent to solving the latter equation for v (continuously in f). First solving for $\hat{v}$, if $\lambda \notin p(i\mathbb{R})$ then

$$\hat{v}(\xi) = \frac{\hat{f}(\xi)}{p(i\xi)-\lambda}\,. \tag{3.6}$$

where v may be obtained via Fourier Inversion [43, Chapter 3]. By differentiating both sides of (3.4) l-times, for $l \leq \ell$, and using the Plancharel theorem,

$$\left\|\partial_x^l v\right\|_{L^2(\mathbb{R}_x)} = \left\|\left(\partial_x^l v\right)^{\wedge}\right\|_{L^2(\mathbb{R}_\xi)} = \left\|\frac{(i\xi)^l}{p(i\xi)-\lambda}\hat{f}\right\|_{L^2(\mathbb{R}_\xi)} \leq \left\|\frac{(i\xi)^l}{p(i\xi)-\lambda}\right\|_{L^\infty(\mathbb{R}_\xi)} \left\|\hat{f}\right\|_{L^2(\mathbb{R}_\xi)}\,.$$

For $l \leq \ell$, the term $\frac{(i\xi)^l}{p(i\xi)-\lambda}$ goes to a constant as $|\xi| \to \infty$, and is uniformly bounded for $|\xi| > R$ for some radius R. The magnitude of the denominator $|p(i\xi)-\lambda|$ is uniformly bounded from below away from zero for $|\xi| \leq R$, and hence the $\left\|\frac{(i\xi)^\ell}{p(i\xi)-\lambda}\right\|_{L^\infty(\xi)}$ term is finite. Thus $v \in H^\ell(\mathbb{R}^n)$. In particular, as $v \in L^2(\mathbb{R}^m)$, then we may invert its Fourier transform to solve for v and thus $\rho(L) \subset \mathbb{C}\backslash p(i\mathbb{R})$.

If λ is on the graph $p(i\mathbb{R})$, i.e. if $\lambda = p(i\xi_0)$, then (3.5) tells us that $\hat{f}(\xi_0) = 0$. As p is non-constant by hypothesis, then there exists some open set U containing ξ_0 so that for all $\xi \in E\backslash\{\xi_0\}$, $\lambda \neq p(i\xi)$. Choose compact set $E \subset U$ with $\xi_0 \in E$, and choose χ_n to be a smooth function that is 1 on $E\backslash\left(\xi_0 - \frac{1}{n}, \xi_0 + \frac{1}{n}\right)$ and 0 on $\left[\xi_0 - \frac{1}{n+1}, \xi_0 + \frac{1}{n+1}\right]$. Choosing $\hat{f}_n = \chi_n$, we may use (3.6) and Fourier inversion to solve for some v_n that attains this f_n, and hence f_n is in the range of $L-\lambda I$. However, the χ_n converge to a function that is 1 on the entirety of E, which cannot correspond to the Fourier transform of some f in the range of $L-\lambda I$ as $\hat{f}(\xi_0) = 0$. By Plancharel, the f_n converge but their limit function is not in the range of $L-\lambda I$. Thus the range of $L-\lambda I$ is not closed, and so the operator fails to be Fredholm and $\lambda \in \sigma_{\text{ess}}(L)$. As this was true for all $\lambda \in p(i\mathbb{R})$, then $p(i\mathbb{R}) \subset \sigma_{\text{ess}}(L)$. As the resolvent and the spectrum form a partition of $\mathbb{C}$, then $\sigma_{\text{ess}}(L) = p(i\mathbb{R})$.

□

Example 3.11. Essential Spectrum of the Laplacian

Consider the Laplacian

$$L = -\partial_x^2 : H^2(\mathbb{R}) \subset L^2(\mathbb{R}) \to L^2(\mathbb{R})$$

As a result from Theorem 3.14, L has only essential spectrum which is the graph of

$$p(i\xi) = -(i\xi)^2 = -\left(-\xi^2\right) = \xi^2, \qquad \xi \in \mathbb{R}$$

Thus the essential spectrum is $[0,\infty)$.

This "special case" of constant coefficients isn't actually that special: since the coefficients of L for our equations of interest — (3.2) and (3.3) — converge exponentially to a constant, then we can view L as a perturbation of its asymptotic constant coefficient counterpart. That is, we can define the asymptotic operators

$$L_{\pm\infty} = \lim_{x\to\pm\infty} L, \tag{3.7}$$

and expect that the spectrum of L would be related to the spectrum of the operators $L_{\pm\infty}$.

There is a rich assortment of results in the theory of spectral perturbations: that is, given an operator A and another operator T, how is the spectrum of the "perturbed" operator $A+T$ related to the original operator A? One of the more classical results is Weyl's essential spectrum theorem, which states that so long as the perturbation T is "sufficiently small" then the essential spectrum of A and $A+T$ are the same.

Theorem 3.12. Weyl's Essential Spectrum Theorem

[24, Theorem 2.2.6, p. 29] Let A and $A+T$ be closed linear operators on a Banach space X. If $A+T$ is a relatively compact perturbation of A, then the following properties hold:

1. *The operator $\lambda I - A$ is Fredholm if and only if $\lambda I - (A+T)$ is Fredholm. Furthermore $ind(\lambda I - A) = ind(\lambda I - (A+T))$.*
2. *The operators A and $A+T$ have the same essential spectrum.*

For a more general treatment, the above results (and more) are laboriously derived in [25, Chapter IV, Theorem 5.35, p. 244].

Theorem 3.13. *[24, Theorem 3.1.11, p. 48] Suppose that the differential operator*

$$L = \partial_x^\ell + a_{n-1}(x)\partial_x^{\ell-1} + \cdots + a_1(x)\partial_x + a_0(x)$$

has $H^1(\mathbb{R})$ coefficients and converges exponentially to the asymptotic operators 3.7. Then L is a relatively compact perturbation of $L_{-\infty}\chi_{(-\infty,0)} + L_\infty \xi_{[0,\infty)}$.

We also mention [24, Lemma 3.1.10, p. 47], which attempts to characterize eigenfunctions as connections from the unstable subspace of $L_{-\infty} - \lambda I$ to the stable subspace of $L_{\infty} - \lambda I$: there the essential spectrum is characterized as the values of λ for which the dimensions of these subspaces change (and hence connecting them is ill-posed). We take this view later when using the Evan's function to find the point spectrum: in that context the essential spectrum are the values of $\lambda \in \mathbb{C}$ where the dimensions of the unstable and stable subspaces of $A(\lambda, x)$ (3.20) change dimension. Put another way, the boundaries of the essential spectrum form the regions where numerical Evan's function calculations (as in Section 3.5) are appropriate. Also note that a similar setup — that of connecting unstable subspaces to stable subspaces — is used in Section 4.1 to numerically generate traveling wave solutions for the modified Kuramoto-Sivashinsky equation.

Another useful consequence of this result is that it gives a way to find the essential spectrum of systems of PDEs. The result characterizes the essential spectrum in terms of the dispersion relation (3.8). This determinant originates from considering plane wave solutions $u = e^{i\xi x - \lambda t}$ and solving for values of ξ that satisfy $u_t + Lu = 0$.

Theorem 3.14. Essential Spectrum of a System of Constant Coefficient Differential Operators

[24, Remark 3.1.14, p. 50] Let $\{A_j\}$ be a collection of ℓ total $d \times d$ constant matrices. Then the essential spectrum of the operator

$$L = \sum_{j=0}^{\ell} A_j \partial_x^j : H^m(\mathbb{R}^n) \subset L^2(\mathbb{R}^n) \to L^2(\mathbb{R}^n)$$

are the values of λ that satisfy the equation, for any value of $\xi \in \mathbb{R}$,

$$\det\left(\lambda I - \sum_{j=0}^{\ell} A_j (i\xi)^j\right) = 0\,. \tag{3.8}$$

Example 3.15. Essential Spectrum of the a System of Constant Coefficient Differential Operators

Consider finding the essential spectrum of the system

$$\begin{aligned} \tau_t &= \tau_x + u_x \\ u_t &= u_{xx} \end{aligned}$$

Using $U = (\tau, u)^T$, then we can write this as

$$U_t = \begin{pmatrix} 1 & 1 \\ 0 & 0 \end{pmatrix} U_x + \begin{pmatrix} 0 & 0 \\ 0 & 1 \end{pmatrix} U_{xx} = A_1 U_x + A_2 U_{xx}$$

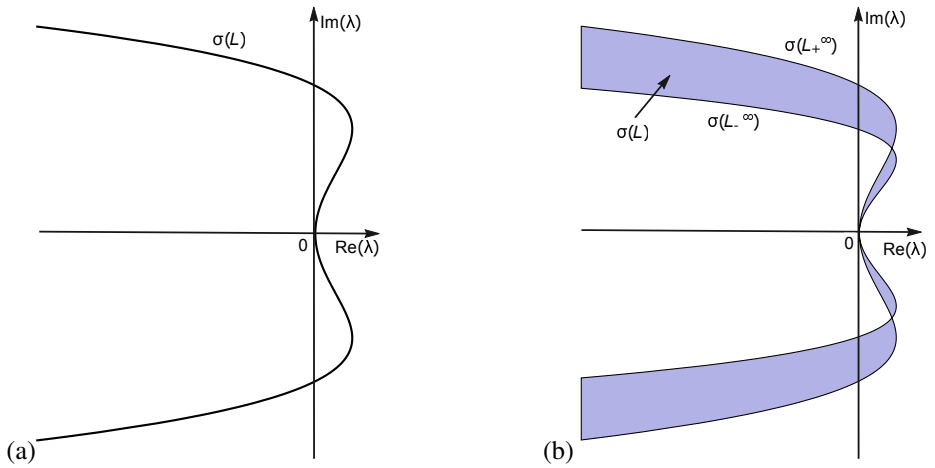

Figure 3.1: The essential spectrum $\sigma_{\text{ess}}(L)$ for the modified Kuramoto-Sivashinsky equation in the case when, for $m_{\pm} = \lim_{x\to\pm\infty} q(x)$, (a) $m_+^2 = m_-^2$ and (b) $m_+^2 \neq m_-^2$. Figure from [22].

Then the dispersion relation is

$$\det\left(\lambda I - A_1(i\xi) - A_2(i\xi)^2\right) = -i\xi^3 + \lambda\xi^2 + \lambda^2 - i\lambda\xi = 0$$

Solving the above for λ,

$$\lambda = i\xi, \qquad \lambda = -\xi^2$$

Allowing ξ to take on values in $\mathbb{R}$, the essential spectrum is the negative real axis (including zero) and the imaginary axis.

This line of reasoning eventually culminates in the following characterization of the essential spectrum.

Theorem 3.16. Essential Spectrum of Linearized Operator L

[24, Theorem 3.1.13, p. 50] Let L be a linearization obtained as in Definition 3.5 and set $\sigma_F(L)$[1] as $\sigma_{ess}(L_{-\infty}) \cup \sigma_{ess}(L_{\infty})$. Then $\sigma_F(L)$ divides $\mathbb{C}$ into a finite collection of open disconnected sets S_j. Each set S_j is either (1) entirely essential spectrum or (2) contains no essential spectrum: i.e. consists of point spectrum and/or resolvent. If $L_{-\infty} = L_{\infty}$, then $\sigma_{ess}(L) = \sigma_F(L)$.

With this result we may finally find the essential spectrum for the linearized operators (3.2) and (3.3) for the modified Kuramoto-Sivashinsky equation and St. Venant respectively.

Lemma 3.17. Essential Spectrum for modified Kuramoto-Sivashinsky

The essential spectrum of the operator L in (3.2), the linearization of the modified Kuramoto-Sivashinsky equation

[1] So named because it is also the Fredholm boundary: places where the Fredholm index changes values.

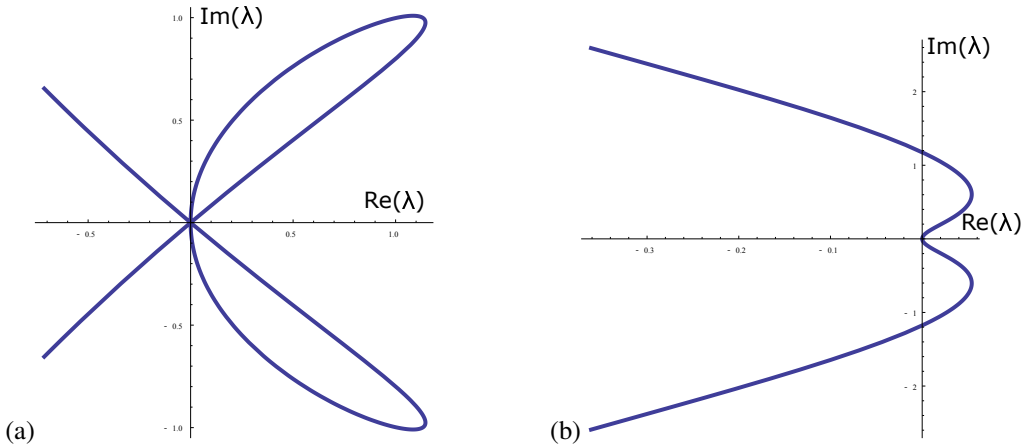

Figure 3.2: The most unstable boundary of the essential spectrum for the St. Venant equations using (a) the [5] Figure 1 parameter values ($r=2$, $s=4$, $u_0=0.96$, $\bar{u}=u_0+c/u_0^2-c\bar{\tau}$, $\nu=0.1$, $F=6$, $c=0.57052639$) and (b) the [5] Figure 7 parameter values ($c\approx 0.7849$, $\bar{u}=1+c-c\bar{\tau}$, $F=9$, $\nu=0.1$).

(2.2), is given as the region between the two curves

$$p_{\pm}(ik) = -(ik)^2 - (ik)^4 + \left(s+3m_{\pm}^2\right)(ik), \qquad k\in\mathbb{R}$$

where $m_{\pm} = \lim_{x\to\pm\infty} q(x)$.

The essential spectrum is given in Figure 3.1. Of particular note is that as the essential spectrum firmly enters the right half plane, then we expect some degree of instability.

Lemma 3.18. Essential Spectrum for St. Venant

The boundary of the essential spectrum of the operator L in (3.3), the linearization of the St. Venant equation (2.5), is given by implicitly solving the equation

$$-c^2k^2 - \frac{ick^3\nu}{\tau_0^2} + k^2c_s^2 - 2ic\lambda k - \frac{ickr}{u_0} + \frac{\lambda k^2\nu}{\tau_0^2} + \lambda^2 + \frac{iks}{\tau_0} + \frac{ik}{\tau_0} + \frac{\lambda r}{u_0} = 0 \tag{3.9}$$

for λ, *where* $(\tau_0,u_0) = \lim_{x\to\pm\infty}(\bar{\tau}(x),\bar{u}(x))$ *and* $k\in\mathbb{R}$.

The most unstable boundaries of the essential spectrum are given in Figure 3.2. Both choices of parameters result in essential spectrum that firmly enters the right half plane.

3.4 Eigenvalue Bounds

Before approaching the point spectrum as a whole, we prove some bounds on the region where eigenvalues can occur. In particular, we show that there is a bounded region of the complex plane where unstable eigenvalues can occur. Later

in Section 3.5 we will define the Evan's function (3.21): this will be an analytic function whose zeros correspond to point spectrum. This reduces the problem of finding unstable point spectrum to that of finding zeros via the argument principle.

In Lemma 3.20 we first show these results for the modified Kuramoto-Sivashinsky equation (2.2), as the fact that it is a scalar equation greatly simplifies things. Later in Lemma 3.23 prove a similar result for the St. Venant equation, but we must contend with the fact that it is a system. The method is based on energy estimates and the key ingredients are (1) the eigenvalue equation $Lu = \lambda u$, (2) the observation that the highest order derivative terms of (2.2) have a negative coefficient, and (3) using the following Sobolev inequality in Lemma 3.19 to reduce the $\|\partial_x u\|_{L^2(\mathbb{R})}$ and $\left\|\partial_x^2 u\right\|_{L^2(\mathbb{R})}$ terms to $\|u\|_{L^2(\mathbb{R})}$ terms. In all of the following let $\langle f, g\rangle = \int_{\mathbb{R}} f\,\bar{g}$ be the $L^2(\mathbb{R})$ inner product, where $\bar{g}$ is the complex conjugate of g.

Lemma 3.19. A Sobolev Inequality

For $j \geq 1$ and a_j arbitrary constants, we have

$$\left\|\partial_x^j u\right\|_{L^2(\mathbb{R})}^2 \leq \frac{1}{4a_j}\left\|\partial_x^{j-1} u\right\|_{L^2(\mathbb{R})}^2 + a_j\left\|\partial_x^{j+1} u\right\|_{L^2(\mathbb{R})}^2. \tag{3.10}$$

Proof. First, start by recalling how the $L^2(\mathbb{R})$-norm is given by the inner product,

$$\left\|\partial_x^j u\right\|_{L^2(\mathbb{R})}^2 = \left\langle \partial_x^j u, \partial_x^j u\right\rangle$$

Then apply integration by parts,

$$\left\|\partial_x^j u\right\|_{L^2(\mathbb{R})}^2 = -\left\langle \partial_x^{j-1} u, \partial_x^{j+1} u\right\rangle$$

Finally apply Cauchy-Schwartz, multiply by $\frac{\sqrt{2}a_j}{\sqrt{2}a_j}$, and use Young's inequality to obtain (3.10). □

This lemma is used to convert terms involving $\partial_x^j u$ to terms involving the previous and next derivatives. In particular the $\|u_x\|_{L^2(\mathbb{R})}$-terms are converted to $\|u\|_{L^2(\mathbb{R})}$ and $\|u_{xx}\|_{L^2(\mathbb{R})}$ terms. As the leading coefficient of (2.2) is negative, this can somehow be used to cancel out the $\|u_{xx}\|_{L^2(\mathbb{R})}$-term. The remaining $\|u\|_{L^2(\mathbb{R})}$ is handled when both sides of the equation are divided by $\|u\|_{L^2(\mathbb{R})}$.

As a technical note we will be performing the calculations for the weighted operator L_a as defined in (5.3) with a chosen to satisfy Theorem 5.2 rather than the expected L from (3.2); we explain why in a paragraph following (3.21). The operator L_a is the same as the operator L but with different coefficients (that depend on a) for all but the highest order $-\partial_x^4$ term.

Lemma 3.20. Eigenvalue Bound for modified Kuramoto-Sivashinsky

Suppose $\lambda \in \mathbb{C}$ is an $L^2(\mathbb{R})$ eigenvalue of L_a (5.3) for the modified Kuramoto-Sivashinsky equation (2.2). Then λ must satisfy the following estimates:

$$Re\ \lambda \leq \frac{1}{2}\left\|\partial_x\left(q^2\right)\right\|_{L^\infty(\mathbb{R})} + \frac{\alpha_2^2}{4} - \alpha_0 - as \tag{3.11}$$

and

$$Re\ \lambda + |Im\ \lambda| \leq \frac{\left\|\alpha_1 + q^2 + s\right\|_{L^\infty(\mathbb{R})}^2}{4 - 6\alpha_3} + \left\|\partial_x\left(q^2\right) - \alpha_0 - 2aq^2 - as\right\|_{L^\infty(\mathbb{R})} + \frac{1-\alpha_3}{2} + \frac{1}{2}\left\|\partial_x\left(q^2\right) - as + \frac{\alpha_2}{2}\right\|_{L^\infty(\mathbb{R})} \tag{3.12}$$

where here

$$\alpha_0 = a^2 + a^4, \qquad \alpha_1 = 2a + 4a^3, \qquad \alpha_2 = 6a^2 + 1, \qquad \alpha_3 = 4a\,.$$

Proof. This lemma follows the general framework of [4, Lemma 2.2]. As the signs of terms will be important, note that $\alpha_j \geq 0$. The eigenvalue equation $L_a w = \lambda w$ for λ may be written as the following ODE,

$$\lambda w = -\partial_x^4 w + \alpha_3 \partial_x^3 w - \alpha_2 \partial_x^2 w + \left[\alpha_1 + q^2 + s\right]\partial_x w + \left[\partial_x\left(q^2\right) - \alpha_0 - 2aq^2 - as\right] w\,. \tag{3.13}$$

Multiplying this by $\bar{w}$, the complex conjugate of w, applying integration by parts, and taking the real part gives

$$\text{Re}\ \lambda\, \|w\|_{L^2(\mathbb{R})}^2 = -\left\|\partial_x^2 w\right\|_{L^2(\mathbb{R})}^2 + \alpha_2 \|\partial_x w\|_{L^2(\mathbb{R})}^2 - (\alpha_0 + as)\|w\|_{L^2(\mathbb{R})}^2 + \frac{1}{2}\int_{\mathbb{R}} \partial_x\left(q^2\right)|w|^2 - \int_{\mathbb{R}} 2aq^2 |w|^2\,. \tag{3.14}$$

In the previous line a fair amount of work isn't shown: that is, each individual term in (3.13) leads to an inner product that must be resolved. Before moving on, we'll show how to find the following three archetypes of terms: terms that result in an $L^2(\mathbb{R})$-norm, terms that disappear because they are perfect derivatives, and terms that cannot be resolved and remain integrals.

First we start with the first term of (3.13). Applying integration by parts twice,

$$\begin{aligned} -\left\langle \partial_x^4 w, w\right\rangle &= \left\langle \partial_x^3 w, \partial_x w\right\rangle \\ &= -\left\langle \partial_x^2 w, \partial_x^2 w\right\rangle \\ &= -\left\|\partial_x^2 w\right\|_{L^2(\mathbb{R})}^2 \end{aligned}$$

This term then ends with an $L^2(\mathbb{R})$-norm. It is also useful to notice that this is a negative $L^2(\mathbb{R})$-term because (2.2) is of even order, and its highest order term has a negative coefficient.

Next we focus on the second term of (3.13). Applying integration by parts,

$$\begin{aligned}\left\langle \alpha_3 \partial_x^3 w, w \right\rangle &= -\left\langle \alpha_3 \partial_x^2 w, \partial_x w \right\rangle \\ &= -\int_{\mathbb{R}} \alpha_3 \partial_x^2 w \, \overline{\partial_x w}\end{aligned}$$

Taking the real part,

$$\begin{aligned}\text{Re } \left\langle \alpha_3 \partial_x^3 w, w \right\rangle &= -\frac{\alpha_3}{2} \int_{\mathbb{R}} \partial_x^2 w \, \overline{\partial_x w} + \overline{\partial_x^2 w} \, \partial_x w \\ &= -\frac{\alpha_3}{2} \int_{\mathbb{R}} \partial_x \left| \partial_x w \right|^2 \\ &= 0\end{aligned}$$

where we have recognized a perfect derivative. Typically the odd order terms of (3.13) will disappear because they are perfect derivatives.

Finally we focus on the first bracketed term of (3.13). The constant terms α_1 and s will lead to a perfect derivative and will disappear. However q^2 depends on x, so the following integration by parts won't result in a perfect derivative.

$$\begin{aligned}\text{Re } \left\langle q^2 \partial_x w, w \right\rangle &= \frac{1}{2} \int_{\mathbb{R}} q^2 \left[\bar{w} \, \partial_x w + w \, \overline{\partial_x w} \right] \\ &= \frac{1}{2} \int_{\mathbb{R}} q^2 \partial_x \left| w \right|^2 \\ &= -\frac{1}{2} \int_{\mathbb{R}} \partial_x \left(q^2 \right) \left| w \right|^2\end{aligned}$$

There's no way to simplify this term so it will remain in an integral form. This will lead to the $L^\infty(\mathbb{R})$ terms in (3.11) and (3.12).

Using Lemma 3.19 with $j = 1$ and $a_1 = \alpha_2$ on (3.14), we have

$$\text{Re } \lambda \left\| w \right\|_{L^2(\mathbb{R})^2}^2 \leq -\left(\alpha_0 + as - \frac{\alpha_2^2}{4} \right) \left\| w \right\|_{L^2(\mathbb{R})}^2 + \frac{1}{2} \int_{\mathbb{R}} \partial_x \left(q^2 \right) \left| w \right|^2 - \int_{\mathbb{R}} 2aq^2 \left| w \right|^2 .$$

Note that $2aq^2 \left| w \right|^2 \geq 0$, so we neglect this negative term in an upper bound. Using an $L^\infty(\mathbb{R})$ estimate on the other integral term results in

$$\text{Re } \lambda \left\| w \right\|_{L^2(\mathbb{R})}^2 \leq \left(\frac{1}{2} \left\| \partial_x \left(q^2 \right) \right\|_{L^\infty(\mathbb{R})} + \frac{\alpha_2^2}{4} - \alpha_0 - as \right) \left\| w \right\|_{L^2(\mathbb{R})}^2 .$$

Dividing both sides by $\left\| w \right\|_{L^2(\mathbb{R})}^2$ results in (3.11).

Starting with (3.13), multiplying by $\bar{w}$, integrating, and taking the imaginary part results in

$$\text{Im } \lambda \, \|w\|^2_{L^2(\mathbb{R})} = \text{Im } \left[\langle -\alpha_3 \partial_x^2 w, \partial_x w \rangle + \langle \left(\alpha_1 + q^2 + s \right) \partial_x w, w \rangle + \langle \left(\left(\partial_x \left(q^2 \right) \right) - \alpha_0 - 2aq^2 - as \right) w, w \rangle \right] .$$

Taking the absolute value of both sides and using Cauchy-Schwartz,

$$\begin{aligned} |\text{Im } \lambda| \, \|w\|^2_{L^2(\mathbb{R})} \leq \alpha_3 \left\| \partial_x^2 w \right\|_{L^2(\mathbb{R})} \|\partial_x w\|_{L^2(\mathbb{R})} + \left| \alpha_1 + q^2 + s \right| \|\partial_x w\|_{L^2(\mathbb{R})} \|w\|_{L^2(\mathbb{R})} \\ + \left| \left\| \partial_x \left(q^2 \right) \right\|_{L^\infty(\mathbb{R})} - \alpha_0 + 2a \left\| q^2 \right\|_{L^\infty(\mathbb{R})} - as \right| \|w\|^2_{L^2(\mathbb{R})} . \end{aligned}$$

From Young's inequality we have

$$\|\partial_x w\|_{L^2(\mathbb{R})} \|w\|_{L^2(\mathbb{R})} \leq \frac{D}{2} \|\partial_x w\|^2_{L^2(\mathbb{R})} + \frac{1}{2D} \|w\|^2_{L^2(\mathbb{R})}$$

valid for any $D > 0$. Taking $D = \dfrac{-\alpha_3 - 2\alpha_3 c + 2c}{\|\alpha_1 + q^2 + s\|_{L^\infty(\mathbb{R})}}$ and combining this with Lemma 3.19 with $j = 1$ and $a_j = \frac{1}{2}$, we have

$$|\text{Im } \lambda| \, \|w\|^2_{L^2(\mathbb{R})} \leq \frac{1}{2} \left\| \partial_x^2 w \right\|^2_{L^2(\mathbb{R})} + \left[\left(\frac{\left\| \alpha_1 + q^2 + s \right\|^2_{L^\infty(\mathbb{R})}}{4 - 6\alpha_3} + \left\| \partial_x \left(q^2 \right) - \alpha_0 - 2aq^2 - as \right\|_{L^\infty(\mathbb{R})} \right) + \frac{1 - \alpha_3}{2} \right] \|w\|^2_{L^2(\mathbb{R})}$$

Note that because we obtained this bound by Cauchy-Schwartz rather than direct calculation, the coefficient on the $\left\| \partial_x^2 w \right\|_{L^2(\mathbb{R})}$-term is positive. While we might not be able to use the same trick as the real part, we are able to use the same equation: returning to (3.14) and using Lemma 3.19 with $j = 1$ and $a_j = \frac{1}{2}$ gives

$$\text{Re } \lambda \, \|w\|^2_{L^2(\mathbb{R})} \leq -\frac{1}{2} \left\| \partial_x^2 w \right\|^2_{L^2(\mathbb{R})} + \left[\frac{1}{2} \left\| \partial_x \left(q^2 \right) \right\|_{L^\infty(\mathbb{R})} - as + \frac{\alpha_2}{2} \right] \|w\|^2_{L^2(\mathbb{R})} .$$

Adding these two bounds together and dividing by $\|w\|_{L^2(\mathbb{R})}$ gives (3.12). □

If one has a numerical approximation to the front solution q, such as the one obtained in Section 4.1, then the eigenvalue bound in Lemma 3.20 can be approximated numerically as well. Figure 3.3 shows the trapezoidal region predicted by Corollary 3.21: eigenvalues λ with $\text{Re } \lambda > -\omega$, for some small $\omega > 0$, are restricted to a bounded set.

Corollary 3.21. Explicit Eigenvalue Bound for modified Kuramoto-Sivashinsky

Suppose $\lambda \in \mathbb{C}$ is an eigenvalue of L_a with $a = 0.3$ from (5.3) acting on $L^2(\mathbb{R})$. Then λ must satisfy the following estimates:

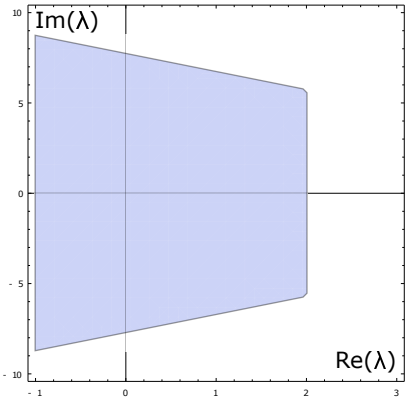

Figure 3.3: The region where eigenvalues may occur as predicted by Corollary 3.21.

$$\begin{aligned} Re\,\lambda &\leq 2 \\ Re\,\lambda + |Im\,\lambda| &\leq 7.7 \end{aligned}$$

We now prove Lemma 3.23, which is the version of Lemma 3.20 for the St. Venant equation (2.5). The proof is similar in form but with an immediate technical difference: as the St. Venant equations are a system, then the eigenvalue equation $Lu = \lambda u$ is now a vector equation and we cannot simply take the $L^2(\mathbb{R})$-norm of each side. Instead, we proceed as in [38, Section 4.1] by defining the following energy function

$$\mathscr{E}_a(U) = \frac{1}{2}\int \left(|u|^2 + |\tau|^2 + \phi_1(x)(\tau_y)^2 + \phi_2(x)(u_y)^2 + \mathrm{Re}\ (\phi_3(x)\tau u_y) \right)$$

where the $\phi_i(x)$ are three currently undetermined real-valued weight functions, and the subscript y indicates differentiation using $\partial_y = \partial_x - a$. This energy function will take the place of $\langle w, w\rangle = \|w\|^2_{L^2(\mathbb{R})}$ in the left hand side of (3.14). We first show that working with ∂_y is not that different than working with ∂_x.

Lemma 3.22. *The $H^1(\mathbb{R})$-norm defined using the derivative ∂_x is equivalent to the $H^1(\mathbb{R})$-norm defined using the derivative ∂_y.*

Proof. In the following we denote the $H^1(\mathbb{R})$-norm using ∂_x by H^1_x and the $H^1(\mathbb{R})$-norm using ∂_y by H^1_y. By definition,

$$\begin{aligned} \|u\|^2_{H^1_y} &= \|u\|^2_{L^2(\mathbb{R}^n)} + \|u_y\|^2_{L^2(\mathbb{R}^n)} \\ &= \|u\|^2_{L^2(\mathbb{R}^n)} + \|(\partial_x - a)u\|^2_{L^2(\mathbb{R}^n)} \\ &\leq (1+a^2)\|u\|^2_{L^2(\mathbb{R}^n)} + \|u_x\|^2_{L^2(\mathbb{R}^n)} \\ &\leq (1+a^2)\|u\|^2_{H^1_x} \end{aligned}$$

For the other direction, let $\langle\cdot,\cdot\rangle$ denote the inner product of $L^2(\mathbb{R}^n)$ and note that

$$\begin{aligned}\|(\partial_x - a)u\|^2_{L^2(\mathbb{R}^n)} &= \langle u_x - au, u_x - au\rangle \\ &= \|u_x\|^2_{L^2(\mathbb{R}^n)} - \langle au, u_x\rangle - \langle u_x, au\rangle + a^2\|u\|^2_{L^2(\mathbb{R}^n)} \\ &= \|u_x\|^2_{L^2(\mathbb{R}^n)} - \int_{\mathbb{R}^n}\partial_x\left(|u|^2\right) + a^2\|u\|^2_{L^2(\mathbb{R}^n)} \\ &= \|u_x\|^2_{L^2(\mathbb{R}^n)} + a^2\|u\|^2_{L^2(\mathbb{R}^n)}\end{aligned}$$

and hence $\|u\|^2_{H^1_x} \leq \|u\|^2_{H^1_y}$. Therefore the two norms are equivalent. □

Lemma 3.23. Eigenvalue Bound for St. Venant Equation

Suppose $\lambda \in \mathbb{C}$ is an $L^2(\mathbb{R})$ eigenvalue of the weighted operator L_a5.4 for the St. Venant equations (2.5). Then there exist constants $C_1, C_2 > 0$ so that Re $\lambda \leq C_1$ and Re $\lambda + C_2|Im\ \lambda| \leq C_1$.

Proof. Let $\langle\cdot,\cdot\rangle$ denote the $L^2(\mathbb{R})$ inner product. We start with the eigenvalue equations $L_a U = \lambda U$ for λu and $\lambda\tau$, which allow us to calculate that

$$2\text{Re}\ \lambda\mathscr{E}_a(U) = \text{Re}\ \left[\langle\phi_1\tau_y, \partial_y(\lambda\tau)\rangle + \langle\phi_2 u_y, \partial_y(\lambda u)\rangle + \langle\phi_3\tau, \partial_y(\lambda u)\rangle + \langle\phi_3 u_y, \lambda\tau\rangle\right] \tag{3.15}$$

We can use the eigenvalue equations to calculate $\partial_y(\lambda\tau)$ and $\partial_y(\lambda u)$. For detailed results of these calculations, see Section 3.6. Focusing on the higher order terms, we have the following inequality.

$$\begin{aligned}2\text{Re}\ \lambda\mathscr{E}_a(U) \leq\ & -\int_{\mathbb{R}}\left(\frac{c}{2}(\phi_1)_y + \frac{3ca}{2}\phi_1 + \alpha\phi_3\right)|\tau_y|^2 - \int_{\mathbb{R}}\left(\frac{\nu}{\bar{\tau}^2}\phi_2\right)|u_{yy}|^2 \\ & + \frac{1}{2}\int_{\mathbb{R}}\left(\phi_1 - \alpha\phi_2 - \frac{\nu}{\bar{\tau}^2}\phi_3\right)(\tau_y\overline{u_{yy}} + \overline{\tau_y}u_{yy}) \\ & + C\left(\|u_{yy}\|_{L^2(\mathbb{R})} + \|u_y\|_{L^2(\mathbb{R})} + \|u\|_{L^2(\mathbb{R})} + \|\tau_y\|_{L^2(\mathbb{R})} + \|\tau\|_{L^2(\mathbb{R})}\right)\left(\|u_y\|_{L^2(\mathbb{R})} + \|u\|_{L^2(\mathbb{R})} + \|\tau\|_{L^2(\mathbb{R})}\right)\end{aligned}$$

As the negative sign on the $|u_{yy}|$-term is beneficial, then we choose ϕ_2 to preserve it. This leads to our first requirement on the weight functions,

$$0 < \phi_2 \equiv \text{const} \ll 1\,.$$

We can't control the sign of the $\tau_y\overline{u_{yy}} + \overline{\tau_y}u_{yy}$ term, so we'll use the weights ϕ_1 and ϕ_3 to make its coefficient zero. This leads to the second requirement that

$$\phi_1 - \alpha\phi_2 - \frac{\nu}{\bar{\tau}^2}\phi_3 = 0\,.$$

We can use this equation to determine ϕ_3, so

$$\phi_3 = \frac{\bar{\tau}^2}{\nu}\left(\phi_1 - \alpha\phi_2\right). \tag{3.16}$$

The negative sign on the $\left|\tau_y\right|$-term is also beneficial, and so we should choose the remaining ϕ_1 to preserve it. Then the condition on its coefficient, after substituting in (3.16), is

$$\frac{c}{2}\left(\phi_1\right)_y + \left(\frac{3ca}{2} + \frac{\alpha\bar{\tau}^2}{\nu}\right)\phi_1 - \frac{\alpha^2\bar{\tau}^2}{\nu}\phi_2 > 0. \tag{3.17}$$

The term $-\frac{\alpha^2\bar{\tau}^2}{\nu}\phi_2$ is always negative, so we temporarily ignore it. We can handle the remainder by having it satisfy the differential equation

$$\frac{c}{2}\left(\phi_1\right)_y + \left(\frac{3ca}{2} + \frac{\alpha^2\bar{\tau}^2}{\nu} - \lim_{x\to\pm\infty}\left[\frac{3ca}{2} + \frac{\alpha^2\bar{\tau}^2}{\nu}\right]\right)\phi_1 = 0. \tag{3.18}$$

This choice was motivated by the fact that in the limit as $x \to \pm\infty$ this tells us that $\left(\phi_1\right)_y \to 0$. We can then explicit solve for ϕ_1,

$$\phi_1 = \exp\left[-\int_{\mathbb{R}}\left(\frac{3ca}{2} + \frac{\alpha\bar{\tau}^2}{\nu} - \lim_{x\to\pm\infty}\left[\frac{3ca}{2} + \frac{\alpha^2\bar{\tau}^2}{\nu}\right]\right)\right]$$

As $\bar{\tau}$ converges to its asymptotic end states exponentially quickly, then the above integral is bounded. As a consequence, ϕ_1 is uniformly bounded from below by a positive number. Substituting (3.18) into (3.17), we can choose the constant value of ϕ_2 sufficiently small so that (3.17) is satisfied.

We have presently chosen the ϕ_i in such a way that there is some positive number $\eta > 0$ so that

$$\begin{aligned} 2\mathrm{Re}\ \lambda\mathscr{E}_a(U) \quad &\leq \quad -\eta\left(\left\|\tau_y\right\|^2_{L^2(\mathbb{R})} + \left\|u_{yy}\right\|^2_{L^2(\mathbb{R})}\right) \\ &\quad +C\left(\left\|u_{yy}\right\|_{L^2(\mathbb{R})} + \left\|u_y\right\|_{L^2(\mathbb{R})} + \|u\|_{L^2(\mathbb{R})} + \left\|\tau_y\right\|_{L^2(\mathbb{R})} + \|\tau\|_{L^2(\mathbb{R})}\right)\left(\left\|u_y\right\|_{L^2(\mathbb{R})} + \|u\|_{L^2(\mathbb{R})} + \|\tau\|_{L^2(\mathbb{R})}\right) \end{aligned} \tag{3.19}$$

Using Young's inequality we may cancel the $\left\|u_{yy}\right\|_{L^2(\mathbb{R})}$ and $\left\|\tau_y\right\|_{L^2(\mathbb{R})}$ terms at the expense of more $\mathscr{E}_a$-term. We then end up with an equation of the form

$$2\mathrm{Re}\ \lambda\mathscr{E}_a(U) \leq \tilde{C}\mathscr{E}_a(U)$$

from which the real part bound for λ follows by dividing both sides by $\mathscr{E}_a$.

Repeating the process of (3.15) for the imaginary part yields

$$2\left|\mathrm{Im}\ \lambda\right|\mathscr{E}_a \lesssim \left\|\tau_y\right\|^2_{L^2(\mathbb{R})} + \left\|u_{yy}\right\|^2_{L^2(\mathbb{R})} + \mathscr{E}_a.$$

Adding some multiple of this to (3.19) and dividing both sides by $\mathscr{E}_a$ yields the $\mathrm{Re}\ \lambda + \left|\mathrm{Im}\ \lambda\right|$-type bound.

□

3.5 Finding the Point Spectrum: The Evan's Function

We start by noting the simplest result regarding the point spectrum: that a system invariant to spatial translations, $\lambda = 0$ is an eigenvalue. By translationally invariant we mean that if $u(x,t)$ is a solution to (1.6), then for any $\gamma \in \mathbb{R}^n$ fixed $u(x+\gamma,t)$ is also a solution. Given a traveling wave solution q, one can explicitly calculate that q' is an eigenfunction of $\lambda = 0$. This is a special case in the theory of an N-parameter symmetry operator, defined later in Definition 5.11. Note however that q' is not necessarily the only eigenfunction of $\lambda = 0$.

Finding the essential spectrum can be handled wholesale through Theorem 3.14, but unfortunately finding the point spectrum can be a far trickier business. We also remark that the characterization of the essential spectrum in Theorem 3.14 is purely analytical (as opposed to numerical), while explicit characterization of the point spectrum are often only analytical for relatively simple systems. The most classical of which is Sturm-Liouville Theory, which concerns differential operators of the form

$$Lu = u_{xx} + a_1(x)u_x + a_0(x)u., \qquad x \in [-1,1]$$

subject to the separated boundary conditions

$$b_1^- p(-1) + b_2^- \partial_x p(-1) = 0, \qquad b_1^+ p(1) + b_2^+ \partial_x p(1) = 0$$

where the coefficients $b_k^\pm$ satisfy $\left(b_1^\pm\right)^2 + \left(b_2^\pm\right)^2 > 0$. See [24, Section 2.3] for a brief overview of the topic. The main result is there are countably many strictly descending real-valued eigenvalues λ_j, which can be ordered in such a way, with $\lambda_j \to -\infty$, that the j-th eigenvalue has an eigenfunction with j simple zeros. This is a powerful result as it gives a criterion for finding the most unstable eigenvalue of L and ensures that only finitely many eigenvalues will have positive real-part.

Unfortunately the systems (2.5) and (2.2) are far from being of Sturm-Liouville type, and fundamentally different techniques must be used. Our main technique is that of the numerical Evan's function. The titular Evan's function is formed as the wronskian of the stable and unstable manifolds, and thus is an analytic function whose zeros correspond to eigenvalues [24, Section 10.2]. The "numerical" part of the numeric Evan's function comes into play as the Evan's function is numerically approximated, and a contour integral and the Argument principle are used to find zeros in a bounded region.

We start by rigorously defining the Evan's function [2, Chapter 3.4]. Note that for ℓ-th order linear differential

operators L the eigenvalue equation $L\phi = \lambda\phi$ is an ODE, and can be written as the first order system

$$W' = A(x,\lambda)W, \qquad W \in \mathbb{R}^{\ell}. \tag{3.20}$$

Furthermore, if the operator L is the linearization about an exponentially asymptotic traveling wave, then we can also define the asymptotic matrices

$$A_{\pm\infty}(\lambda) = \lim_{x\to\pm\infty} A(x,\lambda)$$

and consider the case when the dimension of the unstable subspace U_- of $A_{-\infty}$ and the dimension of the stable subspace S_+ of A_∞ add up to the full dimension ℓ (where $W \in \mathbb{R}^{\ell}$). Viewing (3.20) as an initial value problem posed at $x = -\infty$ and $x = \infty$, separately, both evolving towards $x = 0$ allows one to find a basis $W_1^-(x), \ldots, W_k^-(x)$ and $W_{k+1}^+(x), \ldots, W_\ell^+(x)$ for U_- and S_+ respectively with the property that $\lim_{x\to-\infty} W_i^-(x) = 0$ and $\lim_{x\to\infty} W_i^+(x) = 0$. Then the Evan's function is defined to be

$$D(\lambda) = \det\left(W_1^- \cdots W_k^- W_{k+1}^+ \cdots W_\ell^+\right)\Big|_{x=0} \tag{3.21}$$

hence zeros correspond to values of λ where the unstable subspace U_- meets the stable subspace S_+ creating an eigenfunction.

Note that we are assuming that the dimension of U_- and S_+ remain constant as λ changes: this is sometimes referred to as "consistent splitting." In [24, Lemma 3.1.10, p. 47] it was shown that the boundary of the essential spectrum corresponds to the curves where the dimensions of U_- and S_+ change. Thus so long as one restricts to λ within a region that does not cross the boundary of the essential spectrum the Evan's function is well-defined.

We now present the numeric Evan's function calculations for the modified Kuramoto-Sivashinsky equation. All calculations were performed with the Matlab package STABLAB [2]. As a technical note we will be performing the calculations for the weighted operator L_a as defined in (5.3) with a chosen to satisfy Theorem 5.2 rather than the usual L. This is because in Section 5.2 we will show that the operator L has unstable essential spectrum. In particular, we would not be able to check the entire region of Corollary 3.21 for eigenvalues with positive real part with a contour that does not cross the essential spectrum. Through the use of "exponential weights" — introduced in Section 5.15.1 — for appropriate values of a the weighted operator L_a has no unstable essential spectrum (Theorem 5.2). Furthermore the operator L_a possesses the property that (formally) if ϕ is an eigenfunction of L, then $e^{ax}\phi$ is an eigenfunction of L_a, so the search for unstable point spectrum of L_a is equivalent to finding unstable point spectrum of L.

We can then identify the matrix $A(x,\lambda)$ in (3.20) as

$$A_a(x,\lambda) = \begin{pmatrix} 0 & 1 & 0 & 0 \\ 0 & 0 & 1 & 0 \\ 0 & 0 & 0 & 1 \\ 6\bar{q}\bar{q}' - a^2 - a^4 - 4a\bar{q}^2 - as - \lambda, & 2a + 4a^3, & -6a^2 - 1, & 4a \end{pmatrix}.$$

The asymptotic matrices are

$$A_{a,\pm\infty} = \begin{pmatrix} 0 & 1 & 0 & 0 \\ 0 & 0 & 1 & 0 \\ 0 & 0 & 0 & 1 \\ -a^2 - a^4 - 3am_\pm^2 - as - \lambda, & 2a + 4a^3 + 3m_\pm^2 + s, & -6a^2 - a, & 4a \end{pmatrix}.$$

On the region to the right of the essential spectrum the dimensions of U_- and S_+ are fixed, so it suffices to find their dimensions for just one value of λ. When $a = 0.3$, $s = -2.388$, and $\lambda = 0$ we can calculate that it has eigenvalues of $\mu \approx 1.97862,\ -0.533251 \pm 1.55025i,\ 0.287884$. Hence for all λ to the right then both U_- and S_+ have dimension 2. Further, there exist $W_1^-(x), W_2^-(x)$ a basis of U_- with $W_i^-(x) \to 0$ as $x \to -\infty$, and $W_3^+(x), W_4^+(x)$ a basis of S_+ with $W_i^+(x) \to 0$ as $x \to \infty$. Then our Evan's function is

$$D_a(\lambda) = \det\left(W_1^- W_2^- W_3^+ W_4^+\right)\big|_{x=0}.$$

Before proceeding to the numerics, we discuss a few details of the numerical implementation. Our present objective is to find the $W_i^\pm$ using the ODE (3.20), but note that $W_i^\pm \sim e^{\mu_i}$ where μ_i is given by the eigenvalues of $A_{a,\pm\infty}$. Thus calculations in the regime when $x \to \infty$ (resp. $x \to -\infty$) will be dominated by the $W_i^\pm$ whose eigenvalue has the largest (resp. most negative) real part, making it difficult to find the other $W_i^\pm$. The solution given in [2, Chapter 4, Section 2] and [9, Section 3.3] is the compound matrix method, whose answer is to "lift" the working space $\mathbb{C}^4$ to $\wedge^2\left(\mathbb{C}^4\right)$, the wedge product space. The operator $A_a(x,\lambda)$ is then "lifted" to the operator $A^{(2)}$ defined by $A^{(2)}(e_i \wedge e_j) = (Ae_i) \wedge e_j + e_i \wedge (Ae_j)$. Explicitly, if

$$A = \begin{pmatrix} a_{11} & a_{12} & a_{13} & a_{14} \\ a_{21} & a_{22} & a_{23} & a_{24} \\ a_{31} & a_{32} & a_{33} & a_{34} \\ a_{41} & a_{42} & a_{43} & a_{44} \end{pmatrix},$$

then

$$A^{(2)} = \begin{pmatrix} a_{11}+a_{22} & a_{23} & a_{24} & -a_{13} & -a_{14} & 0 \\ a_{32} & a_{11}+a_{33} & a_{34} & a_{12} & 0 & -a_{14} \\ a_{42} & a_{43} & a_{11}+a_{44} & 0 & a_{12} & a_{13} \\ -a_{31} & a_{21} & 0 & a_{22}+a_{33} & a_{34} & -a_{24} \\ -a_{41} & 0 & a_{21} & a_{43} & a_{22}+a_{44} & a_{23} \\ 0 & -a_{41} & a_{31} & -a_{42} & a_{32} & a_{33}+a_{44} \end{pmatrix}.$$

As the wedge product of vectors is zero if and only if they are linearly dependent, then the Evan's function can also be written as

$$D_a(\lambda) = \left(W_1^- \wedge W_2^-\right) \wedge \left(W_3^+ \wedge W_4^+\right)\big|_{x=0}.$$

The eigenvalues of $A^{(2)}$ are sums of eigenvalues of A and the eigenvectors of $A^{(2)}$ are formed from wedge products of eigenvectors of A. That is, as $W_i^{\pm}$ are the eigenfunctions of A with eigenvalues μ_i, then the eigenfunctions of $A^{(2)}$ are $W_i^{\circ} \wedge W_j^{\circ}$ (where $\circ$ is used as the $+$ or $-$ depend on index i and j) with corresponding eigenvalue $\mu_i + \mu_j$. As a corollary of this, $W_1^- \wedge W_2^-$ will have the eigenvalue with largest real part, and hence will be the dominant term as $x \to \infty$. Similarly, $W_3^+ \wedge W_4^+$ will have the eigenvalue with most negative real part and will be the dominant term as $x \to -\infty$. Since these are the desired terms in their respective regimes, this numerical method is well behaved.

We remark that while the dimensions of this "lifted" space are reasonable, in the general case things may quickly get out of hand. An alternative method is the polar coordinates method, also known as analytic orthogonalization [2, Chapter 4, Section 3].

The last remaining piece of the initial value problem (3.20), albeit using $A^{(2)}$ instead of A, is an initial condition. One uses the method of Kato [2, Chapter 4, Section 4] and [44, Section 6.1] to generate initial conditions that ensure the Evan's function is analytic in λ. Let P_- be the spectral projection into U_- and P_+ be the spectral projection into S_+. Then one solves the two ODEs

$$r_j'(\lambda) = P_{\pm}'(\lambda)\ r_j(\lambda), \qquad r_j(\lambda_0) = r_j^0$$

where the matrices of initial conditions $\left[r_1^0, \ldots, r_\ell^0\right]$ must be of full rank. From [25] one knows that the spectral projections $P_\pm$ are analytic in λ, and one can then show that the solutions $r_j(\lambda)$ vary analytically and are in either U_- or S_+.

In performing the Evan's function calculations we have two goals: (1) verify that there are is no unstable point spectrum, and (2) characterize the eigenvalue $\lambda = 0$. Regarding the latter, recall that $\lambda = 0$ has the eigenfunction q' arising from the translation invariance of the problem. If this is the only eigenfunction, then one can easily create an

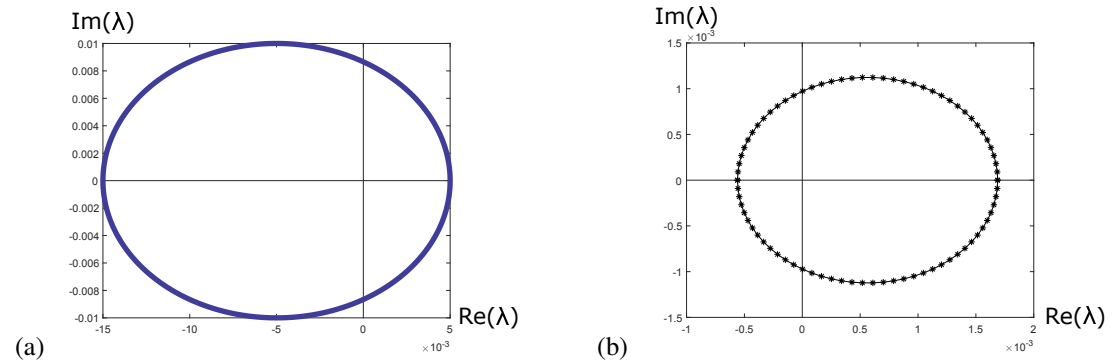

Figure 3.4: Evan's function calculations of L_a from (5.3) with $a = 0.3$ around the origin. (a) The contour used: a small circle around the origin. (b) The numerical Evan's function output, which has a winding number of one.

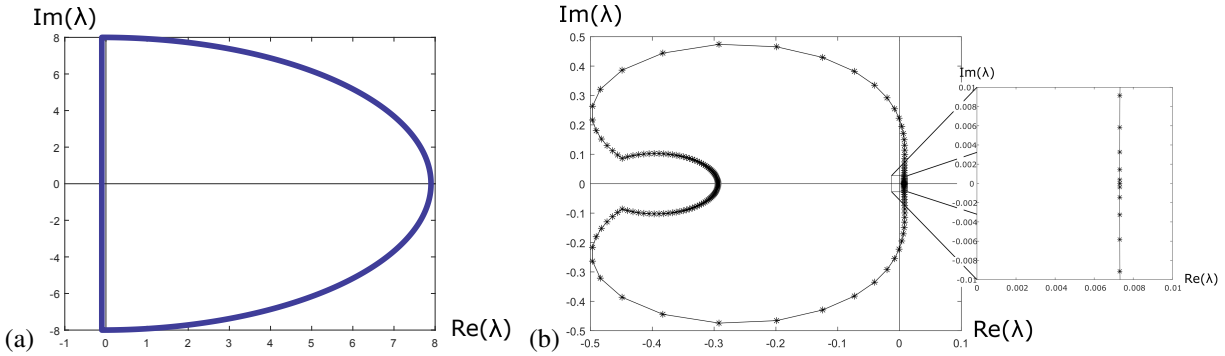

Figure 3.5: Evan's function calculations of L_a from (5.3) with $a = 0.3$ around the region where Corollary 3.21 predicts unstable eigenvalues can occur. (a) The contour used: a semicircle moved slightly to the left (but still entirely to the right of the essential spectrum). (b) The Evan's function output, with an insert showing the what's happening around the origin, and a winding number of one.

explicit spectral projection to remove this eigenvalue and one can continue with the stability argument unperturbed. However, if there was another eigenfunction then we would need to address it. So our first use of the Evan's function is to check the dimension of the eigenspace of $\lambda = 0$. For this we use a very small circular contour about the origin, as seen in Figure 3.4 (a). The output, as seen in Figure 3.4 (b), also resembles a circle and has a winding number of one. This means that q' is also the only eigenfunction of $\lambda = 0$.

To verify there are no unstable point spectrum we perform another Evan's function calculation over the contour in Figure 3.5 (a), which is a contour that contains the region where unstable point spectrum can occur as predicted by Corollary 3.21. This contour is to the right of the essential spectrum: Figure 5.6 (b) shows that when $a = 0.3$ the rightmost part of the essential spectrum occurs when $\text{Re}\,\lambda \approx -0.2$ and the leftmost part of the contour is $\text{Re}\,\lambda \approx -0.1$. The Evan's function output is shown in Figure 3.5 (b) with a winding number of one (which is expected, as $\lambda = 0$ is contained in the contour). Then other than $\lambda = 0$, there is no point spectrum contained in the contour. Note that the contour also contains the areas where point spectrum with small negative real part occur: this produces the spectral gap needed for the Gearhart-Pruss theorem (Theorem 5.6).

3.6 Appendix A: Explicit Calculations of Lemma 3.23

The calculations to rewrite (3.15) are rather lengthy and highly computational, so they were omitted from the proof. However such calculations are vital when implementing numerical Evan's function calculations — in particular consider Corollary 3.21 — so the quantitative results are collected here. We start with three lemmas that aid in the calculations in this section.

Lemma 3.24. Product Rule for ∂_y

For $f, g \in H^1(\mathbb{R})$,

$$(fg)_y = f_y g + f g_x .$$

Proof. This follows from direct calculation.

$$\begin{aligned} (fg)_y &= (fg)_x - afg \\ &= f_x g + f g_x - afg \\ &= f_y g + f g_x . \end{aligned}$$

□

Lemma 3.25. Integration by Parts for ∂_y

For $f, g \in H^1(\mathbb{R})$, we have

$$\int_{\mathbb{R}} f_y g \, dx = -\int_{\mathbb{R}} f\left(g_y + 2ag\right) \, dx .$$

Proof. We start by using integration by parts.

$$\begin{aligned} \int f_y g &= \int (f_x - af) g \\ &= -\int f\left(g_x + ag\right) . \end{aligned}$$

Note that the differential operator $\partial_x + a$ is equivalent to $\partial_y + 2a$: then the lemma follows. □

It is occasionally useful to "collect" derivatives by applying the chain rule in reverse, such as writing $u_x u_{xx}$ as $\partial_x \frac{1}{2} (u_x)^2$, whereby integration by parts can be applied to move the derivatives to other terms. Here we given an equivalent result for ∂_y.

Lemma 3.26. Collecting y-Derivatives

For $u \in H^1(\mathbb{R})$,

$$uu_y = \partial_y\left(u^2\right) - \frac{1}{2}\partial_x\left(u^2\right).$$

Proof. We start with uu_y,

$$uu_y = uu_x - au^2.$$

We may collect the x-derivative of the first term.

$$\begin{aligned} uu_y &= \partial_x\left(\frac{1}{2}u^2\right) - au^2 \\ &= \left(\frac{1}{2}\partial_x - a\right)u^2. \end{aligned}$$

Note that $\frac{1}{2}\partial_x - a$ is $\partial_y - \frac{1}{2}\partial_x$. Thus

$$uu_y = \left(\partial_y - \frac{1}{2}\partial_x\right)u^2.$$

From this the lemma follows. □

In the following we give the bounds associated to each term in (3.15) and give the final bound, omitting the calculations. To save space we use the shorthand "L^2" for $L^2(\mathbb{R})$, and "L^∞" for $L^\infty(\mathbb{R})$, and each integral is over $\mathbb{R}$.

First the terms involving ϕ_1.

$$\begin{aligned} \left\langle \phi_1\tau_y, c\tau_{yy}\right\rangle &= -\int_{\mathbb{R}}\left(\frac{c}{2}\left(\phi_1\right)_y + \frac{3c}{2}a\phi_1\right)\left|\tau_y\right|^2\,dx, \\ \left\langle \phi_1\tau_y, u_{yy}\right\rangle &= \frac{1}{2}\int_{\mathbb{R}}\phi_1\left(\tau_y\bar{u}_{yy} + \bar{\tau}_y u_{yy}\right)\,dx. \end{aligned}$$

Next the terms involving ϕ_2.

$$\begin{aligned} \left\langle \phi_2 u_y, cu_{yy}\right\rangle &\leq \|c\phi_2\|_{L^\infty}\left\|u_y\right\|_{L^2}\left\|u_{yy}\right\|_{L^2}, \\ \left\langle \phi_2 u_y, (\alpha\tau)_{yy}\right\rangle &\leq -\frac{1}{2}\int_{\mathbb{R}}\alpha\phi_2\left(\tau_y\overline{u_{yy}} + \overline{\tau_y}u_{yy}\right)\,dx \\ &\quad + \left(\|(\phi_2)_x\,\overline{\alpha}\|_{L^\infty} + \|\phi_2\overline{\alpha_x}\|_{L^\infty} + \|2\phi_1\overline{\alpha}\|_{L^\infty}\right)\left\|u_y\right\|_{L^2}\left\|\tau_y\right\|_{L^2} \\ &\quad + \left\|\phi_2\left(\overline{\alpha_{xx} - 2\alpha_x a}\right)\right\|_{L^\infty}\left\|u_y\right\|_{L^2}\|\tau\|_{L^2} + \|2\phi_2\overline{\alpha_x}\|_{L^\infty}\left\|u_y\right\|_{L^2}\|\tau_x\|_{L^2}, \\ \left\langle \phi_2 u_y, \nu\left(\frac{u_x}{\bar{\tau}^2}\right)_{yy}\right\rangle &\leq -\int_{\mathbb{R}}\nu\frac{\phi_2}{\bar{\tau}^2}\left|u_{yy}\right|^2\,dx \\ &\quad + \|(\phi_2)_x + 2a\phi_2\|_{L^\infty}\left(\left\|\frac{\nu}{\bar{\tau}^2}\right\|_{L^\infty}\left\|u_y\right\|_{L^2}\left\|u_{yy}\right\|_{L^2} + \left\|\nu\frac{\left(\bar{\tau}^2\right)_x - a\bar{\tau}^2}{\left(\bar{\tau}^2\right)^2}\right\|_{L^\infty}\left\|u_y\right\|_{L^2}^2\right) \end{aligned}$$

$$
\begin{aligned}
&+\|(\phi_2)_x+2a\phi_2\|_{L^\infty}\left\|\nu\frac{a\left(\bar\tau^2\right)_x+a^2\bar\tau^2-\bar\tau^2a^2}{\bar\tau^4}\right\|_{L^\infty}\|u\|_{L^2}\left\|u_y\right\|_{L^2}\\
&+\|\phi_2\|_{L^\infty}\left(\left\|\nu\frac{\left(\bar\tau^2\right)_x-a\bar\tau^2}{\left(\bar\tau^2\right)^2}\right\|_{L^\infty}\left\|u_y\right\|_{L^2}\left\|u_{yy}\right\|_{L^2}+\left\|\nu\frac{a\left(\bar\tau^2\right)_x+a^2\bar\tau^2-\bar\tau^2a^2}{\bar\tau^4}\right\|_{L^\infty}\|u\|_{L^2}\left\|u_{yy}\right\|_{L^2}\right),\\
\left\langle\phi_2u_y,-\left(\bar u^2\tau\right)_y\right\rangle &\leq \|2\phi_2\bar u_x\|_{L^\infty}\left\|u_y\right\|_{L^2}\|\tau\|_{L^2}+\left\|\phi_2\bar u^2\right\|_{L^\infty}\left\|u_y\right\|_{L^2}\left\|\tau_y\right\|_{L^2},\\
\left\langle\phi_2u_y,-\left(2\bar u\bar\tau u\right)_y\right\rangle &\leq \|2\phi_2\left(\bar u_x\bar\tau+\bar u\bar\tau_x\right)\|_{L^\infty}\left\|u_y\right\|_{L^2}\|u\|_{L^2}+\|2\phi_2\bar u\bar\tau\|_{L^\infty}\left\|u_y\right\|_{L^2}^2.
\end{aligned}
$$

Finally the terms involving ϕ_3.

$$
\begin{aligned}
\left\langle\phi_3\tau,cu_{yy}\right\rangle &\leq \|c\phi_3\|_{L^\infty}\|\tau\|_{L^2}\left\|u_{yy}\right\|_{L^2},\\
\left\langle\phi_3\tau,(\alpha\tau)_{yy}\right\rangle &\leq \|\alpha\phi_3\|_{L^\infty}\left\|\tau_y\right\|_{L^2}^2+\|\alpha_x\left((\phi_3)_x+2a\phi_3\right)\|_{L^\infty}\|\tau\|_{L^2}^2\\
&\quad+\|\alpha_x\phi_3+\alpha\left((\phi_3)_x+2a\phi_3\right)\|_{L^\infty}\left\|\tau_y\right\|_{L^2}\|\tau\|_{L^2},\\
\left\langle\phi_3\tau,\nu\left(\frac{u_x}{\bar\tau^2}\right)_{yy}\right\rangle &\leq -\frac{1}{2}\int_{\mathbb{R}}\nu\frac{\phi_3}{\bar\tau^2}\left(\tau_y\bar u_{yy}+\bar\tau_yu_{yy}\right)dx\\
&\quad+\left\|(\phi_3)_y+2a\phi_3\right\|_{L^\infty}\left(\left\|\frac{\nu}{\bar\tau^2}\right\|_{L^\infty}\|\tau\|_{L^2}\left\|u_{yy}\right\|_{L^2}+\left\|\left(\frac{\nu}{\bar\tau^2}\right)_x+\frac{\nu a}{\bar\tau^2}\right\|_{L^\infty}\|\tau\|_{L^2}\left\|u_y\right\|_{L^2}\right)\\
&\quad+\left\|(\phi_3)_y+2a\phi_3\right\|_{L^\infty}\left\|\left(\frac{\nu a}{\bar\tau^2}\right)_x\right\|_{L^\infty}\|\tau\|_{L^2}\|u\|_{L^2}\\
&\quad+\|\phi_3\|_{L^\infty}\left(\left\|\left(\frac{\nu}{\bar\tau^2}\right)_x+\frac{\nu a}{\bar\tau^2}\right\|_{L^\infty}\left\|\tau_y\right\|_{L^2}\left\|u_y\right\|_{L^2}+\left\|\left(\frac{\nu a}{\bar\tau^2}\right)_x\right\|_{L^\infty}\left\|\tau_y\right\|_{L^2}\|u\|_{L^2}\right),\\
\left\langle\phi_3\tau,-\left(\bar u^2\tau\right)_y\right\rangle &\leq \left\|\phi_3\left(\bar u^2\right)_x\right\|_{L^\infty}\|\tau\|_{L^2}^2+\left\|\phi_3\bar u^2\right\|_{L^\infty}\|\tau\|_{L^2}\left\|\tau_y\right\|_{L^2},\\
\left\langle\phi_3\tau,-\left(2\bar u\bar\tau u\right)_y\right\rangle &\leq \|2\phi_3\left(\bar u\bar\tau\right)_x\|_{L^\infty}\|\tau\|_{L^2}\|u\|_{L^2}+\|2\phi_3\bar u\bar\tau\|_{L^\infty}\|\tau\|_{L^2}\left\|u_y\right\|_{L^2}.
\end{aligned}
$$

Chapter 4

Supplementary Numerics

In this chapter we handle a few miscellaneous numerical calculations that play supporting roles elsewhere. Note that while in presenting these methods we primarily focus on the modified Kuramoto-Sivashinsky equation (2.2), such techniques naturally generalize to the St. Venant equations (2.5) as well.

In Section 4.1 we numerically generate the equilibrium solution q as a heteroclinic connection of an unstable eigenspace to a stable eigenspace. This numerical approximation is necessary for the numerical Evan's function calculations in Section 3.5, numerical time evolution in Section 4.2, and when considering ad-hoc periodic solutions formed by concatenating copies of q in Section 5.5.

In Section 4.2 we use the Crank-Nicolson method to numerically calculate the time evolution of a perturbed equilibrium solution q. The results of this are discussed in Section 5.1 and motivates our main stability result Theorem 5.7.

In Section 4.3 we use Hill's method to numerically calculate the spectrum of periodic solutions. This is used when we consider the stability of ad-hoc periodic wave trains formed by concatenating copies of q in Section 5.5.

4.1 Numerically Generating Fronts/Pulses

In this section we focus on numerically generating the traveling wave solution q for the modified Kuramoto-Sivashinsky equation (2.2) — where q satisfies the ODE in (2.3) — with the intention of using it for numerical time evolution in Section 4.2. For simplicity in this section we take $\mu = 0$, but in Section 5.5 we address the case when choosing $\mu \neq 0$. The defining equation (2.3) is a boundary value problem with boundary conditions as $|x| \to \infty$. Thus our main work will be in solving a numerical boundary value problem, although we will need to use projective boundary conditions to reduce this to a boundary value problem on a finite interval. Additionally an initial guess must be provided to the boundary value solver, which will be provided by using the shooting method.

To begin the shooting method we start by rewriting (2.3) as a first order system: by setting $q_j = \partial_x^j q$, we have

$$\begin{aligned} \partial_x q_1 &= q_2 \\ \partial_x q_2 &= q_3 \\ \partial_x q_3 &= -q_2 + q_1^3 + s q_1 \,. \end{aligned} \tag{4.1}$$

This system has the stationary points $\left(\pm\sqrt{-s}, 0, 0\right)$ which we would like to connect via a heteroclinic connection. We may consider arbitrary s, but we require that $s < 0$. Linearizing this system around the stationary points gives the linearization

$$L\vec{q} = \begin{pmatrix} 0 & 1 & 0 \\ 0 & 0 & 1 \\ -2s & -1 & 0 \end{pmatrix} \begin{pmatrix} q_1 \\ q_2 \\ q_3 \end{pmatrix}. \tag{4.2}$$

We ultimately want a heteroclinic orbit that connects the stationary points $\left(\pm\sqrt{-s}, 0, 0\right)$. For ease of presentation in the following, we will be constructing "front" solutions with the orbit going from $\left(-\sqrt{-s}, 0, 0\right)$ to $\left(\sqrt{-s}, 0, 0\right)$. We may also consider "back" solutions going from $\left(\sqrt{-s}, 0, 0\right)$ to $\left(-\sqrt{-s}, 0, 0\right)$: we will do later in Section 5.5.

Numerical calculations from [33] suggest that when $\mu = 0$ then $s \approx -2.388$. We can use Matlab's built in function `eig` to find the eigenvalues and eigenvectors of (4.2). There are three eigenvalues,

$$\lambda \approx 1.48713, \qquad \lambda \approx -0.743565 \pm 1.63054 i$$

which means there is a one-dimensional unstable manifold, spanned by e_u^-, and a two-dimensional stable manifold, spanned by $e_{s,2}^+$ and $e_{s,2}^+$. One can imagine our desired hetereoclinic orbit as leaving $\left(-\sqrt{-s}, 0, 0\right)$ along the unstable manifold and advancing towards $\left(\sqrt{-s}, 0, 0\right)$ along the stable manifold. For our shooting method we will leave $\left(-\sqrt{-s}, 0, 0\right)$ in the direction of e_u^-. That is, we have the initial condition of $\left(-\sqrt{-s}, 0, 0\right) + \varepsilon e_u^-$, where ε is a free parameter. We can then use this initial value along with the equation (4.2) with Matlab's built in ODE solver `ode45`, which implements a paired 4th and 5th order Runge-Kutta method, to solve for the value of $\vec{q}$ after some time (in our numerics we used the interval$[-7, 10]$).

We are then faced with the optimization problem of choosing the value of ε that results in a solution as close to $\left(\sqrt{-s}, 0, 0\right)$ as possible. One can use Matlab's built in function `fminsearch` to perform this optimization, the results of which are given in Figure 4.1. Unfortunately the produced front is a little "lopsided," which we fixed by adding an artificial point to the right using the front's asymptotic value.

With an initial guess in hand, we now advance to the boundary value problem using projective boundary conditions. One can imagine our desired hetereoclinic orbit as leaving $\left(-\sqrt{-s}, 0, 0\right)$ along the unstable manifold and advancing

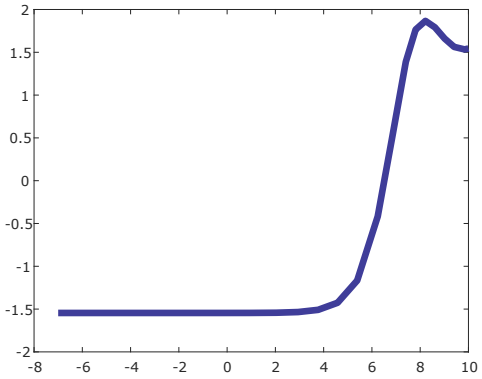

Figure 4.1: The front produced by the shooting method after optimizing over choice of ε.

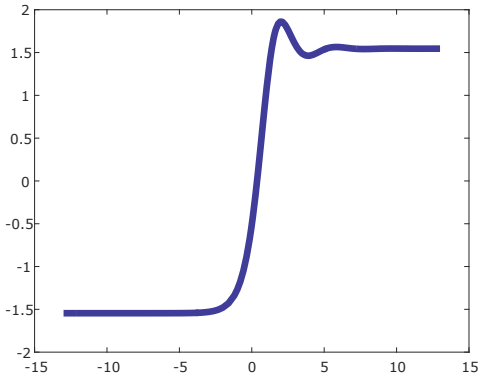

Figure 4.2: The front produced by using projective boundary conditions.

towards $\left(\sqrt{-s},0,0\right)$ along the stable manifold. Along the interval $[-L,L]$ projective boundary conditions may then be obtained by requiring the solution to be orthogonal to the stable manifold at $x=-L$ and orthogonal to the unstable manifold at $x=L$. Explicitly,

$$q\left(-L\right)\cdot e_{s,1}^{-}=0, \qquad q\left(-L\right)\cdot e_{s,2}^{-}=0, \qquad q\left(L\right)\cdot e_{u}^{+}=0\,.$$

The vectors $e_{s,1}^{-},e_{s,2}^{-}$ and e_{u}^{+} were obtained by using Gram-Schmidt to find orthogonal bases to e_{u}^{-} and $e_{s,1}^{+},e_{s,2}^{-}$ respectively. In practice it seemed as though the first two boundary conditions were redundant in some way, so we replaced one with the arbitrary condition that $q_1\left(-L\right)=-\sqrt{-s}+0.001$, intended to counteract the translationally invariant nature of the problem.

One can then use Matlab's built in function bvp4c, which implements a collocation method, to solve this boundary value problem, the result of which is given in Figure 4.2.

The following trick from [14] may be used to vastly increase performance of the boundary value solver. Specifically, that if (4.1) when written as a system is $\partial_x q=\mathscr{F}\left(q\right)$, then we introduce the variable $\tilde{q}$ with $\partial_x\tilde{q}=-\mathscr{F}\left(\tilde{q}\right)$ so rather than working on the region $[-L,L]$, q is the solution on $[0,L]$ and $\tilde{q}$ is the solution running backwards on $[-L,0]$.

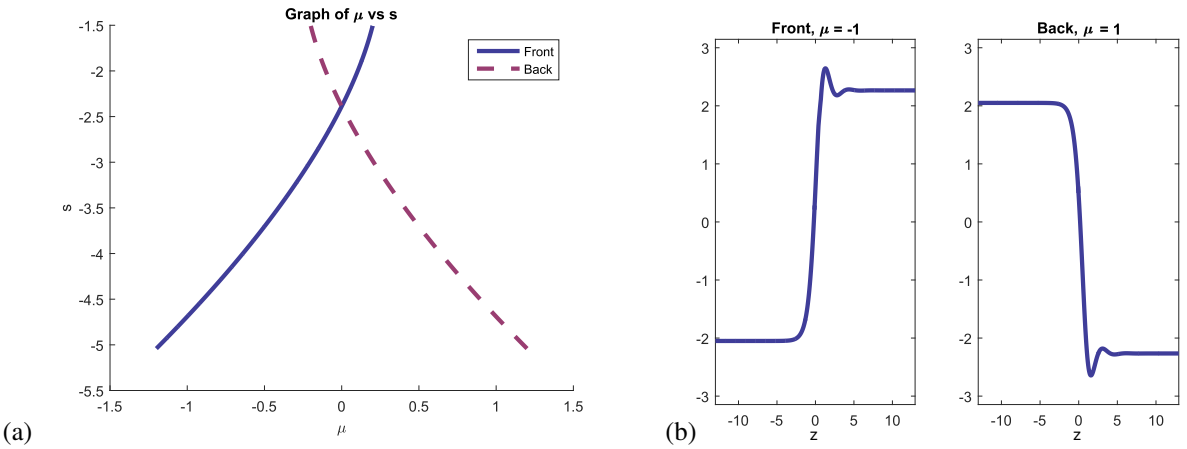

(a) (b)

Figure 4.3: (a) A plot showing how choosing μ affects the speed s, for both fronts and backs. (b) A plot contrasting the asymptotic values of the $\mu = 1$ front and the $\mu = -1$ back.

We then have the additional three-dimensional matching condition that $q(0) = \tilde{q}(0)$ within which we can specify that the front takes on the (arbitrarily chosen) value $\frac{1}{2}$ at $x = 0$.

Finally we now address a lingering mystery: what effect choosing the integration constant $\mu \neq 0$ in (2.3) have? It doesn't affect numerically calculating the front q in Section 4.1 as one can let $\mu \neq 0$ and use this to determine the speed s. One can also calculate backs, which start from the positive asymptotic value and travel towards the positive one.

Later in Section 5.5 we would like to form ad-hoc periodic solutions by concatenating the fronts and backs together, and our choice of μ will affect this. Figure 4.3 (a) summarizes the (numerically calculated) relationship between μ and s. It seems as though the front with $\mu = \alpha$ travels the same speed as the $\mu = -\alpha$ back: this is necessary if we want to concatenate fronts and backs otherwise they would travel at different speeds and the ad-hoc periodic solution would fall apart even without a perturbation. In Figure 4.3 (b) we show how choosing $\mu \neq 0$ changes the asymptotic values: as μ changes the asymptotic values asymmetrically, then fronts and backs only have the same asymptotic values when $\mu = 0$.

4.2 Numerical Time Evolution

We start by reviewing the Crank-Nicolson method [27, Chapter 9.1, p. 182], an implicit method commonly used to solve time evolution problems of the form (1.6). This method is about as efficient as the explicit method but is more amenable to "stiff" equations.

Consider solving the time-evolution problem $u_t = \mathscr{F}(u)$. Discretizing the problem on an $(\Delta x, \Delta t)$ grid so that $u_j^k = u(j\Delta x, k\Delta t)$, or the j-th spatial position and the k-th temporal position. Set $\mathscr{F}_j^k = \mathscr{F}\left(u_j^k\right)$. We consider discretizing

the t-derivative, recalling that the forward and backward Euler methods are respectively

$$\frac{u_j^{k+1}-u_j^k}{\Delta t}=\mathscr{F}_j^k, \qquad \frac{u_j^{k+1}-u_j^k}{\Delta t}=\mathscr{F}_j^{k+1}.$$

The former is an explicit method as one can solve directly for u_j^{k+1}, the future value of u. Conversely the latter is an implicit method as $\mathscr{F}_j^{k+1}$ also depends on the future value of u. The Crank-Nicolson method is the average of these forward and backward Euler methods, explicitly

$$\frac{u_j^{k+1}-u_j^k}{\Delta t}=\frac{1}{2}\left(\mathscr{F}_j^k+\mathscr{F}_j^{k+1}\right) \tag{4.3}$$

We show how the Crank-Nicolson method can be implemented to numerically calculate the time evolution, focusing on (2.2) first as this is a scalar equation which will simplify things. A similar methodology applies to (2.5), but we do not address it explicitly here. Our first goal is to discretize $\mathscr{F}$: with (2.2) in mind, we will need to discretize the terms u_x, u_{xx}, u_{xxxx}, and $\left(u^3\right)_x$.

For both u_x and u_{xx} we use the standard second order difference discretizations [27, Chapter 1],

$$u_x\sim\frac{u_{j+1}^k-u_{j-1}^k}{2\Delta x}, \qquad u_{xx}\sim\frac{u_{j-1}^k-2u_j^k+u_{j+1}^n}{(\Delta x)^2}. \tag{4.4}$$

Note that the u_{xxxx} term will require a five point stencil (compared to the previous two discretization's three point stencils). We use the standard fourth order discretization,

$$u_{xxxx}\sim\frac{u_{j-2}^k-4u_{j-1}^k+6u_j^k-4u_{j+1}^k+u_{j+2}^k}{(\Delta x)^4}.$$

The non-standard term $\left(u^3\right)_x$ can provide some challenge. The naive approach would be the use the discretization for u_x as in (4.4) but using the function u^3 instead, however this caused the overall time evolution to fail. A far better approach is to instead approximate the (equivalent) term $3u^2u_x$, which did work in the eventual time evolution. A plausible explanation is that when u is small, then u^3 is even smaller, so calculating the finite difference for $\left(u^3\right)_x$ is far more ill-posed than calculating it for u_x. We then use the previous discretization for u_x as in (4.4), leading to the discretization

$$3u^2u_x\sim 3\left(u_j^k\right)^2\ \frac{u_{j+1}^k-u_{j-1}^k}{2\Delta x}$$

These discretizations may be combined to calculate $\mathscr{F}_j^k$, with

$$\mathscr{F}_j^k \quad = \quad -\left[\frac{u_{j-1}^k-2u_j^k+u_{j+1}^k}{(\Delta x)^2}\right]-\left[\frac{u_{j-2}^k-4u_{j-1}^k+6u_j^k-4u_{j+1}^k+u_{j+2}^k}{(\Delta x)^4}\right]$$

$$+\left[3\left(u_j^k\right)^2\ \frac{u_{j+1}^k-u_{j-1}^k}{2\Delta x}\right]+\left[s\frac{u_{j+1}^k-u_{j-1}^k}{2\Delta x}\right].$$

This may then be substituted into (4.3) to obtain a system of equations. To emphasize that the u_j^{k+1} are unknown, we rewrite u_j^{k+1} as z_j. This leads to the equation

$$\begin{aligned}0 &= [-2\Delta t]z_{j-2}+\left[8\Delta t-2(\Delta x)^2\Delta t-s(\Delta x)^3\Delta t\right]z_{j-1}+\left[4\left(\Delta x^2\right)\Delta t-12\Delta t-4(\Delta x)^4\right]z_j\\ &+\left[8\Delta t-2(\Delta x)^2\Delta t+s(\Delta x)^3\Delta t\right]z_{j+1}+[-2\Delta t]z_{j+2}+\left[-3(\Delta x)^3\Delta t\right]z_{j-1}z_j^2+\left[3(\Delta x)^3\Delta t\right]z_{j+1}z_j^2\\ &+2(\Delta x)^4\Delta t\mathscr{F}_j^k+4(\Delta x)^4u_j^k\end{aligned}$$

We condense the right hand side into the compact notation $f_j(\vec{z})=0$. We have such a system of equations for each j, so we condense that entire system into the notation $\vec{f}(\vec{z})=0$. Note that due to the $\left(u^3\right)_x$ term this is a nonlinear system in z, so we use Newton's method to solve it. Recall that Newton's method is

$$J_{\vec{f}}\left(z_j^{(n)}\right)\left(z_j^{(n+1)}-z_j^{(n)}\right)=-\vec{f}\left(z_j^{(n)}\right)$$

where $J_{\vec{f}}$ is the Jacobian of $\vec{f}$ with respect to $\vec{z}$, and the (n) in the superscript indicates which iteration of Newton's method this is. As each f_j only depends on $z_{j-2},z_{j-1},z_j,z_{j+1},z_{j+2}$ then the Jacobian will be sparse with values centered around the diagonal. Schematically it will look like

$$J_{\vec{f}}=\begin{bmatrix}\ddots & \ddots & \ddots & \ddots & \ddots & 0 & 0\\ 0 & \frac{\partial f_j}{\partial z_{j-2}} & \frac{\partial f_j}{\partial z_{j-1}} & \frac{\partial f_j}{\partial z_j} & \frac{\partial f_j}{\partial z_{j+1}} & \frac{\partial f_j}{\partial z_{j+2}} & 0\\ 0 & 0 & \ddots & \ddots & \ddots & \ddots & \ddots\end{bmatrix}$$

In order these terms will be

$$\begin{aligned}\frac{\partial f_j}{\partial z_{j-2}} &= -2\Delta t\\ \frac{\partial f_j}{\partial z_{j-1}} &= 8\Delta t-2(\Delta x)^2\Delta t-s(\Delta x)^3\Delta t-3(\Delta x)^3\Delta t\,z_j^2\\ \frac{\partial f_j}{\partial z_j} &= -12\Delta t+4(\Delta x)^2\Delta t-4(\Delta x)^4-6(\Delta x)^3\Delta t\,z_j\left(z_{j+1}-z_{j-1}\right)\\ \frac{\partial f_j}{\partial z_{j+1}} &= 8\Delta t-2(\Delta x)^2\Delta t+s(\Delta x)^3\Delta t+3(\Delta x)^3\Delta t\,z_j^2\\ \frac{\partial f_j}{\partial z_{j+2}} &= -2\Delta t\end{aligned}$$

Note that we have a slight problem at the boundary as the first two and last two f_j depend on z_j that are not

included in the system. For example, f_1 and f_2 depend on z_{-1} and z_{-2}. Since we are only interested in perturbations of an equilibrium solution which reaches its asymptotic values exponentially quickly, we replace any extraneous z_j with said asymptotic values. For example, we would replace the erroneous references to z_{-1} and z_{-2} with the left asymptotic value.

The bulk of the actual numerical method lies in defining the Jacobian and computing the Newton's method to get the next time step. In this context Newton's method converges quite rapidly, so we only run it approximately 5 times for each time step. As the crux of Newton's method is solving a linear system, it is very important to encode the Jacobian as a sparse matrix to take advantage of Matlab's efficient calculation of sparse linear systems.

One useful implementation detail is to use a progress bar over the time steps: this may be implemented with Matlab's built in command `waitbar`. One can also use `tic` and `toc` to calculate the average amount of time to calculate a time step, and thus calculate the time remaining until completion.

The main output is a giant matrix of z-values whose entries are $\left(z_j^k\right)_{j,k}$. While using small time steps, and thus creating a large matrix, is necessary in computing the time evolution, once completed the time axis of the matrix may be truncated to save a significant amount of storage.

To create a visual output of the time evolution, one can use Matlab's built in command `print` to save the output of each time step as an image, and the program `ffmpeg` to combine all the images into a video file.

4.3 Computing the Essential Spectrum for Periodic PDE using Hill's Method

In this section we discuss using Hill's method to numerically calculate the spectrum of a linear differential operator with spatially periodic coefficients. There once existed a program SpectrUW [11] to perform these calculations, however it appears to be no longer available. Here we follow the SpectrUW documentation to implement this method into Matlab.

Firstly, we start with a differential operator L with spatially periodic (on $\left[-\frac{L}{2},\frac{L}{2}\right]$) coefficients $f_k(x)$:

$$L = \sum_{k=0}^{\ell} f_k(x)\,\partial_x^k\,.$$

As the coefficient functions are periodic, then one may use Fourier series to write them:

$$f_k(x) = \sum_{j=-\infty}^{\infty} \hat{f}_{k,j}\, e^{2\pi i\ jx/L}, \qquad k = 0,\dots,\ell \tag{4.5}$$

$$\text{where } \hat{f}_{k,j} = \frac{1}{L}\int_{-\frac{L}{2}}^{\frac{L}{2}} f_k(x)\, e^{-2\pi i\ jx/L}\,dx, \qquad k = 0,\dots\ell, \qquad j \in \mathbb{Z}\,.$$

From standard results in Floquet Theory [10, Section 2.4] the eigenfunctions ψ may be written as

$$\psi(x) = \sum_{j=-\infty}^{\infty} \hat{\psi}_j e^{ix(\xi+\pi j/L)}, \qquad \xi \in \left(-\frac{\pi}{2L}, \frac{\pi}{2L}\right). \tag{4.6}$$

These eigenfunctions satisfy $L\psi = \lambda\psi$, so substituting the eigenfunctions into the eigenvalue equation,

$$\left[\sum_{k=1}^{\ell}\left(\sum_{s=-\infty}^{\infty} \hat{f}_{k,s}\, e^{2\pi i\, sx/L}\right)\partial_x^k\right]\sum_{j=-\infty}^{\infty}\hat{\psi}_j e^{ix(\xi+\pi j/L)} = \lambda\sum_{j=-\infty}^{\infty}\hat{\psi}_j e^{ix(\xi+\pi j/L)}.$$

Calculating all of these derivatives, we then have

$$\sum_{k=1}^{\ell}\sum_{j=-\infty}^{\infty}\sum_{s=-\infty}^{\infty}\hat{\psi}_j\left(\hat{f}_{k,s}\, e^{2\pi i\, sx/L}\right)(i\xi+\pi ij/L)^k e^{ix(\xi+\pi j/L)} = \lambda\sum_{j=-\infty}^{\infty}\hat{\psi}_j e^{ix(\xi+\pi j/L)}.$$

This equation can be viewed as a linear operator acting on the basis $e^{ix(\xi+\pi j/L)}$ with $j\in\mathbb{Z}$: an infinite dimensional matrix. Note that the exponential coming from (4.5) is twice as large as the exponential coming from (4.6), so every other entry in this matrix will be zero. Explicitly, using $\hat{\cdot}$ to denote terms being written in the basis $e^{ix(\xi+\pi j/L)}$, we have $\hat{\psi} = (\ldots,\hat{\psi}_{-1},\hat{\psi}_0,\hat{\psi}_1,\ldots)$ and our eigenvalue equation is $\hat{L}\hat{\psi} = \lambda\hat{\psi}$. Then the entries of the bi-infinite matrix $\hat{L}$ are

$$\hat{L}_{n,m} = \begin{cases} 0 & \text{if } n-m \text{ is odd} \\ \sum_{k=0}^{\ell}\hat{f}_{k,\frac{n-m}{2}}\left(i\xi+i\frac{\pi m}{L}\right)^k & \text{if } n-m \text{ is even} \end{cases}$$

Up to this point everything has been exact. In order to compute this numerically, we truncate the basis $e^{ix(\xi+\pi j/L)}$ with $j\in\mathbb{Z}$ to basis $e^{ix(\xi+\pi j/L)}$ with $j=-N,\ldots,N$. This leads to the truncated equation $\hat{L}_N\hat{\psi}_N = \lambda\hat{\psi}_N$, where now $\hat{L}_N$ is a finite matrix. In particular, this is a standard matrix eigenvalue problem and Matlab's built-in function `eig` can be used to compute the eigenvalues.

The only remaining wrinkle is ξ: we discretize ξ and for each fixed ξ we find all the eigenvalues of $\hat{L}_N$, then at the end we combine them to find an approximation of the spectrum of L.

Implementing this in Matlab consists of three main steps, (1) computing the Fourier coefficients, (2) setting up the matrix $\hat{L}_N$ (and solving the eigenvalue problem with `eig`), and (3) a `for`-loop of the previous two steps over a discretization of ξ. To compute the Fourier coefficients we use Matlab's built-in function `trapz` to use the trapezoidal method to calculate the required integrals.

Chapter 5

Dynamics

In this chapter we discuss the dynamics — both analytical and numerical — of small perturbations to traveling waves of our equations. In particular this contains our main linear stability result for modified Kuramoto-Sivashinsky, Theorem 5.7.

Section 5.1 begins by discussing the result of the numerical time evolution from Section 4.2 for both the modified Kuramoto-Sivashinsky and St. Venant equations and uses this to motivate the idea of exponential weights. These exponential weights will be useful in stabilizing the essential spectrum (originally found in Section 3.3) which will be a necessary ingredient for the Gearhart-Pruss Theorem (Theorem 5.6).

In Section 5.2 we briefly discuss the semigroup formalism, with the goal of developing the Gearhart-Pruss Theorem.

In Section 5.3 we obtain our main linear stability result Theorem 5.7.

In Section 5.4 we discuss nonlinear stability, of which we unfortunately were unable to obtain. In Subsection 5.4.1 we prove a general nonlinear stability argument (that does not apply in our case), and in Subsection 5.4.2 we use this argument to highlight where the particular difficulties in proving nonlinear stability lie.

Finally in Section 5.5 we discuss another method of obtaining stability via ad-hoc periodic wave trains formed by concatenating copies of essentially unstable solutions related to the traveling waves q.

5.1 Time Evolution, Instability, and an Introduction to Exponential Weights

Recall that in Lemmas 3.17 and 3.18 we showed that the essential spectrum of the modified Kuramoto-Sivashinsky and St. Venant equations were unstable. Naively one would assume this leads to some dynamical instability, but of what kind?

Figure 5.1 shows the time evolution for the modified Kuramoto-Sivashinsky equation. We start with the front numerically generated in Section 4.1 that has been perturbed. Figure 5.1 (b) shows the result after a short amount of time: we remark that the perturbation appears to travel leftward through the transition of the front, is damped, then grows again upon leaving the transition. The perturbation also shifts the underlying front to the left a little, which is natural as the system is translation invariant; at best we would be able to show orbital stability, that the result converges

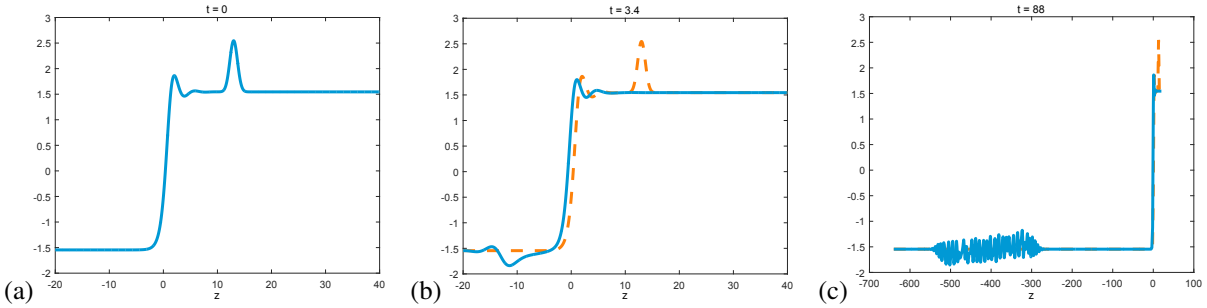

(a) (b) (c)

Figure 5.1: Time evolution of a perturbation to a solitary wave for the modified Kuramoto-Sivashinsky equation (2.2) with $\mu = 0$ and $s = -2.388$. In (a) we show the initial condition, in (b) we show the result after a small amount of time, and in (c) we change the scale to show the result after a long amount of time.

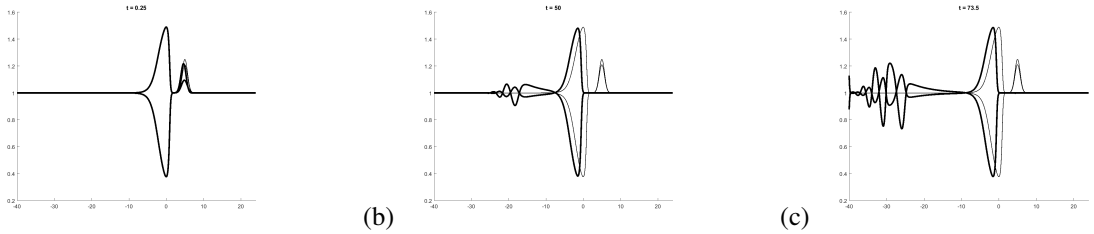

(a) (b) (c)

Figure 5.2: Time evolution of a perturbation to a solitary wave for the St. Venant equation with $c = 0.7849$, $q = 1 + c$, $F = 9$, and $\nu = 0.1$. In (a) we show the initial condition, in (b) we show the result after a small amount of time, and in (c) we show the result after a long amount of time.

asymptotically to a translate of the original front. Figure 5.1 (c) also shows that the amount the front is moved leftward is finite, and is roughly the amount shown in Figure 5.1 (b). Figure 5.1 (c) also shows that the perturbation doesn't ever damp and instead persists, convecting leftward: this is the instability we would expect given the unstable essential spectrum.

One important detail not shown in Figure 5.1 is that the instability that arises appears, from our numerical investigation, to be independent of the size of the initial perturbation. In particular, it seems one cannot control the $L^\infty(\mathbb{R})$-norm of the instability by making the initial perturbation arbitrarily small.

Figure 5.2 shows the time evolution for the St. Venant equation. We start with the pulse and perturbation shown in Figure 5.2 (a). Figure 5.2 (b) shows the result after the perturbation has traveled through the pulse: just like with the modified Kuramoto-Sivashinsky, the perturbation is damped and translates the pulse. In Figure 5.2 (c) we see that the perturbation grows to some size independent of the initial perturbation. In summary, most of the qualitative behavior of the modified Kuramoto-Sivashinsky equation time evolutions are also repeated for the St. Venant equation.

There is one large difference between the two time evolutions presented above though. In Figure 5.3 we show the St. Venant time evolution after a very large amount of time. Most concerning, the perturbation seems to leave copies of the original pulse in its wake, with these copies persisting in time. The modified Kuramoto-Sivashinsky time evolutions do not show this behavior, no matter how long they're run for — the perturbation continues to convects

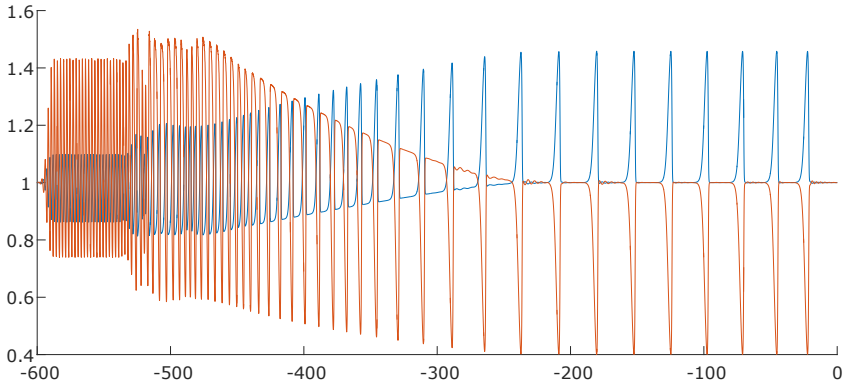

Figure 5.3: Time evolution of the St. Venant equation after a very long time. The variable u is plotted in blue and τ in orange. The perturbation has grown wider and appears to leave copies of the initial pulse in its wake.

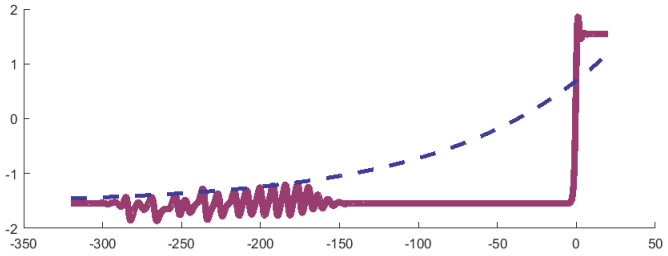

Figure 5.4: A sample perturbation with an exponential function overlaid on it.

leftward while widening. Thus while the modified Kuramoto-Sivashinsky and St. Venant equations have similar behavior near the initial traveling wave, once again the St. Venant equation has unexpected complications.

To summarize, both equations have leftward traveling perturbations that do not decay in time. If we cannot obtain stability in the original $L^2(\mathbb{R})$-space, then how can we obtain stability? Figure 5.4 gives one possible answer: multiply both perturbations by a function that decays as one moves to the left, so as the perturbation travels leftward it damps itself. One of the most robust ways of doing this are the so called exponentially weighted spaces, which use the following L^2-based norm, for $a > 0$,

$$\|f\|_{L^2_a(\mathbb{R})} = \|e^{ax} f\|_{L^2(\mathbb{R})}$$

and we define $L^2_a(\mathbb{R})$ to be the set of functions with finite $L^2_a(\mathbb{R})$-norm. One useful technical trick is to define the weighted perturbation

$$w = e^{ax} v, \qquad w \in L^2(\mathbb{R}), \qquad v \in L^2_a(\mathbb{R}).$$

where the weighted perturbation w can then be studied in the usual space $L^2(\mathbb{R})$. The usual perturbation equations

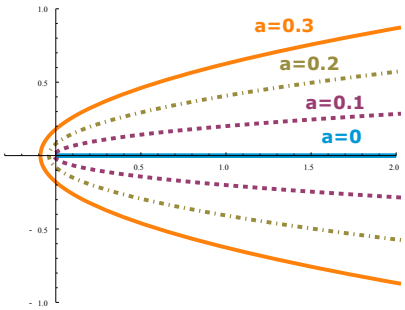

Figure 5.5: The essential spectrum of the weighted Laplacian L_a for different values of a.

(1.9) $v_t = Lv + \mathcal{N}(v)$ can be rephrased in terms of w,

$$w_t = L_a + e^{ax}\mathcal{N}(v), \tag{5.1}$$

where L_a is the conjugated linear operator

$$L_a = e^{ax} L e^{-ax}. \tag{5.2}$$

Also note that the nonlinearity is still a function of both the original unweighted perturbation v and the weighted perturbation w: eg. with $\mathcal{N}(v) = v^2$, then the weighted nonlinearity is wv. This will cause problems later — which we discuss in Subsection 5.4.2 — as one will still need control over the unweighted perturbation v.

Conjugating the linear operator L in this way has the effect of changing its coefficients in the straightforward manner. That is, the product rule tells us that $\partial_x (e^{-ax} v) = (\partial_x - a) v$, hence transforming from L to L_a can be accomplished by replacing each ∂_x with $\partial_x - a$. As we show now, this has the further effect of changing its essential spectrum.

Example 5.1. Spectrum of the Exponentially Weighted Laplacian

Recall that in Example 3.11 we showed that the essential spectrum of the Laplacian $L = -\partial_x^2$ has an essential spectrum of $[0, \infty)$.

We can now calculate that the exponentially weighted Laplacian is

$$L_a = -(\partial_x - a)^2 : H^2(\mathbb{R}) \subset L^2(\mathbb{R}) \to L^2(\mathbb{R})$$

whose essential spectrum is given by the graph of the polynomial

$$p(i\xi) = -(i\xi - a)^2 = \xi^2 + 2ia\xi - a^2, \qquad \xi \in \mathbb{R}.$$

The way in which the exponential weight a changes the essential spectrum of L_a is shown in Figure 5.5. In particular, the essential spectrum moves to the left as the point on this graph with smallest real part is $\lambda = -a^2$.

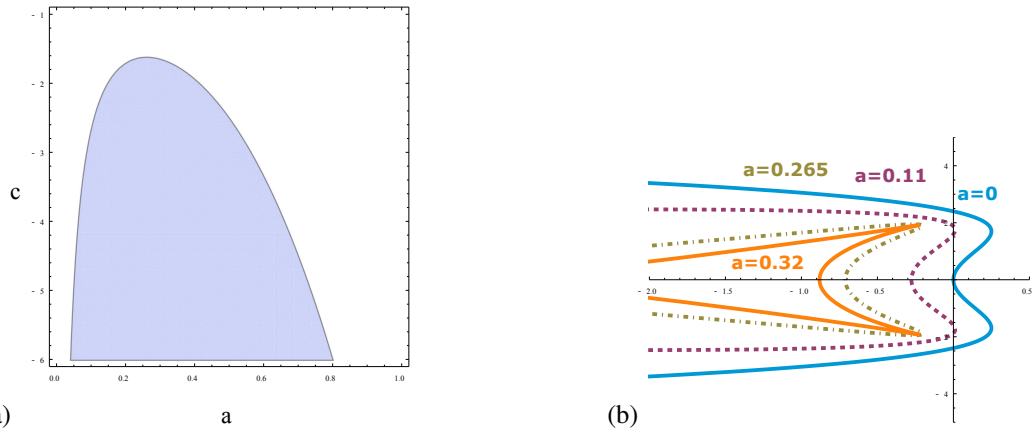

(a) (b)

Figure 5.6: (a) The set of exponential weights a and speeds c for which the essential spectrum is stabilized. (b) The essential spectrum when $s = -1.2$ for different values of a.

This leads to the hope that by changing the exponential weight a, then somehow the essential spectrum will stabilize (by moving entirely into the left half-plane). We will see that for both systems there exist parameter values where the essential spectrum will stabilize.

The weighted linear operator L_a about the traveling wave q — as in (5.2) — for the modified Kuramoto-Sivashinsky equation (2.2) is

$$L_a u = -\partial_x^4 u + 4a\partial_x^3 - \left(6a^2+1\right)\partial_x^2 u + \left(2a+4a^3+3\bar{q}^2+s\right)\partial_x u + \left(6\bar{q}\bar{q}' - a^2 - a^4 - 3a\bar{q}^2 - as\right)u \tag{5.3}$$

Theorem 5.2. Stabilization of the modified Kuramoto-Sivashinsky Essential Spectrum through Exponential Weights

The essential spectrum for the exponentially weighted operator L_a (5.3), for the modified Kuramoto-Sivashinsky equation (2.2), is entirely in the left half-plane provided

$$2s < \frac{-32a^4 - 8a^2 - 1}{4a}.$$

The values of a and s that satisfy this inequality are shown in Figure 5.6 (a).

Proof. The essential spectrum of L_a is given by the graph of the polynomial

$$p(i\xi - a) = -2s(i\xi - a) - (i\xi - a)^4 - (i\xi - a)^2, \qquad \xi \in \mathbb{R}.$$

Our next goal is to find where the real part of the essential spectrum is maximized. The real part of this is

$$\text{Re } p(i\xi - a) = -a^4 + a^2\left(6\xi^2 - 1\right) + 2as - \xi^4 + \xi^2.$$

Through elementary calculus we find that this is maximized when $\xi = \sqrt{\frac{6a^2+1}{2}}$, with a value of

$$\text{Re } p\left(i\sqrt{\frac{6a^2+1}{2}}\right) = -a^4 + \left(3\left(6a^2+1\right)-1\right)a^2 - \frac{1}{4}\left(6a^2+1\right)^2 + \frac{1}{2}\left(6a^2+1\right) + 2as\,.$$

Requiring this to be negative gives the inequality. □

Figure 5.6 (b) shows how the essential spectrum changes as a increases. The value of $a = 0.32$ shown appears to be the exponential weight that moves the essential spectrum the furthest to the left. An interesting effect happens when a is increased past this value, that the essential spectrum moves back to the right. Furthermore, it seems that the essential spectrum becomes unstable at a value of a that matches the exponential decay rates of q. This is also a pragmatic upper limit for the value of a as we need $e^{ax}q'$ to be an eigenfunction of L_a for our result in Theorem 5.7 on the linear dynamics.

The weighted linear operator L_a about the traveling wave $(\bar{\tau}, \bar{u})^T$ — as in (5.2) — for the St. Venant equation (2.5) is

$$L_a\begin{pmatrix}\tau\\ u\end{pmatrix} = \begin{array}{l} c\tau_x - a\tau + u_x - au \\ cu_x - au + (\alpha\tau)_x - a\alpha\tau + \nu\left(\frac{u_x}{\bar{\tau}^2}\right) - \nu a\frac{u_x}{\bar{\tau}^2} - \bar{u}^2\tau - 2\bar{u}\bar{\tau}u \end{array} \tag{5.4}$$

where $\alpha = \bar{\tau}^{-3}\left(F^{-1} + 2c\nu\bar{\tau}_x\right)$.

Showing Theorem 5.2 for modified Kuramoto-Sivashinsky is essentially a calculus problem. However for St. Venant the dispersion relation (3.9) used to find the essential spectrum has complex coefficients, so producing a similar inequality would be difficult. One possibility would be to use the following theorem regarding when roots of a complex coefficient polynomial have positive real part, which can be thought of as a souped up version of Descartes' rule of signs.

Theorem 5.3. Number of Roots of a Complex Polynomial with Positive Real Part

[36, Theorem 11.3.3] Let f be a monic polynomial with possible complex coefficients of degree n, and let $F(z) = -f(iz)$. For $x \in \mathbb{R}$, write

$$\begin{aligned} Re\ F(x) &= x^n + a_1x^{n-1} + \cdots + a_n \\ Im\ F(x) &= 0 + b_1x^{n-1} + \cdots + b_n \end{aligned}$$

and let $\Delta_{2\ell}$ be the Hurwitz determinant

$$\Delta_{2\ell} = \det \begin{pmatrix} a_0 & a_1 & a_2 & \cdots & a_{2\ell-1} \\ b_0 & b_1 & b_2 & \cdots & b_{2\ell-1} \\ 0 & a_0 & a_1 & \cdots & a_{2\ell-2} \\ 0 & b_0 & b_1 & \cdots & b_{2\ell-2} \\ \vdots & \vdots & \vdots & & \vdots \\ 0 & 0 & 0 & \cdots & a_\ell \\ 0 & 0 & 0 & \cdots & b_\ell \end{pmatrix}.$$

Let m be the largest integer in $\{1,\dots,n\}$ such that $\Delta_{2m} \neq 0$. If f has no real zero, then the number p of zeroes of f in the right half-plane is given by

$$p = \frac{n-m}{2} + V^*(1, \Delta_2, \dots, \Delta_{2m})$$

where if $c_0,\dots,c_n$ is a sequence of real numbers such that $c_0 c_n \neq 0$, defining the quantities c_ν^* for $\nu = 0,\dots,n$ to be

$$c_\nu^* = \begin{cases} a_\nu & \text{if } a_\nu \neq 0 \\ (-1)^{j(j-1)/2} & \text{if } a_\nu = \cdots = a_{\nu-j+1} = 0,\ a_{\nu-j} \neq 0,\ j \in \mathbb{N} \end{cases}$$

then V^* is the number of variations of sign in the sequence of non-vanishing numbers $c_0^*,\dots,c_n^*$.

The vastly more cumbersome form of this theorem does not lend itself to a simple inequality as seen in Theorem 5.2. In Figure 5.7 we show how the essential spectrum changes for two parameter values of St. Venant. In (a) the essential spectrum cannot be stabilized as it moves to the right as a increases, and in (b) the essential spectrum is easily stabilized by increasing a. The above theorem, along with continuous dependence of the PDE on the parameters and a, may be used to conclude that for some open set around the parameter values in (b) the essential spectrum may be stabilized for some value of a.

5.2 The Gearhart-Pruss Theorem

In Section 5.1 we found that exponential weights can stabilize the essential spectrum. Couple this with Section 3.5 where we find there are no unstable eigenvalues other than $\lambda = 0$, and we should expect some sort of stability result in the vein of Theorem 1.2.

Recall that Theorem 1.2 largely rested on the behavior of the linear operator $\mathscr{F}'(x_0)$ in (1.3). In this particular

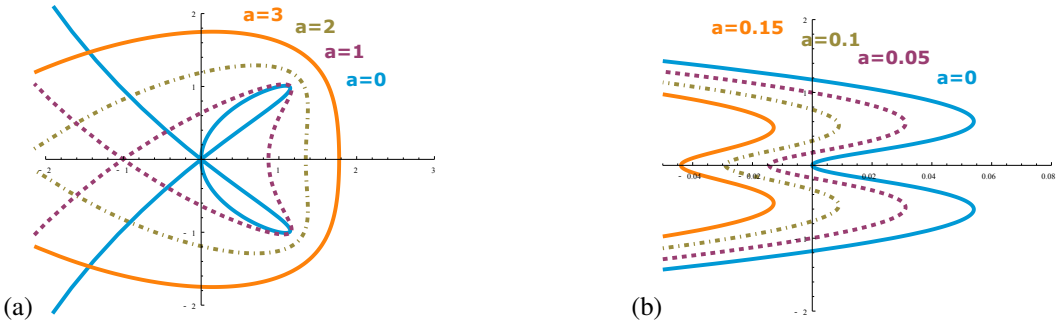

(a) (b)

Figure 5.7: How the most unstable boundary of the essential spectrum for the St. Venant equations changes as a changes using (a) the [5] Figure 1 parameter values ($r=2$, $s=4$, $u_0=0.96$, $\bar{u}=u_0+c/u_0^2-c\bar{\tau}$, $\nu=0.1$, $F=6$, $c=0.57052639$), which cannot be stabilized for any value of a, and (b) the [5] Figure 7 parameter values ($c\approx 0.7849$, $\bar{u}=1+c-c\bar{\tau}$, $F=9$, $\nu=0.1$), which is easily stabilized.

case $\mathscr{F}'(x_0)$ is a $d\times d$ matrix A. The solution to the linear equation $v_t=Av$ is given by the matrix exponential

$$e^{At}=\sum_{j=0}^{\infty}\frac{(At)^j}{j!}, \tag{5.5}$$

where if $v(0)$ is the initial condition, then $v(t)=e^{At}v(0)$ is the solution. One can think of the operator e^{At} as "advancing t units of time," which is a powerful interpretation of the solution that dovetails nicely with the idea of a flow. Matching this view one has the property that $e^{A(t+s)}v(0)=e^{At}e^{As}v(0)$.

To characterize the behavior of the linear solution, first suppose that the matrix A is a diagonalizable: i.e. there exist unitary matrices Q_1,Q_2 and a diagonal matrix D of eigenvalues so that

$$A=Q_1\begin{pmatrix}\lambda_1 & & & \\ & \lambda_2 & & \\ & & \ddots & \\ & & & \lambda_d\end{pmatrix}Q_2\,.$$

Using (5.5) one can calculate the matrix exponential as

$$e^{At}=Q_1\begin{pmatrix}e^{\lambda_1 t} & & & \\ & e^{\lambda_2 t} & & \\ & & \ddots & \\ & & & e^{\lambda_d t}\end{pmatrix}Q_2\,,$$

hence the entries of e^{At} are linear combinations of the $e^{\lambda_i t}$ and the behavior of e^{At} is given by the eigenvalues of A. This gives rise to the condition in Theorem 1.2, as specifically in this case if all the eigenvalues of A have negative real

part then $e^{At}v(0)$ will always decay to zero. In the general case one may use the Jordan normal form to show that all the entries of e^{At} are linear combinations of $t^j e^{\lambda_i t}$, and so the same result holds. Thus the matrix exponential offers a clean and tidy solution to the linear evolution.

In the same way that one can view (1.9) as the PDE analogue of (1.3), one can then wonder if there is a PDE analogue of the matrix exponential. The answer lies in the theory of semigroups.

Definition 5.4. Strongly Continuous or $\mathscr{C}_0$-Semigroup

[18, p. 10] A map $S(\cdot) : \mathbb{R}_+ \to \mathscr{B}(X)$ on a complex Banach space X, where $\mathscr{B}(X)$ are all the bounded linear operators on X, is called a strongly continuous operator semigroup or just $\mathscr{C}_0$-semigroup if the following conditions are fulfilled:

1. $S(0) = I$ and we have $S(t+s) = S(t)S(s)$ for all $t, s \geq 0$
2. For each $x \in X$ the orbit, defined as the map

$$S(\cdot)x : \mathbb{R}_+ \to X,\ t \mapsto e^{Lt}x$$

is continuous

The generator L of $S(t)$ is given by setting

$$\mathscr{D}(L) = \left\{ x \in X \;\middle|\; \text{the limit } \lim_{t \to 0^+} \frac{S(t)x - x}{t} \text{ exists in } X \right\}$$

and defining

$$Lx = \lim_{t \to 0^+} \frac{S(t)x - x}{t}$$

for $x \in \mathscr{D}(L)$. We also say that L generates $S(t)$.

Because semigroups are the generalization of the matrix exponential (5.5), typically one writes e^{Lt} for the semigroup instead of $S(t)$. The following theorem guarantees that all of the differential operators we consider generate $\mathscr{C}^0$-semigroups.

Theorem 5.5. *[24, Lemma 4.1.2, p. 80] Let L be an exponentially asymptotic ℓ-th order differential operator with $H^r(\mathbb{R})$ coefficients, for $1 \leq r < \infty$. If L is well-posed in the sense that there exists $\omega > 0$ such that the operator $L - \lambda$ acting on $H^\ell(\mathbb{R}) \subset L^2(\mathbb{R}) \to L^2(\mathbb{R})$ has a Fredholm index of 0 for Re $\lambda \geq \omega$, then L generates a $\mathscr{C}^0$-semigroup on $H^k(\mathbb{R})$ for all $k \leq r$.*

In particular the weighted operators L_a (5.2) generate $\mathscr{C}^0$-semigroups.

We now state the main result that shows the semigroup has exponential decay under appropriate conditions. Contrast this result, where the resolvent just needs to be uniformly bounded, with Hille-Yoshida or Lumer-Philips theorems where the resolvent needs to have some decay in λ.

Theorem 5.6. Gearhart-Pruss

[24, Theorem 4.1.5, p. 83] Let X be a Hilbert space and assume that $L : \mathscr{D}(L) \subset X \to X$ generates a $\mathscr{C}^0$-semigroup. Let P be a finite codimension spectral projection associated with L. If for some $M, \omega > 0$ the resolvent satisfies

$$\|R(\lambda, L)P\| \leq M$$

for all Re $\lambda \geq -\omega$, then there exists a $C > 0$ such that the semigroup associated with PL satisfies the decay estimate

$$\left\|e^{Lt}Pf\right\|_X \leq Ce^{-\omega t}\|f\|_X .$$

We now show that the resolvent, after projecting off $\lambda = 0$, for the modified Kuramoto-Sivashinsky equation (2.2) is bounded. Recall that in proving Lemma 3.20 the penultimate step was to add the bounds for Re λ and $|\text{Im } \lambda|$ together to get the bound

$$(\text{Re } \lambda + |\text{Im } \lambda|)\|u\|^2_{L^2(\mathbb{R})} \leq \tilde{C}\|u\|^2_{L^2(\mathbb{R})}$$

This was obtained by starting with the eigenvalue problem $L_a u = \lambda u$. If instead one starts from the equation $\lambda u = L_a u + f$, then $u = (\lambda - L_a)^{-1} f$ and we can use this to obtain a resolvent bound. The first step was to consider the inner product with u to form $\langle \lambda u, u\rangle$, so the only new term is $\langle f, u\rangle$. Using Cauchy-Schwartz and Young's inequality,

$$(\text{Re } \lambda + |\text{Im } \lambda|)\|u\|^2_{L^2(\mathbb{R})} \leq C'\|u\|^2_{L^2(\mathbb{R})} + \|f\|^2_{L^2(\mathbb{R})}$$

Then after re-arranging,

$$\|u\|^2_{L^2(\mathbb{R})} \leq \frac{1}{\text{Re } \lambda + |\text{Im } \lambda| - C'}\|f\|^2_{L^2(\mathbb{R})}$$

This more or less establishes the resolvent bound we need. Note that technically we need a bound for $\|u\|_{H^2(\mathbb{R})}$, not $\|u\|_{L^2(\mathbb{R})}$. We can repeat the process starting from the equations $\lambda u_x = L_a u_x + f_x$ and $\lambda u_{xx} = L_a u_{xx} + f_{xx}$ to obtain the following bounds,

$$(\text{Re } \lambda + |\text{Im } \lambda|)\|u_x\|^2_{L^2(\mathbb{R})} \lesssim \|u\|^2_{L^2(\mathbb{R})} + \|u_x\|^2_{L^2(\mathbb{R})} + \|f_x\|^2_{L^2(\mathbb{R})}$$

$$(\text{Re } \lambda + |\text{Im } \lambda|)\|u_{xx}\|^2_{L^2(\mathbb{R})} \lesssim \|u_{xx}\|^2_{L^2(\mathbb{R})} + \|u_x\|^2_{L^2(\mathbb{R})} + \|u\|^2_{L^2(\mathbb{R})} + \|f_{xx}\|^2_{L^2(\mathbb{R})}$$

Also note that in the above there are terms like u_{xxxx}, for which $u \in H^2(\mathbb{R})$ is technically not defined. So we prove

the bounds for $u \in \mathscr{C}_0^\infty$, then extend the final bounds to $u \in H^2(\mathbb{R})$ by density. Finally once everything is combined, we have the bound

$$\|u\|_{H^2(\mathbb{R})}^2 \leq \frac{1}{\text{Re } \lambda + |\text{Im } \lambda| - C'} \|f\|_{H^2(\mathbb{R})}^2 .$$

From this bound we see that for $|\lambda|$ sufficiently large (such as $|\lambda| > \beta$) the resolvent is bounded. Combining the results of Theorem 5.2 and Section 3.5, and projecting away the eigenvalue $\lambda = 0$ with a projection P (discussed in the next section, 5.3), gives us a spectral gap: there exists some $\omega > 0$ so that for all Re $\lambda \geq -\omega$, the resolvent $PR(\lambda, L)$ is defined. As the resolvent is analytic, then we may obtain a uniform bound for $|\lambda|$ sufficiently small (such as $|\lambda| < \beta$) and Re $\lambda \geq -\omega$, and we may apply Gearhart-Pruss.

Recall that the eigenvalue bound Lemma 3.23 for St. Venant fundamentally works the same as Lemma 3.20, and hence we may repeat the same calculations to apply Gearhart-Pruss to St. Venant as well.

5.3 Linear Dynamics

In this section we leverage the Gearhart-Pruss theorem (Theorem 5.6) to obtain the following stability result for the linear initial value problem

$$\begin{cases} w_t = L_a w \\ w(0) = w_0 . \end{cases} \tag{5.6}$$

Theorem 5.7. Asymptotic Linear Orbital Stability for the modified Kuramoto-Sivashinsky Equation

Let q be a traveling front solution of (2.2) and suppose that there exists an $a > 0$ such that the following hold:

1. *$\lambda = 0$ is a simple eigenvalue of L_a acting on $L^2(\mathbb{R})$ with eigenfunction $e^{ax}q'$,*
2. *there exists a $\omega > 0$ such that*

$$\sigma(L_a) \setminus \{0\} \subset \{\lambda \in \mathbb{C} \mid Re\ \lambda < -\omega\} .$$

Then given any $w_0 \in H^2(\mathbb{R})$ there exists a constant $\gamma_\infty \in \mathbb{R}$ and a solution $w(x,t)$ of (5.6) that is global in time and satisfies

$$\left\| w(\cdot,t) - \gamma_\infty e^{a\cdot} q' \right\|_{H^2(\mathbb{R})} \lesssim e^{-\omega t} \|w_0\|_{H^2(\mathbb{R})} \tag{5.7}$$

for all $t > 0$.

We remark that the numerical Evan's function calculations in Section 3.5 suggest that these hypotheses on the spectrum are satisfied.

As Gearhart-Pruss requires a spectral gap, the first order of business is to construct a spectral projection to remove the $\lambda = 0$ eigenvalue. While one can generically create a spectral projection with a contour integral using the resolvent,

in this case we can "explicitly" write the projection. Through the Fredholm alternative we know the dimension of $\ker L_a^*$ is 1: i.e. it is the span of some function ψ^a. As $e^{ax}q' \in \ker L_a$ and $\lambda = 0$ is a simple eigenvalue, then there are no generalized eigenvalues and $e^{ax}q' \notin \text{Range}\,(L_a)$, which by the Fredholm alternative tells us that $e^{ax}q' \notin \ker(L_a^*)^\perp$ as well, and so $\langle \psi^a, e^{ax}q' \rangle \neq 0$ (where $\langle \cdot, \cdot \rangle$ denotes the $L^2(\mathbb{R})$-inner product). Then we may write the spectral projection explicitly as

$$Pf = \frac{\langle \psi^a, f \rangle}{\langle \psi^a, e^{ax}q' \rangle} e^{ax}q', \qquad P : L^2(\mathbb{R}) \to L^2(\mathbb{R}) .$$

Given a solution w of (5.6), we can decompose it as

$$w(x,t) = Pw(x,t) + (I-P)\,w(x,t) .$$

Note that $L_aPf = 0$, so $e^{L_at}Pf = Pf$. Then defining

$$\gamma_\infty = \frac{\langle \psi^a, w(x,0) \rangle}{\langle \psi^a, e^{ax}q' \rangle}$$

and using that $w(x,t) = e^{L_at}w(x,0)$,

$$w(x,t) = \gamma_\infty q' + e^{Lt}(I-P)\,w(0) .$$

We can re-arrange this equation to solve for $e^{L_at}(I-P)\,w(0)$ and apply Gearhart-Pruss to obtain (5.7). We can also interpret this stability result in the context of the original solution u of (2.2). Note that (5.7) can also be written as

$$\left\| v(\cdot,t) - \gamma_\infty q' \right\|_{H_a^2(\mathbb{R})} \lesssim e^{-\omega t} \left\| v_0 \right\|_{H_a^2(\mathbb{R})}$$

where $H_a^2(\mathbb{R})$ is an exponentially weighted $H^2(\mathbb{R})$. This means that the perturbation converges to $\gamma_\infty q'$ in $H_a^2(\mathbb{R})$. Returning to the original equation $u(x,t) = q(x) + v(x)$, then we see that

$$u(x,t) \quad \to \quad q(x) + \gamma_\infty q'(x) \text{ in } H_a^2(\mathbb{R}) \text{ as } t \to \infty \tag{5.8}$$

$$\approx \quad q(x+\gamma_\infty) \tag{5.9}$$

where the latter approximation follows from Taylor's theorem. This justifies the use of the term "orbital stability" in Theorem 5.7. This would also be our expected behavior for any nonlinear argument.

Also note that under a similar hypothesis Gearhart-Pruss also applies to St. Venant, so we may propose a similar linear asymptotic orbital stability result for St. Venant.

5.4 Nonlinear Dynamics

5.4.1 Basic Nonlinear Stability Argument

In this subsection we work through Theorem 4.3.5 of [24] which gives a basic nonlinear stability argument. Unfortunately this stability argument will not work for our equations: the difficulty lies in the polynomial inequalities following (5.18), as we would need control over the unweighted perturbation v — which Section 5.1 shows isn't easily controlled — as well as the weighted perturbation w. Still, this basic argument will serve as a starting point for Subsection 5.4.2 where we discuss in detail the difficulties in proving nonlinear stability.

Theorem 5.8. Basic Nonlinear Stability Argument

[24, Theorem 4.3.5, p. 93] Consider the nonlinear problem

$$\partial_t u = \mathscr{F}(u)$$

where $\mathscr{F} : H^m(\mathbb{R}) \subset L^2(\mathbb{R}) \to L^2(\mathbb{R})$ has an N-fold symmetry T. Suppose that $\mathscr{F}(q) = 0$ and that the linearization $L = \nabla_u \mathscr{F}(q)$ and the nonlinearity $N(v) = \mathscr{F}(q+v) - Lv$ satisfy the following hypotheses,

1. *The operator L has a spectral gap; that is, there exists an $\omega > 0$ such that*

$$\sigma(L) \cap \{\lambda \in \mathbb{C} \mid Re\ \lambda \geq -\omega\} = \{0\}$$

2. *The eigenfunctions of $\lambda = 0$ (i.e., the kernel of L) consists of N simple eigenfunctions, each one associated with one of the N-fold symmetries T. (See (5.10) and the surrounding discussion for more details.)*

3. *The resolvent is bounded; specifically, if P is the spectral projection to the eigenspaces of 0, then the resolvent of the complementary projection is bounded: i.e. there exists $M, \omega > 0$ so that for all Re $\lambda > -\sigma$,*

$$\left\| R(\lambda; L) P^C \right\| \leq M$$

4. *The linearization is well behaved; specifically the gradient $\nabla_u \mathscr{F}$ is locally Lipschitz on bounded sets, i.e. for each $R > 0$ with $\|u\|_{H^m(\mathbb{R})} \leq R$, $\|v\|_{H^m(\mathbb{R})} \leq R$, then*

$$\|(\nabla_u \mathscr{F}(u) - \nabla_u \mathscr{F}(v)) w\|_{H^m(\mathbb{R})} \leq M \|u - v\|_{H^m(\mathbb{R})} \|w\|_{H^m(\mathbb{R})}$$

5. The nonlinearity is locally quadratic; i.e. there exist $R > 0$, $C > 0$ so that for all $\|v\|_Y \leq R$ we have

$$\|\mathscr{N}(v)\|_{H^m(\mathbb{R})} \leq C\|v\|^2_{H^m(\mathbb{R})}$$

Then for any $\tilde{\omega} \in (0,\omega)$ the manifold $\mathscr{M}_T$ of equilibria is asymptotically orbitally stable in $\|\cdot\|_{H^m(\mathbb{R})}$ with exponential rate $\tilde{\omega}$.

But first we'll say a little about the "manifold $\mathscr{M}_T$ of equilibria" and "asymptotically orbitally stable." For stability we would naively expect the perturbed solution to return to the original solitary wave q: Lyapunov stability from Definition 1.1. However, as Theorem 5.7 shows, at least at the linear level for the modified Kuramoto-Sivashinsky equation the perturbed wave settles down to a translate of the original wave. Both of the equations (2.2) and (2.5) are invariant to spatial translations in that if $u(x,t)$ is a solution, then $u(x+\gamma,t)$ will also be a solution. We need to account for this invariance in our notion of stability. In this case we would define $\mathscr{M}_T$ to be all translates of the traveling wave q. In general the N-fold symmetries (Definition 5.11) will determine the manifold $\mathscr{M}_T$ of equilibria. Orbital stability is defined to be Lyapunov stability to some particular element of $\mathscr{M}_T$.

Example 5.9. Translation Symmetry

We define the translation operator T by

$$T(\gamma)q(x) = q(x+\gamma).$$

Then we can see we have the properties that $T(0) = I$, $T(\gamma)T(\delta)q = T(\gamma+\delta)q$, and $T(-\gamma)T(\gamma)q = q$.

Further, we can define the generator T', or "linear approximation," through the limit, considered in $H^m(\mathbb{R})$,

$$T' = \lim_{\gamma\to 0}\frac{T(\gamma)-T(0)}{\gamma} = \partial_x.$$

Taylor's theorem gives us the estimate

$$\left\|T(\gamma)u - u - \gamma T'u\right\|_{H^m(\mathbb{R})} \leq M|\gamma|^2.$$

Another relatively common symmetry is rotational symmetry. Typically it occurs in complex systems, where rotation can be manifested as multiplying by "$e^{i\theta}$."

Example 5.10. Rotational Symmetry

We define rotational symmetry as

$$T(\theta)\phi = e^{i\theta}q.$$

Again we have the properties that $T(0) = I$, $T(\theta)T(\varphi)q = T(\theta+\varphi)q$, and $T(-\theta)T(\theta)q = q$.

Further, we can define the generator T', or "linear approximation," through the limit, considered in $H^m(\mathbb{R})$,

$$T' = \lim_{\theta\to 0} \frac{T(\theta) - T(0)}{\gamma} = \partial_\theta \left(e^{i\theta}\right)|_{\theta=0} = i.$$

Then the estimate

$$\|T(\theta)u - u - i\theta u\| \leq M|\gamma|^2$$

again arises through Taylor's theorem, though this time by expanding $e^{i\theta}$ into a Taylor series.

Motivated by these specific properties of the above symmetries, we define the generalized notion of a symmetry.

Definition 5.11. *N*-**Parameter Symmetry Operator**

[24, p. 86] We say that a given evolution PDE $u_t = \mathscr{F}(u)$ has an N-parameter symmetry operator if there exist N independent and commuting linear operators $T_j \in \mathscr{C}^1(\mathbb{R}, \mathscr{B}(Y))$ that satisfy

1. $T_j(0) = I$,
2. Preserves the addition structure of $\mathbb{R}$;
   $T_j(s+t) = T_j(s)T_j(t) = T_j(t)T_j(s)$,
3. Commute with one another,
   $T_i(\gamma)T_j(\theta) = T_j(\theta)T_i(\gamma)$,
4. The PDE is invariant under this symmetry,
   $T_j(\gamma)\mathscr{F}(u) = \mathscr{F}(T_j(\gamma)u)$.

We also assume that each symmetry is an isometry, i.e. $\left\|T_j(\gamma)u\right\|_{H^m(\mathbb{R})} = \|u\|_{H^m(\mathbb{R})}$ for all γ, and that the generator is defined by the limit, considered in $H^m(\mathbb{R})$,

$$T_j' = \lim_{\gamma\to 0} \frac{T_j(\gamma) - T_j(0)}{\gamma}$$

exists and is a bounded operator from $H^m(\mathbb{R})$ to $L^2(\mathbb{R})$. Finally, we also require the generator to be a linear estimation in the sense that for u sufficiently small,

$$\left\|T_j(\gamma)u - u - \gamma T_j'u\right\|_{H^m(\mathbb{R})} \leq M|\gamma|^2.$$

Finally we combine the individual T_j together into the full symmetry operator

$$T(\vec{\gamma}) = T_1(\gamma_1) T_2(\gamma_2) \dots T_N(\gamma_N) .$$

One important observation is that $T_j' q$ are always in the kernel of L; as $\mathscr{F}(T_j(\gamma) q) = 0$ for all γ, then $\partial_\gamma \mathscr{F}(T_j(\gamma) q) = 0$. Interchanging the derivative, we also have

$$\mathscr{F}\left(\partial_\gamma T_j(\gamma) q\right) = \mathscr{F}\left(T_j' q\right) = 0 . \tag{5.10}$$

Then an alternative statement of hypothesis 2) of Theorem 5.8 is that *only* these $T_j' q$ are in the kernel.

Lemma 5.12. *Under the hypotheses of Theorem 5.8, given the adjoint eigenfunctions ψ_i^a we have that* $\ker(L^a) = span\{\psi_1^a, \dots, \psi_N^a\}$ *with the property that*

$$\left\langle T_i' q, \psi_j^a \right\rangle = \delta_{ij} . \tag{5.11}$$

Proof. As $\lambda = 0$ is an eigenvalue, then L is a Fredholm operator with Fredholm index 0. Recall from the Fredholm alternative (Theorem 3.4) combined with the definition of the Fredholm Index (Definition 3.1) we have that, for L^* the adjoint of L,

$$\dim(\ker L) = \dim(\ker L^*)$$

so this combined with hypothesis 2) of Theorem 5.8 establishes that $\ker L^*$ should be N dimensional. Recall that we also had the property that

$$\mathscr{R}(L) = [\ker L^a]^\perp .$$

For (5.11) to be true, then it is sufficient that each $T_i' q$ isn't perpendicular to $\ker L^*$. However, we identified $[\ker L^*]^\perp$ as $\mathscr{R}(T)$. If $Lf = T_i' q$, then $L^2 f = 0$ and we have a generalized eigenspace for $T_i' q$ of dimension 2. This cannot happen as by hypothesis 2) of Theorem 5.8 each $T_i' q$ is a simple eigenfunction. □

To explain the purpose of this construction, first note that given the basis $\left\{T_1' q, \dots, T_N' q\right\}$ for the eigenspace of $\lambda = 0$, the spectral projection P can in general be written as

$$Pf = \sum_{j=1}^{N} \sum_{i=1}^{N} \frac{\langle \psi_i^a, f \rangle}{\left\langle \psi_i^a, T_j' q \right\rangle} T_j' q .$$

(This can be confirmed by noting that the complementary projection, $I - P$, is orthogonal to all ψ_i^a, and so it takes

elements to $(\ker L^a)^\perp$.) This construction allows us to eliminate an index of summation and write the projection as

$$Pf = \sum_{j=1}^{N} \frac{\left\langle \psi_j^a, f \right\rangle}{\left\langle \psi_j^a, T_j' q \right\rangle} T_j' q \tag{5.12}$$

where we also get the necessary condition that each $\left\langle \psi_j^a, T_j' q \right\rangle$-term is nonzero.

Recall that hypotheses 1) and 3) of Theorem 5.8 mean that the hypotheses of the Gearhart-Pruss theorem (Theorem 5.6) are satisfied. We would then like to follow the argument in Section 5.3 used to obtain the linear dynamics by considering the evolution of $e^{Lt} Pw(0)$ and $e^{Lt} P^C w(0)$. In particular, we would like to use the intuition of (5.9) — that the part of v that doesn't decay exponentially via Gearhart-Pruss can be written as $q(x+\gamma_\infty)$ — to calculate $e^{Lt} Pw(0)$. Our first lemma says that we really can decompose a solution into a part that decays exponentially and a translation of ϕ.

Lemma 5.13. *[24, Lemma 4.3.3, p. 92] There exist $\delta > 0$ and smooth functions $\gamma : H^m(\mathbb{R}) \to \mathbb{R}^N$ and $\beta : H^m(\mathbb{R}) \to H^m(\mathbb{R})$ satisfying $\gamma(0) = 0$, $\beta(0) = 0$ and that for all $q \in \mathscr{M}_T$ and all $\|v\|_Y \leq \delta$,*

$$u = q + v = T(\gamma(v)) q + \beta(v)$$

and further that $\beta(v) \in (\ker L^a)^\perp$.

Proof. First, using the Taylor series-like property of the symmetry,

$$T(\gamma) q = q + \sum_{j=1}^{N} \gamma_j T_j' q + T_{\mathscr{N}}$$

where $T_{\mathscr{N}}$ is quadratic in γ.

Solving for $\beta(v)$,

$$\beta(v) = q + v - T(\gamma) q = v - \sum_{j=1}^{N} \gamma_j T_j' q - T_{\mathscr{N}}. \tag{5.13}$$

Requiring that $\beta \in (\ker L^a)^\perp$ requires that for all the ψ_j^a that span $\ker L^a$, we have

$$0 = \left\langle \beta, \psi_j^a \right\rangle = \left\langle v, \psi_j^a \right\rangle - \sum_{i=1}^{N} \gamma_j \left\langle T_i' q, \psi_j^a \right\rangle - \left\langle T_{\mathscr{N}}, \psi_j^a \right\rangle.$$

If we set $g(\gamma, v) = \left(\left\langle v, \psi_1^a \right\rangle, \left\langle v, \psi_2^a \right\rangle, \ldots, \left\langle v, \psi_N^j \right\rangle \right)$, then $g(0,0) = 0$ and $D_\gamma g(0,0) = -I_N \neq 0$. (This follows from $\left\langle T_i' \phi, \psi_j^a \right\rangle = \delta_{ij}$.) Then by the implicit function theorem there is a neighborhood of $(0,0)$ and a smooth function $\gamma(v)$ so that $g(\gamma(v), v) = 0$ on that neighborhood. From (5.13) we see that $\beta(v)$ is smooth as well.

□

With this decomposition in hand, we turn to the main theorem.

Proof. (Of Theorem 5.8)

First, consider initial data u_0 close enough to q so that we can apply the decomposition in Lemma 5.13. The goal is to show that $u(t)$ stays close to q, and in particular converges to some nearby "translate" $T(\gamma_\infty)q$.
Starting off with the decomposition given by Lemma 5.13,

$$u(t) = T(\gamma(t))q + v, \qquad P^C v = 0. \tag{5.14}$$

In the sequel we will write $\gamma(t)$ as just γ, but it is important to remember the time dependence.
Substituting (5.14) into the evolution equation $u_t = \mathscr{F}(u)$, then we obtain

$$u_t = \mathscr{F}(u) = \mathscr{F}(T(\gamma)q + v).$$

For the left hand side, we again substitute the decomposition (5.14) for u. For the right hand side, we take the Taylor expansion about $T(\gamma)q$. We then obtain the perturbation equation

$$v_t + \sum_{j=1}^{N} (\gamma_j)_t T_j'(T(\gamma)q) = \mathscr{F}(T(\gamma)q) + [\nabla_u \mathscr{F}(T(\gamma)q)](u - T(\gamma)q) + \mathscr{N} \tag{5.15}$$

where the nonlinearity $\mathscr{N}$, by hypothesis, is quadratic in $\|v\|_{H^m(\mathbb{R})}$. First, note that $\mathscr{F}(T(\gamma)q) = 0$. Next, note that while we have a "linear operator" $L_\gamma = \nabla_u \mathscr{F}(T(\gamma)q)$, it is time dependent through $\gamma(t)$, so we cannot directly apply semigroup estimates on L_γ. That being said, our perturbation equations are currently

$$v_t + \sum_{j=1}^{N} (\gamma_j)_t T_j'(T(\gamma)q) = L_\gamma v + \mathscr{N}.$$

To get rid of the time dependence, we first write $L_\gamma v = L_0 v + \left[L_\gamma - L_0\right] v$, where L_0 is $L_{\gamma(0)}$. Using our hypothesis on the Lipschitz continuity of $\nabla_u \mathscr{F}$, we have that $\left\| \left[L_\gamma - L_0\right] v \right\|_{H^m(\mathbb{R})} \leq C|\gamma| \|v\|_{H^m(\mathbb{R})}$. Then we will "hide" the $\left[L_\gamma - L_0\right] v$ term in the nonlinearity by considering the new nonlinearity $\mathscr{R} = \mathscr{N} + \left[L_\gamma - L_0\right] v$.

To help with the later modulation equations (i.e. being perpendicular to ψ_j^q), we would like to express $T_j'(T(\gamma)q)$ in terms of $T_j'q$. We first write $T_j'(T(\gamma)q) = T_j'q + T_j'(T(\gamma)q - q)$. The latter term is a problem, but we can use the Taylor series of T to write $T(\gamma)q - q$ as $\gamma T_j'q$ plus a higher order term. As q is smooth, then $T_j'q$ is bounded by some constant, so $\|T(\gamma)q - q\|_{H^m(\mathbb{R})} = \mathscr{O}(|\gamma|)$. Assuming the operator norm of T_j' is bounded as well, then $\left\| T_j'(T(\gamma)q - q) \right\|_{H^m(\mathbb{R})} = \mathscr{O}(|\gamma|)$. Then we write these as error terms $t_j = T_j'(T(\gamma)q - q)$.

With these approximation in mind, the modulation equations are

$$v_t + \sum_{j=1}^{N} (\gamma_j)_t \left(T_j' q + t_j\right) = L_0 v + \mathscr{R} \tag{5.16}$$

where $\mathscr{R}$ satisfies $\|\mathscr{R}\| = \mathscr{O}\left(|\gamma| \|v\|_{H^m(\mathbb{R})} + \|v\|^2_{H^m(\mathbb{R})}\right)$.

Our next goal is to see how γ and v behave in time. For this, we consider applying the spectral projection P and its complement P^C. Applying P will remove all v terms (recall (5.14)), and we will get an evolution equation for just γ. Applying P^C will allow us to use our exponential decay estimate on $P^C L_0$.

First, we consider applying P. Recall from (5.12) that

$$Pf = \sum_{i=1}^{N} \frac{\langle \psi_i^a, f\rangle}{\langle \psi_i^a, T_i' q\rangle} T_i' q\,.$$

so it suffices to take the inner product of the modulation equation 5.16 with ψ_i^a. Taking this inner product, we obtain

$$\langle \psi_i^a, v_t\rangle + \sum_{j=1}^{N} (\gamma_j)_t \left(\langle \psi_i^a, T_j' q\rangle + \langle \psi_i^a, t_j\rangle\right) = \langle \psi_i^a, L_0 v\rangle + \langle \psi_i^a, \mathscr{R}\rangle\,.$$

As $Pv = 0$, then $\langle \psi_i^a, v\rangle = 0$. Noting that ψ_i^a is time independent and taking the t-derivative, $\frac{d}{dt}\langle \psi_i^a, v\rangle = \langle \psi_i^a, v_t\rangle = 0$. Using the definition of an adjoint, $\langle \psi_i^a, L_0 v\rangle = \langle L_0^a \psi_i^a, v\rangle = 0$.

Recall that we constructed the ψ_i^a so that $\left\langle \psi_i^a, T_j' q\right\rangle = \delta_{ij}$. Then if we define the matrix M where the entry $M_{ij} = \left\langle \psi_i^a, t_j\right\rangle$ and the vector $\vec{r}$ where the i-th component is $r_i = \langle \psi_i^a, \mathscr{R}\rangle$, we can view this as the evolution equation

$$(I_N + M)\,\gamma_t = \vec{r}\,.$$

For γ sufficiently small, then $I_N + M$ is invertible, and $\left\|(I_N+M)^{-1}\right\| \approx 1$. Since the ψ_i^a are orthonormal and $\|\mathscr{R}\|_{H^m(\mathbb{R})} = \mathscr{O}\left(|\gamma|\|v\| + \|v\|^2\right)$, then

$$|\gamma_t| = \mathscr{O}\left(|\gamma| \|v\|_{H^m(\mathbb{R})} + \|v\|^2_{H^m(\mathbb{R})}\right)\,.$$

Returning the the perturbation equation, if instead we apply P^C we have

$$P^C v_t + P^C \sum_{j=1}^{N} (\gamma_j)_t \left(T_j' q + t_j\right) = P^C L_0 v + P^C \mathscr{R}\,.$$

Recall from (5.14) that we specifically constructed v so that $P^C v = v$. Further, as P^C is a spectral projection it commutes

with L_0, and so $P^C L_0 v = L_0 v$ as well. Naturally, $P^C T_j' \phi = 0$. Then this projection of the perturbation equation is

$$v_t + \sum_{j=1}^{N} (\gamma_j)_t P^C t_j = L_0 v + P^C \mathscr{R}.$$

Since we now have estimates on both t_j and γ_t, we can combine this with the nonlinearity to make $\mathscr{R}_f = P^c \mathscr{R} - \sum_{j=1}^{N} (\gamma_j)_t P^C t_j$. As $\left\|t_j\right\|_{H^m(\mathbb{R})} = \mathscr{O}(|\gamma|)$, and we're taking γ sufficiently small, then we can bound this term by a constant. Then as $\mathscr{R}$ and γ_t have the same estimate, we have $\left\|\mathscr{R}_f\right\|_{H^m(\mathbb{R})} = \mathscr{O}\left(|\gamma| \|v\|_{H^m(\mathbb{R})} + \|v\|^2_{H^m(\mathbb{R})}\right)$. This results in the relatively simple evolution equation

$$v_t = L_0 v + \mathscr{R}_f. \tag{5.17}$$

With this agreeable version of the perturbation equation and nonlinearity that we can estimate, the stage is set for the heart of the nonlinear analysis. Fix an exponential decay rate $\tilde{\omega} \in (0, \omega)$ and define the quantities

$$M_v(t) = \sup_{0 \le s \le t} \left(e^{\tilde{\omega} s} \|v(s)\|_{H^m(\mathbb{R})}\right), \qquad M_\gamma(t) = \sup_{0 \le s \le t} |\gamma(s)|. \tag{5.18}$$

Note that if the quantity M_v gives us the estimate $\|v(s)\|_{H^m(\mathbb{R})} \le e^{-\tilde{\omega} s} M_v(t)$ for all $0 < s \le t$, so if M_v is bounded, then we get exponential decay.

We use Duhamel on the simplified perturbation equation (5.17) to solve for $v(t)$, so

$$v(t) = e^{L_0 t} v_0 + \int_0^t e^{L_0 (t-s)} \mathscr{R}_f \, ds.$$

Note that hypotheses 1) and 3) ensure that $P^C L_0$ satisfies the hypotheses of the Gearhart-Pruss theorem (Theorem (5.6)), which in turn gives exponential decay of the linear solution $e^{L_0 t} v_0$. Thus $\left\|e^{L_0 t} v(0)\right\|_{H^m(\mathbb{R})} \le C e^{-\omega t} \|v(0)\|_{H^m(\mathbb{R})}$.

Using the estimate that $\left\|\mathscr{R}_f\right\|_{H^m(\mathbb{R})} = \mathscr{O}\left(|\gamma| \|v\|_{H^m(\mathbb{R})} + \|v\|^2_{H^m(\mathbb{R})}\right)$, we have the estimate

$$\|v(t)\|_{H^m(\mathbb{R})} \le C e^{-\omega t} \|v(0)\|_{H^m(\mathbb{R})} + C \int_0^t e^{-\omega(t-s)} \left(|\gamma| \|v(s)\|_{H^m(\mathbb{R})} + \|v(s)\|^2_{H^m(\mathbb{R})}\right) ds.$$

Using the estimate $\|v(s)\|_{H^m(\mathbb{R})} \le e^{-\tilde{\omega} s} M_v$ to introduce the M_v and $|\gamma| \le M_\gamma$ to introduce M_γ,

$$\|v(t)\|_{H^m(\mathbb{R})} \le C e^{-\omega t} \|v(0)\|_{H^m(\mathbb{R})} + C e^{-\omega t} \int_0^t \left[e^{(\omega - \tilde{\omega}) s} M_\gamma M_v + e^{(\omega - 2\tilde{\omega}) s} M_v^2\right] ds$$

Note that M_v, M_γ are independent of s, so we can evaluate these integrals directly. The $\int_0^t e^{\omega s} \, ds$ become $e^{\omega t}$, which cancels with the existing $e^{-\omega t}$ terms. We also use that $e^{-\omega t} \le e^{-\tilde{\omega} t}$ to reduce the exponential coming from linear

decay. Then grouping everything under the same constant,

$$\|v(t)\|_{H^m(\mathbb{R})} \leq C\left[e^{-\tilde{\omega}t}\|v(0)\|_{H^m(\mathbb{R})} + e^{-\tilde{\omega}t}M_\gamma M_v + e^{-2\tilde{\omega}t}M_v^2\right]. \tag{5.19}$$

While we may have written t in the above, it technically applies for all $t' \in [0,t]$. With this in mind, we can change t to t', multiply by $e^{\tilde{\omega}t'}$, then take the supremum over all $t' \in [0,T]$ to convert $\|v(t)\|_{H^m(\mathbb{R})}$ to M_v, and in particular the bound

$$M_v \leq C\left[\|v_0\| + M_\gamma M_v + M_v^2\right].$$

To obtain a similar inequality for M_γ, we need to backtrack to the evolution equation $\gamma_t = \mathscr{O}\left(|\gamma|\,\|v\|_{H^m(\mathbb{R})} + \|v\|^2_{H^m(\mathbb{R})}\right)$. Using M_v, M_γ to bound these terms and integrating from 0 to t' gives that

$$\left|\gamma\left(t'\right)\right| \leq C_2\left[M_\gamma M_v + M_v^2\right].$$

As this holds for all $t' \in [0,T]$, it also holds for M_γ, so

$$M_\gamma \leq C_2\left[M_\gamma M_v + M_v^2\right].$$

Now we use M_v, M_γ to show nonlinear stability. Recall that we were a little vague in choosing u_0. To rectify this, suppose we choose u_0 such that $M_v(t) \leq \frac{1}{2C_2}$ for all $t \in [0,\underline{T}]$. Our goal is to extend $\underline{T}$ to infinity.

First, using this bound for M_v, we have that

$$M_\gamma \leq \frac{1}{2}M_\gamma + C_2 M_v^2.$$

Subtracting $\frac{1}{2}M_\gamma$ from both sides and renormalizing,

$$M_\gamma \leq 2C_2 M_v^2.$$

Using this bound, we can rewrite the inequality for M_v as

$$M_v \leq C_3\left[\|v(0)\| + M_v^2 + M_v^3\right]. \tag{5.20}$$

Without loss of generality, take $C_3 > 1$. Thus it suffices to set $x = M_v$ and consider the polynomial inequality

$$-x^3 - x^2 + x - \|v(0)\|_{H^m(\mathbb{R})} \leq 0.$$

Note that when $\|v(0)\|_{H^m(\mathbb{R})} = 0$ then $x = 0$ is a root, and that the x-derivative when $x = 0$ is 1. Choosing $\|v(0)\|_{H^m(\mathbb{R})} > 0$ will shift the graph vertically downwards. For $\|v(0)\|_{H^m(\mathbb{R})}$ non-zero but sufficiently small, the polynomial will take on a negative value at $x = 0$ and cross the x-axis. In particular this means that when $t = 0$, $x = M_v(0) = \|v(0)\|_{H^m(\mathbb{R})}$ which will satisfy the polynomial inequality, and hence M_v satisfies the polynomial inequality for all time. □

5.4.2 As Applied to modified Kuramoto-Sivashinsky and the St. Venant Equation

In (5.8) we develop our guess for the nonlinear stability result, a standard asymptotic orbital stability result possibly phrased as "given a solution u, we have $\|u(\cdot,t) - q(\cdot + \gamma(t))\|_{H^2_a} \lesssim e^{-\omega t} \|u(0)\|_{H^2_a(\mathbb{R})}$ where $\gamma(t)$ is some function converging exponentially to a constant." Unfortunately we were unable to prove the full nonlinear instability result. In this section we detail the complications and technical issues that arise,many of which have seemingly not been reported in the literature before.

The main problem comes down to the interaction between the exponential weight and the nonlinearity. For the modified Kuramoto-Sivashinsky equation the perturbation equations (1.9) — obtained by decomposing the solution as $q(x) + v(x,t)$ and substituting this into the PDE, with a more detailed definition in (5.15) — are

$$v_t = -v_{xx} - v_{xxxx} + cv_x + 6qq'v + 3q^2v_x + 3q'v^2 + 6qvv_x + 3v^2v_x - \gamma' q' . \tag{5.21}$$

We'll focus on the v^2v_x term. Recall that we defined the weighted perturbation to be $w = e^{ax}v$, and when rewriting this perturbation equation (5.21) in terms of w to obtain the weighted perturbation equation (5.1), the nonlinearity becomes $e^{ax}\mathcal{N}(v)$. Considering just this one term, our weighted nonlinearity may be written as either

$$e^{ax}v^2v_x = wvv_x \qquad \text{or } \sim v^2w_x .$$

(The $\sim$ is used as there are additional terms arising from the product rule.) Recall that from Section 5.1 the $L^2(\mathbb{R})$-norm of the weighted perturbation w may become small, but the unweighted perturbation v remains large (in both an $L^2(\mathbb{R})$ and $L^\infty(\mathbb{R})$ sense). However, no matter where the weight is placed, one still needs some control over the original unweighted perturbation v. In particular, this is a problem when attempting to find a polynomial bound as in (5.20) of the general nonlinear stability theorem. For the weighted perturbation w we could define M_w in a similar manner as in (5.18), i.e. $M_w(t) = \sup_{0\le s\le t}\left(e^{\tilde{\omega}s}\|w(s)\|_{H^m(\mathbb{R})}\right)$. We cannot do the same for M_v as we do not expect exponential decay of the $H^m(\mathbb{R})$-norm. One possible solution would be to define $M_v(t) = \sup_{0\le s\le t}\|w(s)\|_{L^\infty(\mathbb{R})}$, but this term doesn't become arbitrarily small.

One naive solution to this would be to split the exponential weight into thirds, with

$$e^{ax}\mathscr{N}(v) = \left(e^{\frac{1}{3}ax}v\right)^2\left(e^{\frac{1}{3}ax}v_x\right).$$

Then one could define

$$M_{\tilde{w}}(t) = \sup_{0\le s\le t}\left(e^{\tilde{\omega}s}\left\|e^{\frac{1}{3}ax}v(s)\right\|_{H^m(\mathbb{R})}\right)$$

and hopefully use this to find a polynomial bound as in (5.20). We remark that looking at Figure 5.6 there appear to be speeds s and weights a where both a and $\frac{1}{3}a$ will stabilize the essential spectrum and hence it may be possible that both M_w and $M_{\tilde{w}}$ to be bounded. Unfortunately with this method one would then have to mind both weights $e^{ax}v$ and $e^{\frac{1}{3}ax}v$ simultaneously. The main issue arises in the analogue of (5.19), as the left hand side is $\|w\|_{H^m(\mathbb{R})}$, and taking the supremum in t gives an M_w term, not the desired $M_{\tilde{w}}$ term. That is, one would have $M_w(t) \le f(M_{\tilde{w}}(t))$ where f is some polynomial. It is clear that $M_w(t) \le M_{\tilde{w}}(t)$, but one would need the opposite inequality to convert this into a polynomial inequality like (5.20).

The more typical solution, such as in [16, 6, 31], is to prove some sort of a priori estimate for the unweighted perturbation v, typically in the $L^\infty(\mathbb{R})$-norm. In our case we wouldn't expect $\|v\|_{L^\infty(\mathbb{R})}$ to become arbitrarily small given arbitrarily small initial perturbations — hence this may not help finish the nonlinear stability argument — but rigorously showing that $\|v\|_{L^\infty(\mathbb{R})}$ is at least bounded would be an interesting result on its own.

For technical reasons when trying to establish an $L^\infty(\mathbb{R})$-norm bound for the perturbation one usually uses the Banach space $L^2_{\text{ul}}(\mathbb{R})$ of uniformly local weighted $L^2(\mathbb{R})$ functions. To define this space, first choose a positive and bounded weight function $\rho(x) \in C^2(\mathbb{R})$ for which $\int \rho(x)\ dx = 1$ and $|\rho'(x)|, |\rho''(x)| \le \rho(x)$ for all $x \in \mathbb{R}$. One possible choice is $\rho(x) = \frac{1}{\pi}\operatorname{sech} x$. Also define the rescaling $\rho_b(x) = \rho(bx)$. This space uses the norm

$$\|u\|^2_{L^2_{\text{ul}}(\mathbb{R})} = \sup_{y\in\mathbb{R}}\int_{\mathbb{R}}\rho(x+y)\,|u(x)|^2\ dx$$

and the space itself is defined to be

$$L^2_{\text{ul}}(\mathbb{R}) = \left\{u \in L^2_{\text{loc}}(\mathbb{R}) \;\middle|\; \|u\|_{L^2_{\text{ul}}(\mathbb{R})} < \infty \text{ and } \|u(\cdot+y)-u(\cdot)\|_{L^2_{\text{ul}}(\mathbb{R})} \to 0 \text{ as } y \to 0\right\}.$$

One can also use this methodology to define uniformly local Sobolev spaces $H^k_{\text{ul}}(\mathbb{R})$, and that different choices of weight function $\rho(x)$ result in the same spaces with equivalent norms. These spaces also have the following properties.

Lemma 5.14. *[16, Lemma 2.1] There is a constant K_0 with the following properties:*

1. *$H^1_{ul}(\mathbb{R})$ is an algebra and embeds continuously into the space of uniformly continuous functions with $\|u\|^2_{L^\infty(\mathbb{R})} \le K_0\|u\|_{L^2_{ul}(\mathbb{R})}\|u\|_{H^1_{ul}(\mathbb{R})}$ for all $u \in H^1_{ul}(\mathbb{R})$.*

2. *For each* $0 < b < 1$, *then* $\|u\|^2_{L^2_{ul}(\mathbb{R})} \leq K_0 (1+b) \|u\|_{L^2_{ul}(\mathbb{R},\rho_b)}$ *for all* $u \in L^2_{ul}(\mathbb{R})$.

3. *We have* $-\int_{\mathbb{R}} \rho_b u \left(1+\partial_x^2\right)^2 u \, dx \leq \frac{7b^2}{2} \int_{\mathbb{R}} \rho_b u^2 \, dx$ *for all* $u \in H^4_{ul}(\mathbb{R})$.

The first result shows that the $L^2_{\text{ul}}(\mathbb{R})$-norm more or less provides an upper bound for the $L^\infty(\mathbb{R})$-norm. Intuitively this is because the weight function is shifted all around, so there's no place on the real line for a function to hide its poor behavior.

The third result gives a slight hint as to why the $L^2_{\text{ul}}(\mathbb{R})$-norm is easier to work with rather than the $L^\infty(\mathbb{R})$-norm. Ignoring the translation invariance, fundamentally $\|\cdot\|_{L^2_{\text{ul}}(\mathbb{R})}$ is defined as an inner product. That means one can use energy type estimates, such as those in Section 5.20 which heavily relied upon integration by parts, to form inequalities. The following is an adaptation of the third result but using the linear operator from the modified Kuramoto-Sivashinsky equation.

Lemma 5.15. *Let* ρ *be an integrable weight function with* $|\rho''(x)| \leq \rho(x)$ *for all* $x \in \mathbb{R}$. *For* $b \in \mathbb{R}$, *set* $\rho_b(x) = \rho(bx)$. *Then, for all* $u \in H^4_{ul}(\mathbb{R})$, *the following estimate holds:*

$$\int_{\mathbb{R}} \rho_b u \left(-\partial_x^4 - \partial_x^2 + s\partial_x\right) u \, dx \leq \left(\frac{b^4}{4} + \frac{3b^2}{2} - \frac{bs}{2} + 1\right) \int_{\mathbb{R}} \rho_b u^2 \, dx$$

Proof. First, a side calculation. By integration by parts,

$$\int \rho_b u u_x = -\int \rho_b' u^2 - \int \rho_b u u_x .$$

From which we conclude

$$\int \rho_b u u_x = -\frac{1}{2} \int \rho_b' u^2 .$$

Returning to the main equation, from integration by parts,

$$\begin{aligned}
\int \rho_b u \left(-\partial_x^4 - \partial_x^2 + s\partial_x\right) u \, dx &= \int \left[\rho_b' u u_{xxx} + \rho_b u_x u_{xxx}\right] - \rho_b u u_{xx} - \frac{s}{2} \rho_b' u^2 \\
&= \int -\left[\rho_b'' u u_{xx} + \rho_b' u_x u_{xx}\right] - \left[\rho_b' u_x u_{xx} + \rho_b u_{xx}^2\right] - \rho_b u u_{xx} - \frac{s}{2} \rho_b' u^2 \\
&= \int \rho_b'' \left(-u u_{xx} + u_x^2\right) - \rho_b \left(u u_{xx} + u_{xx}^2\right) - \frac{s}{2} \rho_b' u^2 .
\end{aligned}$$

From the proof of [31, Lemma 3.8], we have

$$\int \rho_b u_x^2 \leq \frac{b^2}{2} \int \rho_b u^2 + |u u_{xx}| .$$

Applying this,

$$\int \rho_b u \left(-\partial_x^4 - \partial_x^2 + s\partial_x\right) u \, dx \leq \int \rho_b \left(\left(2+b^2\right) |u u_{xx}| - u_{xx}^2 + \left(\frac{b^4}{2} - \frac{bs}{2} \right) u^2 \right).$$

Using Cauchy with epsilon with $\varepsilon = \frac{\left(2+b^2\right)}{\sqrt{2}}$, $|u|\,|u_{xx}| \leq \frac{\left(2+b^2\right)^2}{4} u^2 + u_{xx}^2$, and the result follows. □

However, the papers [16, Lemma 3.5] that use this technique concern themselves with reaction-diffusion equations — time evolution PDEs where the highest order term is $-u_{xx}$ and where there are no derivatives in the nonlinearity. In particular these equations are of a fundamentally different structure than either the modified Kuramoto-Sivashinsky or St. Venant equations. The arguments in [16, Lemma 3.5] heavily rely upon this structure to obtain their estimates. In particular a problem arises when attempting to follow the strategy in [16, Lemma 3.5] is that in their equation (1.2) the nonlinearity is $-u^3$: as the modified Kuramoto-Sivashinsky does not have this term, then we are unable to establish the sign of a certain quantity.

Another interesting result would be to prove that the perturbation only travels to the left. The most promising way of doing this would likely be a technique that resembles [28, Lemma 16], [29, Section 2, Lemma 1], or [30, Lemma 3]. The details of each of these differ slightly, but the setup is to define the quantity

$$\mathscr{I}(t) = \int_{\mathbb{R}} |u(x,t)|^2 \, \psi(x-t) \, dx$$

where $\psi(x) = \arctan(x)$ or a similar function and show that $\mathscr{I}(t)$ is monotone increasing in time. Note that $\mathscr{I}$ is more or less an energy, so by calculating $\frac{d}{dt}\mathscr{I}(t)$ one can use integration by parts to shift the derivatives to the ψ term. Then part of the trick is defining an ODE for ψ whose solution is given by a function that resembles arc tangent. Again, because the PDEs they consider differ in structure from the modified Kuramoto-Sivashinsky equation, it is not clear if an amenable ODE for ψ can even be constructed.

A final remark regarding obstacles to obtaining a polynomial bound such as (5.20) is the fact that the nonlinearity for the modified Kuramoto-Sivashinsky $v^2 v_x$ contains a derivative. Naively choosing M_v to be based on the $H^m(\mathbb{R})$-norm, the derivative in the nonlinearity would force a term like M_v but using the $H^{m+1}(\mathbb{R})$-norm, and hence the iteration couldn't close. In contrast to the previous problems of this subsection, this problem does have a working solution in the form of damping estimates. An example of one is given in Lemma 6.9 which applies to an equation with a nonlinearity like uu_x, for which one obtains an inequality like

$$\|u\|_{H^2} \leq e^{-\beta t} \|u(0)\|_{H^2} + C \int_0^T e^{-\beta(t-s)} \|u(s)\|_{H^1(\mathbb{R})} \, ds.$$

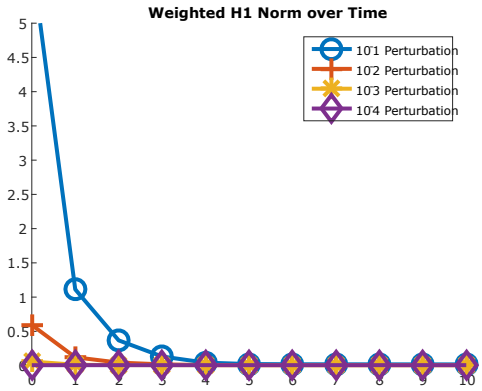

Figure 5.8: The weighted $H^1_a(\mathbb{R})$-norm of the perturbation for the modified Kuramoto-Sivashinsky equation, with $a = 0.3$, as a function of time. Note that time has been truncated to show the rapidity of decay. The perturbations used are rescalings of that in Figure 5.1.

This allows us to bound higher order Sobolev spaces by lower order ones, in exchange for some exponential growth, and allows us to complete the iteration of (5.20) by using M_ν defined using the same $H^m(\mathbb{R})$-norm. In principle such a result should be true for the modified Kuramoto-Sivashinsky equation, although the complexity of the weighted linear operator L_a in (5.3) necessitates a well-planned bookkeeping system for the calculations. The result for the St. Venant equation was proved in [38, Section 4.2].

One extra problem that shows up exclusively for the St. Venant case was shown in Figure 5.3: the fact that the perturbation seemingly leaves copies of the original pulse in its wake. The most promising solution would be to return to the original ansatz $q(x+\gamma(t))+v(x,t)$ and account for some number of copies of the original pulse, perhaps rewriting it as $u(x,t) = \sum_{j=1}^{N} q_j(x+\gamma_j(t))+v(x,t)$.

Finally, we end this section on a hopeful note by reviewing Figure 5.8 which shows the time evolution of the weighted $H^1_a(\mathbb{R})$-norm of the perturbations for the modified Kuramoto-Sivashinsky equation. All of the perturbation sizes show exponential decay: so while it may not be clear how to prove the nonlinear stability result, we believe such a result should be true.

5.5 Stabilizing via Ad-hoc Periodic Wave Trains

We start this section by considering the modified Kuramoto-Sivashinsky equation. First, let us recall that numerical time evolution suggests that a transition from one slope to another is unstable in the standard space $L^2(\mathbb{R})$. We investigated these transitions because they model an observable physical phenomenon and hence should be stable themselves. Since something must be stable — otherwise it would not be physically observable — maybe the secret lies not in a single transition but the repeating effect of them. After all, the pictures of the surface in [33] show not just one transition but many: what if choosing to investigate only a single transition neglects some sort of important effect?

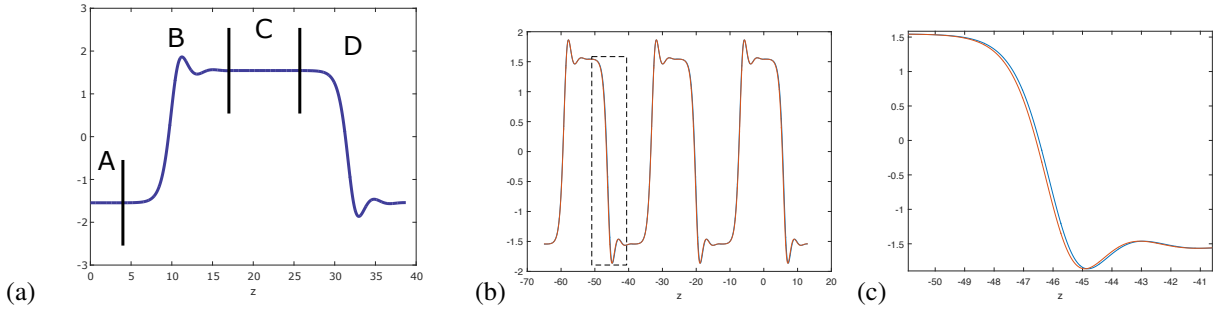

(a) (b) (c)

Figure 5.9: (a) A schematic of one cell block for the ad-hoc periodic wave train. (b) A comparison of an ad-hoc periodic wave train with the computed numerical solution, found by using the boundary value problem from Section 4.1 with the ad-hoc periodic wave train as an initial guess. (c) A zoom-in on the dashed part of (a), showing how well they agree.

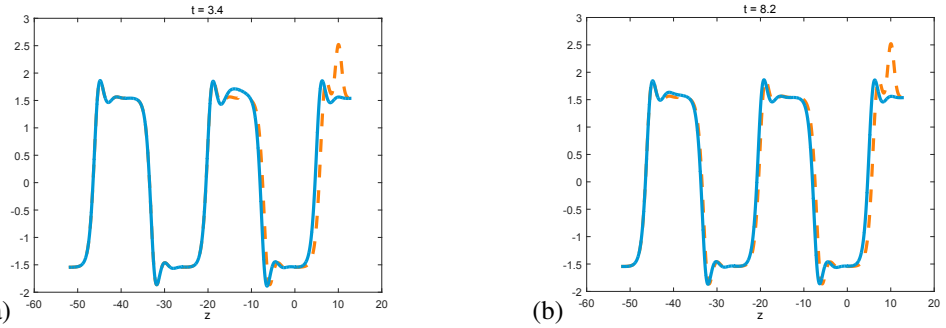

(a) (b)

Figure 5.10: The time evolution of an ad-hoc periodic wave train formed by concatenating a $\mu = 0$ front with a $\mu = 0$ back solution. The initial condition is shown in orange, and the solutions at time (a) $t = 3.4$ and (b) $t = 8.2$ are shown. In (b) the perturbation is barely visible around $z = -20$, and in (c) the perturbation is almost undetectable near $z = -40$.

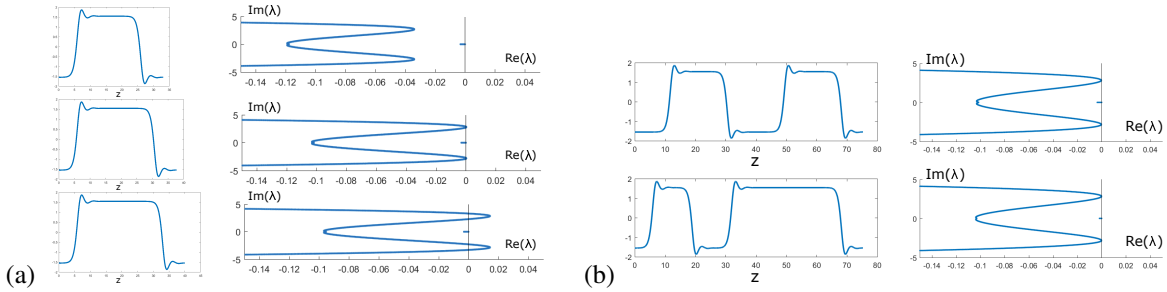

Figure 5.11: (a) Three different front-back pairs with variable spacing and their corresponding essential spectrum. (b) Periodic cells with two front-back pairs and variable spacing. Note that despite using different spacings, both of their total spacings sum up to 2η and that for both the essential spectrum is just touching the imaginary axis.

With this in mind we attempt to investigate how repetition affects stability. We simplify the situation by considering ad-hoc periodic wave train formed by concatenating a front, a back, and some amount of space in-between them. Specifically, we'll be constructing "cell blocks", as in Figure 5.9(a), by concatenating a front, some amount of "spacing" which lingers on the front's right asymptotic value, a back, more spacing which uses the back's right asymptotic value, then possibly repeating this process with more fronts and backs. Each spacing can be independently varied and the resulting cell block will be repeated periodically to create a periodic solution. Of note is that each front and back itself needs a certain amount of space to reach its asymptotic values. If there isn't enough, then the solution is always unstable no matter what spacing is used. This amount of space to use for each front and back was chosen arbitrarily.

While these solutions may be ad-hoc, they do resemble the observed phenomenon in [33] by having many alternating slope transitions. Figure 5.9 (b) and (c) also show that the ad-hoc periodic wave trains are good approximations for a periodic solution. There is one major difference in that the observed physical phenomenon's slope transitions do not necessarily occur in regular intervals and are not periodic. These ad-hoc wave trains are a compromise where we can investigate irregular spacings by changing the cell blocks, while periodically repeating these cell blocks allows us to use Hill's Method (from Section 4.3) to easily calculate the spectrum.

The time evolution in Figure 5.10 provides a hint to the general dynamics of these ad-hoc wave trains when subjected to small localized perturbations. In general the leftward moving perturbation is damped as it moves through each slope transition while it grows when it is otherwise in the region of constant slope. Then by placing enough transitions close enough together the perturbation can be repeatedly damped, eventually disappearing.

Rephrasing this intuition in terms of the spectrum, the general trend is that increasing the spacings moves the spectrum to the right and so makes the solution more unstable. This can be observed in Figure 5.11 (a), where one spacing parameter for a one front-back pair is successively increased. Refining this observation, there seems to be a critical spacing η where the spectrum just touches the imaginary axis: any more spacing is unstable, any less is stable. What is perhaps more surprising is that for n front-back pairs, the *sum* of all the spacings is compared to the critical

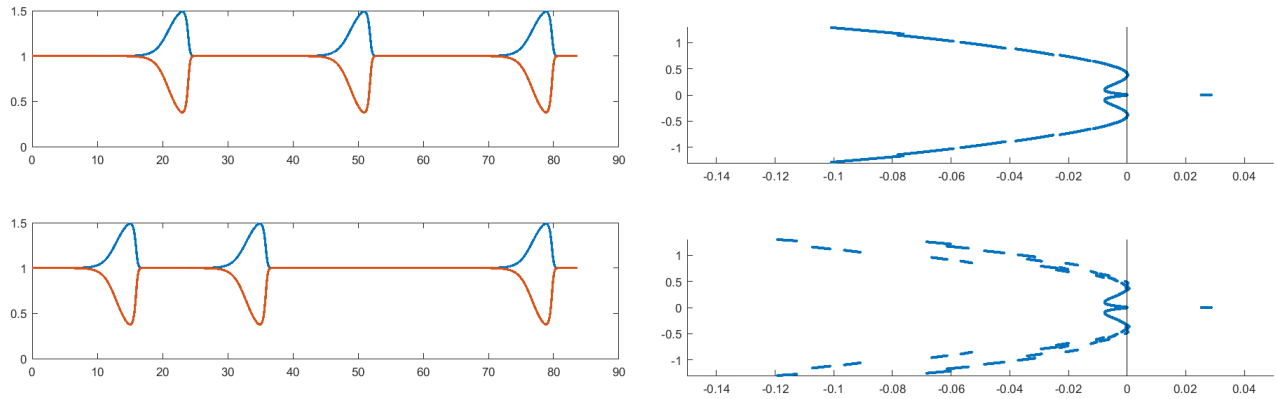

Figure 5.12: Periodic cells for the St. Venant equation with three pulses and variable spacing. Blue is the u-variable and orange is the τ variable. Note that despite using different spacings, both of their total spacings are the same and that for both the essential spectrum is just touching the imaginary axis.

number $n\eta$: any more spacing is unstable, any less is stable. This is demonstrated in Figure 5.11 (b) where the spacing of two front-back pairs is allowed to vary, but the total spacing is kept at 2η, and the spectrum keeps just touching the imaginary axis. In particular, the instability can be given a relatively large space to grow in, so long as this is balanced by a few close front-back pairs.

So far in this section we have been focusing on the behavior ad-hoc periodic wave trains specifically for the modified Kuramoto-Sivashinsky equation. However, all of this investigation was actually inspired by Figures 11 to 13 from [5]: which are essentially Figure 5.10 for the St. Venant equation. Some preliminary numerics, such as Figure 5.12, suggest that St. Venant allows for the same behavior for ad-hoc periodic wave trains, right down to the result that it is the total spacing that matters, not how it's distributed.

All of these results suggest that the modified Kuramoto-Sivashinsky and St. Venant equations might admit a robust array of repeating but not necessarily periodic traveling wave solutions. An open problem would be to show their existence and to consider their dynamics. For modified Kuramoto-Sivashinsky in particular these results suggest that starting with solitary traveling waves may not be the right approach to modeling the stable nanoscale patterns.

Chapter 6

Using the Bloch Transform to Characterize Unstable Initial Conditions

In much of the preceding, the fact that there was unstable essential spectrum served to complicate matters: the main complication being that in the time evolution — as featured in Section 5.1 — the essential spectrum caused oscillatory instabilities that could not be controlled by making the initial perturbation smaller. As a consequence of this, the main linear stability result Theorem 5.7 could only be proved in an exponentially weighted space.

In contrast, the eigenvalue $\lambda = 0$ posed no problems as it was quickly eliminated with a spectral projection. This leads to the natural question about whether or not such a neat and tidy spectral projection could be constructed to handle the unstable essential spectrum as well.

In this chapter we propose a methodology — detailed in 6.2.2 — for constructing such a projection P and use this projection to show that any initial perturbation which activates a sufficiently unstable portion of the essential spectrum will lead to instability. In particular, this projection will be used to characterize the linear growth of the initial perturbation. Hence any spectral projection for the essential spectrum must at least remove some portion of the unstable part.

In particular this result is proved in the context of periodic PDEs, as there the essential spectrum is given as point spectrum of a family of related operators — this is detailed in Subsection 6.2.1.

6.1 Setup

We consider a reaction-diffusion type system of real-valued partial differential equations of the form

$$\begin{cases} u_t(x,t) = Lu(x,t) + \mathcal{N}(u(x,t)) & x \in \mathbb{R},\ t > 0 \\ u(x,0) = u_0(x) & u \in \mathbb{R}^d \end{cases} \tag{6.1}$$

posed on $X = H^n(\mathbb{R})$, an appropriate Sobolev subspace of $L^2(\mathbb{R})$, where L is an $2n$-th order linear differential operator of the form

$$L = \sum_{j=0}^{2n} a_j(x)\,\partial_x^j \tag{6.2}$$

with real-valued 2π-periodic coefficient functions $a_j(x)$. Other periods may be considered by rescaling x. For simplicity we also assume that L is a sectorial operator. We assume the nonlinear operator $\mathscr{N}$ satisfies the following polynomial estimate,

$$\|\mathscr{N}(u)\|_X \leq \|u\|_X^p \qquad \text{for some } p > 1. \tag{6.3}$$

Note that in general the perturbation equation (1.9) may be of this form provided L is the linearization around a periodic equilibrium solution. While we did not consider the modified Kuramoto-Sivashinsky equation (2.2) or St. Venant equations (2.5) in this context, the numerics in Subsection 5.5 suggest that periodic equilibrium solutions exist for the modified Kuramoto-Sivashinsky equation and for St. Venant periodic equilibrium solutions do exist [38].

For the local dynamics, traditionally one uses the following definition of stability.

Definition 6.1. Let ϕ be an equilibrium solution and u be a perturbation (as above) which satisfies (6.1). The equilibrium solution ϕ is said to be *stable* (in the norm $\|\cdot\|$) if for all $\varepsilon > 0$ there exists a $\eta > 0$ so that requiring $\|u_0\| < \eta$ ensures that $\|u(t)\| < \varepsilon$ for all time. Otherwise ϕ is said to be *unstable*.

Typically the focus has been showing that equilibrium solutions are stable. In contrast, we are particularly interested in the case when the $L^2(\mathbb{R})$ spectrum of L, $\sigma(L)$, is "spectrally unstable": when $\sigma(L) \cap \{z \in \mathbb{C} \mid \operatorname{Re} z > 0\} \neq \emptyset$. In particular, this may be in the context of Subsection 5.5 for a sufficiently large spacing.

In [17, 19] it is shown that spectral instability leads to instability. This is done by constructing a specific initial perturbation u_0 which results in a poorly behaved solution, thus precluding stability. In particular in [19] the initial perturbation u_0 is taken to be a perturbation which "activates" the most unstable part of $\sigma(L)$, roughly speaking that it projects into the most unstable subspaces. Hence the presence of any unstable essential spectrum precludes stability in the sense of Definition 6.1.

However if some sort of projection could be constructed that removes all of the unstable essential spectrum, then one may be able to show stability in the sense of 6.1. This problem may be rephrased in the following way: suppose that u_0 is an initial perturbation that "activates none of the unstable essential spectrum." Then we would like to show that the initial perturbation u_0 is stable in the following sense.

Definition 6.2. An initial perturbation u_0 of (6.1) is said to be *stable* (in the norm $\|\cdot\|$) if for all $\varepsilon > 0$ there exists an $\eta > 0$ so that for all $0 < \delta < \eta$, if u_δ is the solution to (6.1) with initial perturbation δu_0, then $\|u_\delta(t)\| < \varepsilon$ for all time. Otherwise u_0 is said to be *unstable*.

With this definition in mind, [19] shows that the initial perturbation which activates the rightmost part of $\sigma(L)$ is unstable. But what if an initial perturbation activates any other part of $\sigma(L) \cap \{z \in \mathbb{C} \mid \operatorname{Re} z > 0\}$? A naive guess would be that if u_0 activates $\sigma(L) \cap \{z \in \mathbb{C} \mid \operatorname{Re} z > 0\}$ it is unstable, and if it does not it is stable. If that were the case, then one would obtain stability of ϕ for a wide range of initial perturbations.

Our main result is a step in this direction with Theorem 6.7 which concludes that if an initial perturbation activates an sufficiently unstable subset of $\sigma(L) \cap \{z \in \mathbb{C} \mid \operatorname{Re} z > 0\}$, then that initial perturbation is unstable. This result applies to many reaction-diffusion type systems with periodic equilibrium solutions, including but not limited to scalar reaction diffusion, FitzHugh-Nagumo [35], the Klausmeier model for vegetation stripe formulation [41, 40], and the Belousov-Zhabotinskii reaction [7]. This methodology is robust enough that in Theorem 6.10 we show how it may be extended to dissipative systems of conservation laws such as Kuramoto-Sivashinsky [4, 20] and the St. Venant equation [3, 38].

To see how a spectral instability may lead to a nonlinear instability, we recall from Duhamel's equation the solution of (6.1) can be decomposed as

$$u(x,t) = e^{Lt}u_0(x) + \int_0^t e^{L(t-s)}\mathcal{N}(u(x,s))\, ds, \tag{6.4}$$

which uses the solution semigroup e^{Lt} to write the solution in terms of a linear part and a nonlinear part.

The stability of the linear part is directly influenced by point spectrum of L. Suppose L had an eigenfunction ψ with eigenvalue λ with $\operatorname{Re}\lambda > 0$: then choosing ψ as an initial perturbation, the linear part would be $e^{\lambda t}\psi$ and we would have exponential growth. While in general the $L^2(\mathbb{R})$ spectrum of L will not contain such eigenvalues, as the coefficient functions $a_j(x)$ in (6.2) were taken to be 2π-periodic then Floquet theory gives the $L^2(\mathbb{R})$ spectrum of L as the collection of $L^2_{\text{per}}[0,2\pi)$ point spectrum of the one-parameter family of operators $L_\xi = e^{-i\xi x}Le^{i\xi x}$ with $\xi \in \left[-\frac{1}{2},\frac{1}{2}\right)$ [21, Proposition 3.1]. The respective domains $L^2(\mathbb{R})$ and $L^2_{\text{per}}[0,2\pi)$ are connected through the Bloch Transform. (This theory and its preliminaries are developed in Subsection 2.1, and that specific spectral result is given in Proposition 6.3). In Subsection 2.2 we use the Bloch Transform to define the projection (6.15) which allow us to use this unstable point spectrum of L_ξ to conclude exponential growth for the linear part of (6.4).

This clarifies the notion of "u_0 activating an unstable part of $\sigma(L)$" as "the Bloch Transform of u_0 contains some sufficiently unstable eigenspace of some L_ξ." A further area of study would be to see if this Bloch transform view gives any insight into specifically how the initial perturbation goes unstable.

To handle the nonlinear part of (6.4), we apply the reverse triangle inequality to obtain the following lower bound for the solution,

$$\left| \left\| e^{Lt}u_0 \right\|_X - \left\| \int_0^t e^{L(t-s)}\mathcal{N}(u(x,s))\, ds \right\|_X \right| \leq \|u(x,t)\|_X . \tag{6.5}$$

In Section 3 we prove an upper bound on the growth of the nonlinear part, which when contrasted with the exponential growth of the linear part gives instability.

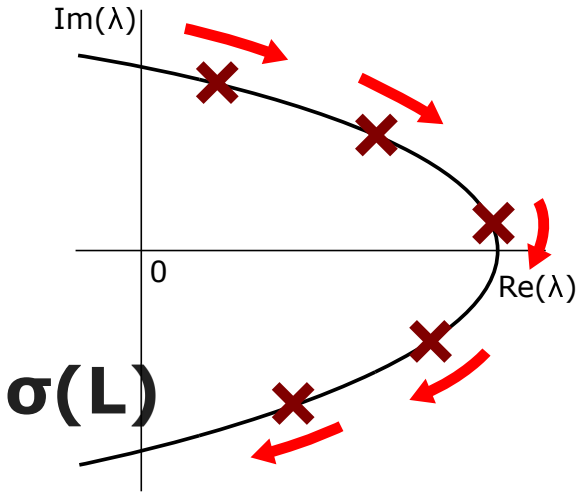

Figure 6.1: Eigenvalues λ of L_ξ given as maroon x's. As ξ changes, each individual eigenvalue moves holomorphically with its path given in red. (It is artistic license that the paths are unidirectional.) The spectrum of L, $\sigma(L)$, is graphed in black. The union of all of these eigenvalues λ forms $\sigma(L)$.

6.2 Spectral Properties

6.2.1 Characterization of the Spectrum

The operator L from (6.1) is a linear differential operator with 2π-periodic coefficients, so standard results in Floquet theory [10, Section 2.4] tell us that there are no $L^2(\mathbb{R})$ eigenfunctions: the spectrum is entirely essential. Furthermore, the spectrum of L can be determined from the following one-parameter family of Bloch operators L_ξ,

$$L_\xi = e^{-i\xi x} L e^{i\xi x} \qquad \text{defined on } L^2_{\text{per}}[0,2\pi),\ \xi \in \left[-\frac{1}{2},\frac{1}{2}\right). \tag{6.6}$$

Given the form of L in (6.2), the Bloch operators take the following explicit form,

$$L_\xi = \sum_{j=0}^{n} a_j(x)\,(\partial_x + i\xi)^j\,. \tag{6.7}$$

Proposition 6.3. *[21, Proposition 3.1] Consider the operator L as in (6.2) acting on $L^2(\mathbb{R})$ with domain $H^1(\mathbb{R})$ and the associated Bloch operators $\{L_\xi\}_{\xi\in[-\frac{1}{2},\frac{1}{2})}$ acting on $L^2_{per}[0,2\pi)$ with domain $H^1_{per}[0,2\pi)$. Then λ is in the $L^2(\mathbb{R})$ spectrum of L if and only if there exists some $\xi \in [-\frac{1}{2},\frac{1}{2})$ so that λ is in the $L^2_{per}[0,2\pi)$ spectrum of L_ξ with an eigenfunction of the form $e^{i\xi x}v(x)$ with $v \in H^1_{per}[0,2\pi)$.*

As the resolvent of each L_ξ with domain $H^1_{\text{per}}[0,2\pi)$ is a compact operator, then the spectrum of L_ξ is a countable set of isolated eigenvalues with finite multiplicity [12]. Note that from (6.7), ξ appears in L_ξ as a polynomial and so L_ξ is holomorphic as a function of ξ, and thus [25, Theorem 1.7 from VII-§1] given a closed curve Γ that separates

the spectrum, its corresponding spectral projection is holomorphic in ξ and [25, Theorem 1.8 from VII-§1] any finite system of eigenvalues which depend holomorphically on ξ. See Figure 6.1 for a depiction of the spectral picture.

In particular, let λ be an eigenvalue of L_{ξ_0} and Γ be a curve that contains λ and no other eigenvalue of L_{ξ_0}. Then there is some interval $I \subset \left[-\frac{1}{2}, \frac{1}{2}\right)$, with $\xi_0 \in I$, so that the following spectral projection

$$\tilde{P}_\lambda(\xi) = \frac{1}{2\pi i} \int_\Gamma R\left(\zeta, L_\xi\right)\, d\zeta \tag{6.8}$$

is holomorphic on I, where $R\left(\zeta, L_\xi\right)$ is the resolvent of L_ξ.

The Bloch transform may be used to relate the domain of the Bloch operators $\left\{L_\xi\right\}_{\xi \in \left[-\frac{1}{2}, \frac{1}{2}\right)}$ to the domain of L. To explain the former domain, first fix ξ and consider $g(\xi, \cdot) \in \mathscr{D}\left(L_\xi\right) = H^1_{\text{per}}[0, 2\pi)$. The Bloch transform requires the map $\xi \in \left[-\frac{1}{2}, \frac{1}{2}\right) \mapsto g(\xi, \cdot) \in H^1_{\text{per}}[0, 2\pi)$ be $L^2\left(\left[-\frac{1}{2}, \frac{1}{2}\right); H^1_{\text{per}}[0, 2\pi)\right)$, identifying this as the domain of the Bloch operators $\left\{L_\xi\right\}_{\xi \in \left[-\frac{1}{2}, \frac{1}{2}\right)}$. We define the Bloch transform of $f \in L^2(\mathbb{R})$ to be the unique function $\check{f} \in L^2\left(\left[-\frac{1}{2}, \frac{1}{2}\right); L^2_{\text{per}}[0, 2\pi)\right)$ which satisfies

$$f(x) = \int_{-1/2}^{1/2} \check{f}(\xi, x)\, e^{i\xi x}\, d\xi\,. \tag{6.9}$$

We have uniqueness because there is an explicit formula for $\check{f}$; starting from the Fourier inversion formula, if we break the integral into blocks of the form $[j - 1/2, j + 1/2]$ with $j \in \mathbb{Z}$,

$$f(x) = \frac{1}{2\pi} \int_{\mathbb{R}} \hat{f}(\xi)\, e^{i\xi x}\, d\xi = \int_{-1/2}^{1/2} \left(\sum_{j \in \mathbb{Z}} \hat{f}(\xi + j)\, e^{ijx} \right) e^{i\xi x}\, d\xi\,.$$

Then explicitly,

$$\check{f}(\xi, x) = \sum_{j \in \mathbb{Z}} \hat{f}(\xi + j)\, e^{ijx}\,.$$

From Parseval's theorem we see that the Bloch transform is an isometry,

$$\|f\|^2_{L^2(\mathbb{R})} = 2\pi \int_{-1/2}^{1/2} \left\|\check{f}(\xi, \cdot)\right\|^2_{L^2(\mathbb{R} \setminus 2\pi\mathbb{Z})}\, d\xi\,. \tag{6.10}$$

We can also use the Bloch transform to write the linear evolution e^{Lt} in terms of the linear evolution of the Bloch operators [23, Equation 1.15]. Specifically, given an $f_0 \in L^2(\mathbb{R})$, we have

$$e^{Lt} f_0(x) = \frac{1}{2\pi} \int_{-1/2}^{1/2} e^{i\xi x} e^{L_\xi t} \check{f}_0(\xi, x)\, d\xi\,. \tag{6.11}$$

6.2.2 Bloch-Space Projections

Our first goal is to use the unstable spectrum of L to show that the linear part of (6.4) has some sort of exponential growth. We assume that the spectrum of L is unstable, so let $\lambda \in \sigma(L) \cap \{z \in \mathbb{C} \mid \mathrm{Re}\, z > 0\}$. In Proposition 6.3 we characterized the $L^2(\mathbb{R})$ spectrum of L in terms of the $L^2_{\mathrm{per}}[0,2\pi)$ eigenvalues of the one-parameter family of Bloch operators L_ξ: there must be some $\xi_0 \in \left[-\frac{1}{2},\frac{1}{2}\right)$ so that λ is an eigenvalue of L_{ξ_0} with eigenfunction $\phi(\xi_0,x)$. Note that ϕ when considered as an initial perturbation has exponential growth as $e^{L_{\xi_0}t}\phi = e^{\lambda t}\phi$, albeit in $L^2_{\mathrm{per}}[0,2\pi)$. We use the Bloch Transform (6.9) to extend ϕ into some function in $L^2(\mathbb{R})$ that has exponential growth.

First we extend $\phi(\xi,x)$ to more ξ values than just ξ_0. Using the spectral projection around a single eigenvalue of L_{ξ_0}, $\tilde{P}_\lambda(\xi)$ introduced in (6.8), for ξ in some interval I we may continuously define $\phi(\xi,x) = \tilde{P}_\lambda(\xi)\,\phi(\xi_0,x)$. We restrict the contour Γ and interval I to be sufficiently small so that

$$\beta = \inf \mathrm{Re}\,\Gamma > 0\,, \tag{6.12}$$

then we can use the Bloch Transform to define the following function in $L^2(\mathbb{R})$,

$$f_0(x) = \frac{1}{2\pi}\int_I e^{i\xi x}\phi(\xi,x)\; d\xi\;. \tag{6.13}$$

As each $\phi(\xi,x)$ is a linear combination of eigenfunction of L_ξ with eigenvalues λ' that satisfy $\mathrm{Re}\lambda' > \beta$, then $\left\| e^{L_\xi t}\phi(\xi,x)\right\|_{L^2_{\mathrm{per}}[0,2\pi)} > e^{\beta t}\left\|\phi(\xi,x)\right\|_{L^2_{\mathrm{per}}[0,2\pi)}$. Hence when using (6.10) and (6.11) we have the estimate that

$$\begin{aligned}\left\|e^{Lt}f_0\right\|^2_{L^2(\mathbb{R})} &= \frac{1}{2\pi}\int_I \left\|e^{\lambda_i(\xi)t}\phi_i(\xi,\cdot)\right\|^2_{L^2(\mathbb{R}\setminus 2\pi\mathbb{Z})} \\ &\geq \frac{1}{2\pi}e^{\beta t}\inf_{\xi\in I}\left\|\phi_i(\xi,\cdot)\right\|^2_{L^2(\mathbb{R}\setminus 2\pi\mathbb{Z})}\,.\end{aligned}$$

The intuition behind this is constructing an initial perturbation that is close to the eigenfunction $\phi(\xi_0,x)$. In the sequel our strategy changes to instead defining a projection P that recognizes when such "eigenfunctions" are present in an initial perturbation u_0. This has the advantage of being widely applicable to all initial perturbations rather than just a constructed few.

As a technical issue we require any such "eigenfunctions" to have a sufficient level of exponential growth. To that end we first define the following quantity which will be the maximum rate of exponential growth an initial perturbation u_0 contains,

$$\lambda_M(u_0) = \sup\left\{\mathrm{Re}\;\lambda \;\middle|\; \tilde{P}_\lambda(u_0)^\vee \neq 0, \lambda \in \sigma\left(L_\xi\right) \text{ for any } \xi \in \left[-\frac{1}{2},\frac{1}{2}\right)\right\}, \tag{6.14}$$

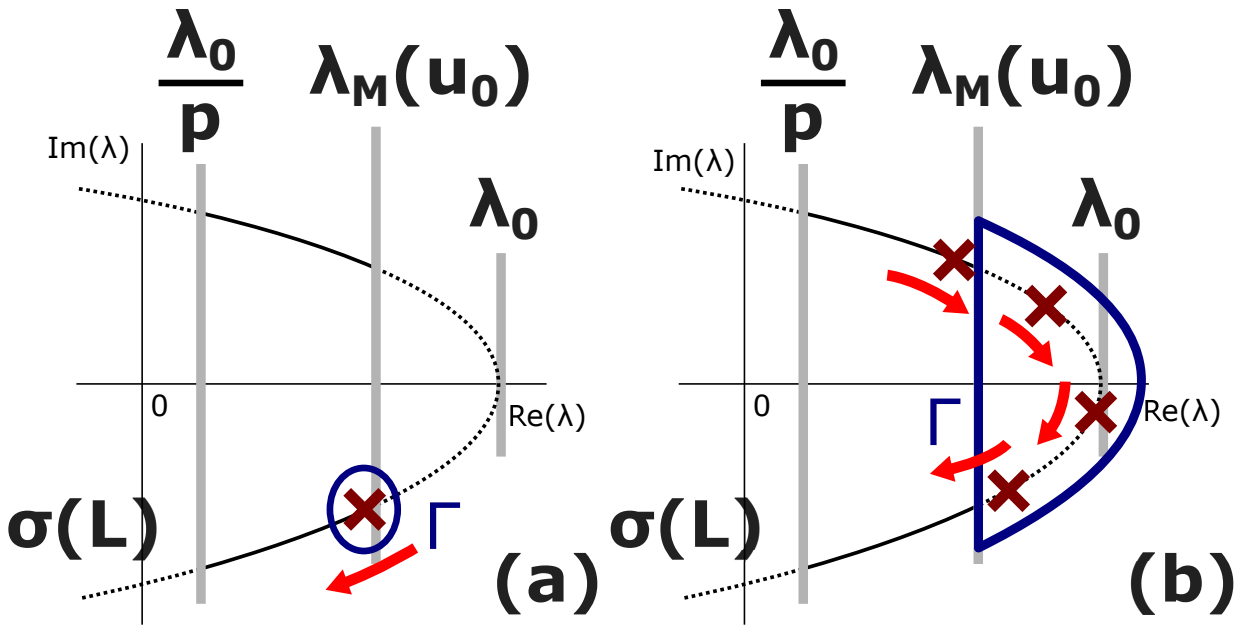

Figure 6.2: The spectrum of L, $\sigma(L)$, with the lines Re $z = \frac{\lambda_0}{p}$, Re $z = \lambda_M(u_0)$, and Re $z = \lambda_0$ shown. (a) The contour Γ chosen for P which is chosen close to an eigenvalue $\lambda(\xi_0)$, which in turn is close to λ_M. The interval I is chosen sufficiently small so that no other eigenvalues enter the region enclosed by Γ. (b) The contour Γ chosen for P'. Note that as ξ varies, eigenvalues may enter or exit the region enclosed by Γ: Hypothesis 6.5 claims that this happens finitely many times, so we may consider finitely many ξ-intervals I_j where the number of eigenvalues (counted by multiplicity) enclosed by Γ is a constant.

where $\tilde{P}_\lambda$ is a spectral projection to the eigenspace of λ as defined in equation (6.8). Note that the condition in (6.14) is analogous to requiring "$\lambda \in \sigma(L)$," but accounts for the technicality that if λ is an eigenvalue for multiple L_ξ then $\tilde{P}_\lambda$ as defined in (6.8) is not unique.

We will construct this projection P analogously to (6.13): as $\phi(\xi_0, x)$ was extended to $\phi(\xi, x)$ by prepending $\tilde{P}_\lambda$, we shall do so here as well. We choose our $\tilde{P}_\lambda$ so that λ is arbitrarily close to λ_M. That is, let $\varepsilon > 0$ with $0 < \lambda_M - \varepsilon < \lambda_M$. Then choose an eigenvalue λ of L_{ξ_0} with $\tilde{P}_\lambda(u_0)^\vee \neq 0$ so that $\lambda_M - \text{Re}\,\lambda < \frac{\varepsilon}{2}$, and restrict the contour Γ and interval I containing ξ_0 so that $\lambda_M - \inf \text{Re}\,\Gamma < \varepsilon$ and $\tilde{P}_\lambda(\xi)$ is holomorphic on I. See Figure 6.2 (a) for an illustration. We may then use the Bloch Transform (6.9) to define the following projection,

$$Pu(x) = \int_I e^{i\xi x} \tilde{P}_\lambda(\xi)\, \check{u}(\xi, x)\, d\xi\,. \tag{6.15}$$

To see that P is a projection, first note that by the uniqueness of (6.9) we see that $(Pu)^\vee = \tilde{P}_\lambda \check{u}$, and so $P^2 u = Pu$. Secondly, applying 6.10 and that $\|\tilde{P}_\lambda\|_{L^2_{\text{per}}[0,2\pi)} \leq 1$ gives that $\|P\|_{L^2(\mathbb{R})} \leq 1$. Furthermore the spectral projection $\tilde{P}_\lambda(\xi)$ commutes with the semigroup $e^{L_\xi t}$ for each ξ [42, Theorem 3.14.10], which we can use to show that P commutes with e^{Lt} as well. This construction resembles the constant fiber direct integral from section XIII.16 of [37].

Lemma 6.4. *Suppose u_0 is an initial perturbation to (6.1). Then there exists some constant $C > 0$ depending only on*

u_0 so that for any $\omega < \lambda_M$ sufficiently close to λ_M defined in (6.14), we have the linear growth estimate

$$C\delta e^{\omega t} \leq \left\| e^{Lt}\delta u_0 \right\|_X .$$

Proof. As P is a projection, then

$$\|Pu\|_X \leq \|u\|_X .$$

So it suffices to show this exponential growth for the projected linear part $Pe^{Lt}\delta u_0$. Set $\varepsilon = \lambda_M - \omega$ and recall the choice of λ in (6.15), restricting the interval I so that $\tilde{P}_\lambda(\xi)(u_0)^\vee \neq 0$ for all $\xi \in I$. As $\tilde{P}_\lambda(\xi)(u_0)^\vee$ is a linear combination of eigenfunctions of L_ξ with eigenvalues λ' that satisfy $\operatorname{Re}\lambda' > \omega$, $\left\| e^{L_\xi t} \right\|_{L^2_{\text{per}}[0,2\pi)} > e^{\omega t}$, and after applying (6.10),

$$\begin{aligned} \left\| Pe^{Lt}\delta u_0 \right\|_X &\geq \int_I \left\| e^{L_\xi t}\tilde{P}(\xi)(\delta u_0)^\vee(\xi,\cdot)\; e^{i\xi\cdot} \right\|_{L^2_{\text{per}}[0,2\pi)} d\xi \\ &\geq \delta e^{\omega t} \int_I \inf_{\xi\in I} \left(\left\| \tilde{P}(\xi)(u_0)^\vee(\xi,\cdot) \right\|_{L^2_{\text{per}}[0,2\pi)} \right) d\xi . \end{aligned}$$

□

Our instability argument requires that λ_M be sufficiently large to attain a certain minimum level of exponential growth. To define this level, we first need to determine an upper bound of $\lambda_M(u_0)$ over all choices of initial perturbations u_0,

$$\lambda_0 = \sup\{\operatorname{Re}\lambda \mid \lambda \in \sigma(L)\} . \tag{6.16}$$

Note that as L was assumed to be sectorial, then λ_0 is necessarily finite. As part of the upcoming Hypothesis 6.5 we assume that this quantity is finite. We later determine in Theorem 6.7 that a sufficient level of exponential growth is attained if $\frac{\lambda_0}{p} < \lambda_M$, where p is the power of the nonlinearity as in equation (6.3). Put another way, if we define

$$\Sigma_U = \sigma(L) \cap \left\{ \operatorname{Re}(z) > \frac{\lambda_0}{p} \;\middle|\; z \in \mathbb{C} \right\}$$

then there is a sufficient amount of exponential growth if for some $\lambda \in \Sigma_U$, λ an eigenvalue of L_{ξ_0}, we have that $\tilde{P}_\lambda(u_0)^\vee \neq 0$. This is what is precisely meant by saying u_0 "activates" the unstable part of the spectrum. We now make a hypothesis on Σ_U, that eigenvalues do not enter and exit it too many times.

Hypothesis 6.5. *For each initial perturbation u_0 of (6.1) with $\frac{\lambda_0}{p} < \lambda_M(u_0)$, there is a finite partition of $\left[-\frac{1}{2},\frac{1}{2}\right)$ into intervals I_j so that the number of eigenvalues of L_ξ (defined in (6.7), counted by multiplicity) in*

$$A_{u_0} = \Sigma_U \cap \{z \in \mathbb{C} \mid Re\; z > \lambda_M(u_0)\}$$

is constant for $\xi \in I_j$.

For a visual depiction of this latter assumption, see Figure 6.2 (b), where eigenvalues are allowed to enter and exit a contour Γ enclosing only A_{u_0} — and no other part of $\sigma(L)$ — only finitely many times. In [13, Figure 6] [39, Figure 3] a numerical calculation of the point spectrum of L_ξ appears to agree with this hypothesis.

As it stands, a naive exponential growth upper bound for u_0 — that is, obtained solely by looking at the spectrum of L — would be $e^{\lambda_0 t}$. If we bound the nonlinear part in (6.4) by this exponential function $e^{\lambda_0 t}$, then it would overshadow the lesser growth $e^{(\lambda_M - \varepsilon)t}$ that (6.15) can provide for the linear part. But we can take advantage of the fact that for all $\lambda \in \sigma(L)$ with $\operatorname{Re}\lambda > \lambda_M$, then $\tilde{P}_\lambda u_0 = 0$ (for any choice of $\tilde{P}_\lambda$). Thus intuitively u_0 should "ignore" that part of the spectrum, and the exponential growth upper bound should instead be $e^{\lambda_M t}$.

Lemma 6.6. *Suppose that (6.1) satisfies Hypothesis 6.5 and let u_0 be an initial perturbation with $\frac{\lambda_0}{p} < \lambda_M(u_0)$. Then there exists some constant $C > 0$ depending only on u_0 so that we have the linear growth estimate*

$$\left\| e^{Lt} \delta u_0 \right\|_X \leq C\delta e^{\lambda_M t}.$$

Proof. We start by using Hypothesis 6.5 to find intervals I_j a finite partition of $\left[-\frac{1}{2}, \frac{1}{2}\right)$ so that the number of eigenvalues of L_ξ (counted by multiplicity) in A_{u_0} is constant for each $\xi \in I_j$. Let Γ be a curve that encloses all of A_{u_0} and no other part of $\sigma(L)$ (see Figure 6.2 (b)). Then we define the following spectral projection,

$$\tilde{P}'(\xi) u = \int_\Gamma R\left(\zeta, L_\xi\right) \, d\zeta.$$

Note that by construction $\left(I - \tilde{P}'(\xi)\right)(u_0)^\vee(\xi, x) = (u_0)^\vee(\xi, x)$. Combining this with (6.11),

$$e^{Lt} u_0(x) = \frac{1}{2\pi} \sum_j \int_{I_j} e^{i\xi x} e^{L_\xi t} \left(I - \tilde{P}'(\xi)\right)(u_0)^\vee(\xi, x) \, d\xi$$

and [42, Theorem 3.14.10] we see that $\tilde{P}'$ commutes with $e^{L_\xi t}$ and $\left\| \left(I - \tilde{P}'(\xi)\right) e^{L_\xi t} \right\|_{L^2_{\text{per}}[0,2\pi)} \leq e^{\lambda_M t}$. This gives the growth estimate. □

6.3 Nonlinear Instability

We now state our main instability result. With Definition 6.2 in mind we start by defining u_δ, for $\delta > 0$, to be the solution to the following evolution equation,

$$\begin{cases} (u_\delta(x,t))_t = Lu_\delta(x,t) + \mathcal{N}(u_\delta(x,t)) \\ u_\delta(x,0) = \delta u_0(x)\,. \end{cases} \tag{6.17}$$

Showing that the initial perturbation u_0 is unstable is equivalent to showing that u_δ cannot be made arbitrarily small by taking δ arbitrarily small. In our instability theorem we find an explicit time T where the solution fails to be arbitrarily small.

Theorem 6.7. *Consider the initial value problem (6.1), with L a sectorial operator with 2π-periodic coefficients as defined in (6.2), and $\mathcal{N}$ a nonlinear operator satisfying the polynomial estimate (6.3). Assume that Hypothesis 6.5 holds and let u_0 be an initial perturbation with $\lambda_M(u_0) > \lambda_0/p$. Then u_0 is unstable in the sense of Definition 6.2 as there exist $\varepsilon > 0$ and $\eta > 0$ sufficiently small so that for all $\delta < \eta$, at the time T when*

$$e^{\lambda_M(u_0)T} = \frac{2\eta}{\delta}\,, \tag{6.18}$$

we have

$$\|u_\delta(\cdot,T)\|_{L^2(\mathbb{R})} > \varepsilon\,,$$

where $\lambda_M(u_0)$ is given in equation (6.14), λ_0 is given in equation (6.16), and p is given in equation (6.3).

Recall from the introduction that our general strategy was to use (6.5) to pit the exponential growth of the linear term obtained from the unstable spectrum of L against the nonlinear term's slower growth. The former was developed in Lemmas 6.4 and 6.6, so we handle the latter below.

Lemma 6.8. *For $u_0, u_\delta, T, \lambda_M(u_0), \lambda_0, p$ as in Theorem 6.7, then if $\lambda_M(u_0) > \lambda_0/p$ we have*

$$\|u_\delta(\cdot,t)\|_X \le \delta C e^{\lambda_M(u_0)t} \qquad \text{for } t \le T\,.$$

Proof. For $t \le T$ we define the quantity

$$\rho(t) = \sup_{0\le s\le t} \|u_\delta(s)\|_X e^{-\lambda_M s}\,. \tag{6.19}$$

To prove the result, it is sufficient to show that $\rho(t)$ is uniformly bounded for $t \le T$. We start by taking the norm of (6.4). From Lemma 6.6 we have that $\left\|e^{Lt}\delta u_0\right\|_X \le \delta C e^{\lambda_M t}$, and as L is sectorial[1] then $\left\|e^{Lt}\right\|_X \le e^{\lambda_0 t}$. Then after recalling (6.3), we have

$$\|u_\delta(\cdot,t)\|_X \le \delta C e^{\lambda_M t} + \int_0^t e^{\lambda_0(t-s)} \|u_\delta(\cdot,s)\|_X^p \, ds\,.$$

[1]The assumption that L is sectorial may be relaxed so long as we have this same semigroup estimate and λ_0 is finite.

Then we multiply and divide the nonlinear term by $e^{-p\lambda_M s}$, apply (6.19), evaluate the integral, and note that $\rho(t)$ is monotone increasing to obtain

$$\|u_\delta(\cdot,t)\|_X \leq \delta C e^{\lambda_M t} + \rho(t)^p \frac{e^{p\lambda_M t} - e^{\lambda_0 t}}{p\lambda_M - \lambda_0}. \tag{6.20}$$

Recall the hypothesis $\lambda_0/p < \lambda_M$, and note that it implies

$$e^{\lambda_0 t} < e^{p\lambda_M t} \quad \text{and} \quad 0 < p\lambda_M - \lambda_0,$$

so we may focus solely on the larger exponential growth.

Note that this upper bound (6.20) also applies for all $\|u_\delta(\cdot,s)\|_X$ for $s \leq t$. Multiplying both sides by $e^{-\lambda_M s}$ and taking the supremum over all $s \leq t$ yields

$$\rho(t) \leq \delta C + \rho(t)^p \frac{e^{(p-1)\lambda_M t}}{p\lambda_M - \lambda_0}. \tag{6.21}$$

Replacing the right hand side exponential term's t with T, recalling (6.18), and dividing both sides by δ,

$$\frac{\rho(t)}{\delta} \leq C + \frac{(2\eta)^{p-1}}{p\lambda_M - \lambda_0} \left(\frac{\rho(t)}{\delta}\right)^p.$$

Setting $z = \frac{\rho(t)}{\delta}$ leads to the equivalent polynomial inequality valid for $t \leq T$,

$$0 \leq C - z + \frac{(2\eta)^{p-1}}{p\lambda_M - \lambda_0} z^p. \tag{6.22}$$

This polynomial has a critical point at

$$z = \frac{1}{2\eta} \left(\frac{p\lambda_M - \lambda_0}{p}\right)^{\frac{1}{p-1}} > 0.$$

And at this critical point the polynomial takes on the value

$$C - \frac{1}{2\eta} \left[\left(\frac{p\lambda_M - \lambda_0}{p}\right)^{\frac{1}{p-1}} \left(1 + \frac{1}{p}\right)\right].$$

Then so long as η is smaller than some expression that only involves p, λ_M, λ_0, then the polynomial will be negative at some z-value to the right of $z = 0$. In particular, it will have a root to the right of $z = 0$.

When $t = 0$, $z = \frac{\|u_\delta(0)\|}{\delta} = 1$, so choosing η sufficiently small will satisfy the polynomial inequality initially at $t = 0$. Then the existence of a root means that z is uniformly bounded for $t \leq T$, and hence the uniform bound for ρ

for $t \leq T$. □

Now we can use this lemma to establish an upper bound for the nonlinear growth in (6.4) and finally prove Theorem 6.7.

Proof. (Of Theorem 6.7)

Lemma 6.4, when $t = T$, gives us that

$$C\eta \leq \left\| e^{LT} \delta u_0 \right\|_X . \tag{6.23}$$

From Lemma 6.8, we can bound the nonlinear part of u_δ by

$$\left\| \int_0^t e^{L(t-s)} \mathscr{N}\left(u_\delta(s)\right)\, ds \right\|_X \quad \leq \quad \left(C\delta e^{\lambda_M t} \right)^p \int_0^t e^{\lambda_M (t-s)}\, ds .$$

In particular, when $t = T$, we have

$$\left\| \int_0^T e^{L(T-s)} \mathscr{N}\left(u_\delta(s)\right)\, ds \right\|_X \leq \bar{C}\eta^p . \tag{6.24}$$

Then if η is chosen sufficiently small so that $C\eta \geq \bar{C}\eta^p$, then by the reverse triangle inequality we have

$$0 < C\eta - \bar{C}\eta^p \leq \left| \left\| e^{LT} \delta u_0 \right\|_X - \left\| \int_0^T e^{L(T-s)} \mathscr{N}\left(u_\delta\right) \right\|_X \right| \leq \left\| u_\delta(T) \right\| .$$

Note that the leftmost term $C\eta - \bar{C}\eta^p$ is a positive constant independent of δ: this becomes our ε, which completes the proof. □

6.4 Extension to Dissipative Systems of Conservation Laws

Recall that our main Theorem 6.7 was proven in the context of reaction-diffusion type systems of the form (6.1): specifically for systems with no derivatives in the nonlinearity. Some examples of such systems would be scalar reaction diffusion, FitzHugh-Nagumo [35], the Klausmeier model for vegetation stripe formulation [41, 40], and the Belousov-Zhabotinskii reaction [7]. However, our general methodology is sufficiently robust enough that it can apply more widely to dissipative systems of conservation laws. As a specific example, consider the following Korteweg-de-Vries/Kuramoto-Sivashinsky (KdV-KS) equation

$$p_t + pp_x + p_{xxx} + \beta\left(p_{xx} + p_{xxxx}\right) = 0 \tag{6.25}$$

with $0 < \beta \ll 1$, which arises in the context of inclined thin film flow [20]. It was shown in [1, 20] that this equation admits periodic traveling wave solutions ϕ whose linearization satisfies Hypothesis 6.5. If we consider solutions of the form $p(x,t) = \phi(x) + u(x,t)$, we find that u satisfies the following perturbation equation [4, Lemma 3.3][2]

$$u_t + u_{xxx} + \beta(u_{xx} + u_{xxxx}) + \phi u_x + \phi' u + u u_x = 0. \tag{6.26}$$

Our goal is to characterize which initial perturbations u_0 of our traveling wave ϕ will result in an unstable solution p. Note that the nonlinearity uu_x does not in any standard Sobolev space satisfy a polynomial estimate of the form (6.3). Nevertheless we can use the following damping estimate as in [4, Proposition 3.4] to obtain a workable analogue. For completeness we reproduce the proof of this damping estimate.

Lemma 6.9. *Let u be a solution to (6.26). Then u satisfies the following nonlinear damping estimate*

$$\|u\|_{H^2} \leq e^{-\beta t} \|u(0)\|_{H^2} + C \int_0^T e^{-\beta(t-s)} \|u(s)\|_{H^1(\mathbb{R})} \, ds \tag{6.27}$$

for some constant $C > 0$.

Proof. Let $\langle \cdot, \cdot \rangle$ denote the $L^2(\mathbb{R})$ inner product. Using integration by parts,

$$\frac{1}{2} \frac{d}{dt} \left(\|u\|^2_{H^2(\mathbb{R})} \right) = \langle u_t, u - u_{xx} + u_{xxxx} \rangle . \tag{6.28}$$

We can obtain u_t from (6.26). Using Cauchy-Schwartz, Young's inequality, and the fact that $\|u\|_{L^\infty(\mathbb{R})} \leq \|u\|_{H^1(\mathbb{R})}$ allows us to bound the nonlinear term,

$$\langle u u_x, u_{xxxx} - u_{xx} \rangle \leq \frac{1}{2} \|u\|_{L^\infty(\mathbb{R})} \left(\left(1 + \frac{1}{2\beta} \|u\|_{L^\infty(\mathbb{R})} \right) \|u_x\|^2_{L^2(\mathbb{R})} + \|u_{xx}\|^2_{L^2(\mathbb{R})} \right) + \frac{\beta}{2} \|u_{xxxx}\|_{L^2(\mathbb{R})} .$$

The remainder of (6.28) can be handled with integration by parts and recognizing perfect derivatives, resulting in the bound

$$\frac{1}{2} \frac{d}{dt} \left(\|u\|^2_{H^2(\mathbb{R})} \right) \leq \sum_{j=0}^{3} \alpha_j \left\| \partial_x^j u \right\|^2_{L^2(\mathbb{R})} - \frac{\beta}{2} \|u_{xxxx}\|^2_{L^2(\mathbb{R})} , \tag{6.29}$$

where the α_j are non-negative constants depending on δ, $\left\| \partial_x^k \phi \right\|_{L^\infty}$ for $k = 0, 1, 2, 3, 4$, and $\|u\|_{L^\infty}$.

Before proceeding we derive a useful Sobolev interpolation inequality. Using integration by parts, for integer $j \geq 1$ we have

$$\left\| \partial_x^j u \right\|^2_{L^2(\mathbb{R})} = - \left\langle \partial_x^{j-1} u, \partial_x^{j+1} u \right\rangle .$$

[2] A slight discrepancy arises in that [4] considers a modulation $\psi(x,t)$ so that $u(x,t) = p(x + \psi(x,t), t) - \phi(x)$ and that here we neglect such a modulation.

Using Cauchy-Schwartz and Young's inequality with an arbitrary positive constant a_j yields the inequality

$$\left\|\partial_x^j u\right\|_{L^2(\mathbb{R})}^2 \leq \frac{1}{4a_j}\left\|\partial_x^{j-1} u\right\|_{L^2(\mathbb{R})}^2 + a_j\left\|\partial_x^{j+1} u\right\|_{L^2(\mathbb{R})}^2 .$$

Taking a linear combination of the $j = 2,3$ cases, for appropriate choices of the a_j and a sufficiently large constant $\tilde{C} > 0$, we can obtain the following Sobolev interpolation inequality

$$\left(\alpha_2 + \frac{\beta}{2}\right)\|u_{xx}\|_{L^2(\mathbb{R})}^2 + \alpha_3\|u_{xxx}\|_{L^2(\mathbb{R})}^2 \leq \tilde{C}\|u_x\|_{L^2(\mathbb{R})}^2 + \frac{\beta}{2}\|u_{xxxx}\|_{L^2(\mathbb{R})}^2 . \tag{6.30}$$

Combining (6.30) and (6.29) gives, for some constant $C > 0$,

$$\frac{1}{2}\frac{d}{dt}\left(\|u\|_{H^2(\mathbb{R})}^2\right) \leq -\frac{\beta}{2}\|u\|_{H^2(\mathbb{R})}^2 + C\|u\|_{H^1(\mathbb{R})}^2 .$$

The estimate (6.27) then follows from Gronwall's inequality. □

The key ingredient to the damping estimate was that the leading term $-\beta u_{xxxx}$ of (6.26) was negative: such an estimate is not necessarily limited to the specific PDE (6.25). In particular a damping estimate also holds for the St. Venant equation [38, Proposition 4.2], which is a hyperbolic-parabolic system of balance laws. In light of this, we introduce a general requirement on the nonlinearity, that for constants $\theta > 0$, $C > 0$, $T > 0$, $n \geq 2$, $p > 1$, and $t < T$,

$$\|\mathscr{N}(u(t))\|_{H^n(\mathbb{R})} \leq \|u(t)\|_{H^1(\mathbb{R})}^{p-1}\left(e^{-\theta t}\|u(0)\|_{H^n(\mathbb{R})} + C\int_0^T e^{-\theta(t-s)}\|u(s)\|_{H^1(\mathbb{R})}\, ds\right) . \tag{6.31}$$

We can then prove an alternate instability result.

Theorem 6.10. *Consider the initial value problem (6.1), with L a sectorial operator with 2π-periodic coefficients as defined in (6.2), and $\mathscr{N}$ a nonlinear operator instead satisfying the estimate (6.31). Assume that Hypothesis 6.5 holds and let u_0 be an initial perturbation which satisfies both $\frac{\lambda_0+\theta}{p-1} < \lambda_M(u_0)$ and $\frac{\lambda_0}{p} < \lambda_M(u_0)$, then u_0 is unstable in the sense of Definition 6.2 as there exist $\varepsilon > 0$ and $\eta > 0$ sufficiently small so that for all $\delta < \eta$, at the time T when*

$$e^{\lambda_M(u_0)T} = \frac{2\eta}{\delta} , \tag{6.32}$$

we have

$$\|u_\delta(\cdot,T)\|_{L^2(\mathbb{R})} > \varepsilon ,$$

where $\lambda_M(u_0)$ is given in equation (6.14), λ_0 is given in equation (6.16), and u_δ is the solution to (6.17).

Remark 6.11. In Lemma 6.9 we show that (6.26) satisfies a nonlinear estimate of the form (6.31) with $\theta = \beta$. However,

equation (6.30) of the proof can be modified to obtain any $0 < \theta < \beta$, so the θ in the requirement that $\frac{\lambda_0+\theta}{p-1} < \lambda_M$ is not restrictive.

Proof. Here we take $X = H^1(\mathbb{R})$. Lemmas 6.4 and 6.6 and the proof of Theorem 6.7 apply with no further modification, provided we can establish an estimate as in Lemma 6.8.

We again define ρ as in (6.19) and start by concentrating on the nonlinear term of (6.4). By the triangle inequality and (6.31),

$$\begin{aligned}\int_0^t \left\| e^{L(t-s)} \right\|_X \|\mathscr{N}(u(s))\|_X \, ds \quad &\leq \quad \int_0^t e^{\lambda_0(t-s)} \|u(s)\|_X^{p-1} e^{-\theta s} \|u(0)\|_{H^n(\mathbb{R})} \, ds \\ &\quad + C \int_0^t e^{\lambda_0(t-s)} \|u(s)\|_X^{p-1} \int_0^s e^{-\theta(s-s')} \left\|u\left(s'\right)\right\|_X \, ds' \, ds .\end{aligned}$$

We multiply and divide by appropriate powers of $e^{\lambda_M s}$, bound by ρ, and evaluate the integrals to obtain the analogue of (6.20),

$$\begin{aligned}\|u_\delta(t)\|_X \quad &\leq \quad \delta C e^{\lambda_M t} + \rho^{p-1}(t) \|u_\delta(0)\|_{H^n} \frac{e^{((p-1)\lambda_M-\theta)t} - e^{\lambda_0 t}}{(p-1)\lambda_M - (\theta+\lambda_0)} \\ &\quad + \left(\frac{C\rho^p(t)}{\theta+\lambda_M}\right) \left(\frac{e^{p\lambda_M t} - e^{\lambda_0 t}}{p\lambda_M - \lambda_0} - \frac{e^{((p-1)\lambda_M-\theta)t} - e^{\lambda_0 t}}{(p-1)\lambda_M - (\theta+\lambda_0)}\right).\end{aligned} \tag{6.33}$$

Note that the hypotheses $\frac{\lambda_0+\theta}{p-1} < \lambda_M$ and $\frac{\lambda_0}{p} < \lambda_M$ imply that

$$e^{\lambda_0 t} < e^{((p-1)\lambda_M-\theta)t} \quad \text{and} \quad e^{\lambda_0 t} < e^{p\lambda_M t},$$

so we may focus solely on the larger exponential growth.

The upper bound in (6.33) also applies for all $\|u_\delta(s)\|_X$ for $s \leq t$. Then after multiplying both sides of the inequality by $e^{-\lambda_M t}$ and taking the supremum over all $s \leq t$, we have the analogue of (6.21),

$$\rho(t) \leq \delta C + a_{p-1} \rho^{p-1}(t) e^{(p-2)\lambda_M t} + a_p \rho^p(t) e^{(p-1)\lambda_M t},$$

where a_{p-1} and a_p depend only on C, p, λ_0, λ_M, θ, and $\|u_\delta(0)\|_{H^n}$.

Replacing the right hand side exponential terms' t with T, recalling (6.32), dividing both sides by δ and setting $z = \frac{\rho(t)}{\delta}$, then we have the analogue of (6.22),

$$0 \leq a_p \eta^{p-1} z^p + a_{p-1} \eta^{p-2} \delta z^{p-1} - z + C. \tag{6.34}$$

To find a zero of this polynomial, we compare it with the linear function $C - z$. In particular, on the interval $[0, L]$ we have

$$\left|\left(a_p \eta^{p-1} z^p + a_{p-1} \eta^{p-2} \delta z^{p-1} - z + C\right) - (C - z)\right| \leq a_p \eta^{p-1} L^p + a_{p-1} \eta^{p-2} \delta L^{p-1}.$$

Choosing $L = C + 1$ has the function $C - z$ taking on the value -1 when $z = L$, and taking η sufficiently small ensures that the polynomial (6.34) takes on a negative value when $z = L$. As that same polynomial takes on the positive value C when $z = 0$, then it has a zero. As a consequence, then ρ is uniformly bounded. □

Bibliography

[1] Blake Barker. Numerical proof of stability of roll waves in the small-amplitude limit for inclined thin film flow. *Journal of Differential Equations*, 257(8):2950–2983, October 2014.

[2] Blake Barker, Jeffrey Humpherys, Joshua Lytle, and Kevin Zumbrun. STABLAB: A MATLAB-Based Numerical Library for Evans Function Computation, June 2015.

[3] Blake Barker, Mathew A. Johnson, Pascal Noble, L. Miguel Rodrigues, and Kevin Zumbrun. Whitham averaged equations and modulational stability of periodic traveling waves of a hyperbolic-parabolic balance law. *Journes Equations aux dérivées partielles*, pages 1–24, 2010.

[4] Blake Barker, Mathew A. Johnson, Pascal Noble, L. Miguel Rodrigues, and Kevin Zumbrun. Nonlinear modulational stability of periodic traveling-wave solutions of the generalized Kuramoto-Sivashinsky equation. *Physica D: Nonlinear Phenomena*, 258:11–46, 2013.

[5] Blake Barker, Mathew A. Johnson, L. Miguel Rodrigues, and Kevin Zumbrun. Metastability of solitary roll wave solutions of the St. Venant equations with viscosity. *Physica D: Nonlinear Phenomena*, 240(16):1289–1310, August 2011.

[6] Margaret Beck, Anna Ghazaryan, and Björn Sandstede. Nonlinear convective stability of travelling fronts near Turing and Hopf instabilities. *Journal of Differential Equations*, 246(11):4371–4390, June 2009.

[7] Grigory Bordyugov, Nils Fischer, Harald Engel, Niklas Manz, and Oliver Steinbock. Anomalous dispersion in the Belousov-Zhabotinsky reaction: Experiments and modeling. *Physica D: Nonlinear Phenomena*, 239(11):766–775, June 2010.

[8] William E. Boyce and Richard C. DiPrima. *Elementary Differential Equations and Boundary Value Problems*. John Wiley & Sons, Inc., 8th edition, 2005.

[9] Leon Brin. Numerical testing of the stability of viscous shock waves. *Mathematics of computation*, 70(235):1071–1088, 2001.

[10] Carmen Chicone. *Ordinary differential equations with applications*, volume 34. Springer Science & Business Media, 2006.

[11] Bernard Deconinck, Firat Kiyak, John D. Carter, and J.Nathan Kutz. SpectrUW: A laboratory for the numerical exploration of spectra of linear operators. *Mathematics and Computers in Simulation*, 74(4-5):370–378, March 2007.

[12] Lawrence C. Evans. *Partial Differential Equations*. Volume 19 of Graduate studies in mathematics. American Mathematical Society, second edition, 1998.

[13] M. Osman Gani and Toshiyuki Ogawa. Instability of periodic traveling wave solutions in a modified FitzHugh-Nagumo model for excitable media. *Applied Mathematics and Computation*, 256:968–984, April 2015.

[14] Anna Ghazaryan, Jeffrey Humpherys, and Joshua Lytle. Spectral Behavior of Combustion Fronts with High Exothermicity. *SIAM Journal on Applied Mathematics*, 73(1):422–437, January 2013.

[15] Anna Ghazaryan, Yuri Latushkin, and Stephen Schecter. Stability of Traveling Waves for a Class of Reaction-Diffusion Systems That Arise in Chemical Reaction Models. *SIAM Journal on Mathematical Analysis*, 42(6):2434–2472, January 2010.

[16] Anna Ghazaryan and Björn Sandstede. Nonlinear Convective Instability of Turing-Unstable Fronts near Onset: A Case Study. *SIAM Journal on Applied Dynamical Systems*, 6(2):319–347, January 2007.

[17] Dan Henry. *Geometric theory of semilinear parabolic equations*. Number 840 in Lecture notes in mathematics. Springer, Berlin, 3. printing edition, 1993. OCLC: 257019414.

[18] Dirk Hundertmark, Martin Meyries, Lars Machinek, and Roland Schnaubelt. Operator semigroups and dispersive equations. In *16th Internet Seminar on Evolution Equations*, 2013.

[19] Jiayin Jin, Shasha Liao, and Zhiwu Lin. Nonlinear Modulational Instability of Dispersive PDE Models. *Arch. Ration. Mech. Anal.*, 231:1487–1530, 2019.

[20] Mathew Johnson, Pascal Noble, L. Rodrigues, and Kevin Zumbrun. Spectral stability of periodic wave trains of the Korteweg-de Vries/Kuramoto-Sivashinsky equation in the Korteweg-de Vries limit. *Transactions of the American Mathematical Society*, 367(3):2159–2212, 2015.

[21] Mathew A. Johnson. Stability of Small Periodic Waves in Fractional KdV-Type Equations. *SIAM Journal on Mathematical Analysis*, 45(5):3168–3193, January 2013.

[22] Mathew A. Johnson, Gregory D. Lyng, and Connor Smith. On the Dynamics of Traveling Fronts Arising in Nanoscale Pattern Formation. *arXiv preprint arXiv:1810.02233*, 2018.

[23] Mathew A. Johnson and Kevin Zumbrun. Nonlinear stability of periodic traveling wave solutions of systems of viscous conservation laws in the generic case. *Journal of Differential Equations*, 249(5):1213–1240, September 2010.

[24] Todd Kapitula and Keith Promislow. *Spectral and Dynamical Stability of Nonlinear Waves*, volume 185 of *Applied Mathematical Sciences*. Springer New York, New York, NY, 2013.

[25] Tosio Kato. *Perturbation theory for linear operators*. Classics in mathematics. Springer-Verlag, Berlin, 1995.

[26] Peter D. Lax. Integrals of nonlinear equations of evolution and solitary waves. *Communications on pure and applied mathematics*, 21(5):467–490, 1968.

[27] Randall J. LeVeque. *Finite difference methods for ordinary and partial differential equations: steady-state and time-dependent problems*. Society for Industrial and Applied Mathematics, Philadelphia, PA, 2007. OCLC: ocm86110147.

[28] Yvan Martel and Frank Merle. A Liouville theorem for the critical generalized Korteweg–de Vries equation. *Journal de mathématiques pures et appliquées*, 79(4):339–425, 2000.

[29] Yvan Martel and Frank Merle. Asymptotic Stability of Solitons for Subcritical Generalized KdV Equations. *Archive for Rational Mechanics and Analysis*, 157(3):219–254, April 2001.

[30] Yvan Martel and Frank Merle. Asymptotic stability of solitons of the subcritical gKdV equations revisited. *Nonlinearity*, 18(1):55–80, January 2005.

[31] Alexander Mielke and Guido Schneider. Attractors for modulation equations on unbounded domains-existence and comparison. *Nonlinearity*, 8(5):743, 1995.

[32] Pascal Noble. Linear stability of viscous roll waves. *Communications in Partial Differential Equations*, 32(11):1681–1713, 2007.

[33] Daniel A. Pearson and R. Mark Bradley. Theory of terraced topographies produced by oblique-incidence ion bombardment of solid surfaces. *Journal of Physics: Condensed Matter*, 27(1):015010, 2014.

[34] Robert L. Pego and Michael I. Weinstein. Asymptotic stability of solitary waves. *Communications in Mathematical Physics*, 164(2):305–349, 1994.

[35] Jens D.M. Rademacher, Björn Sandstede, and Arnd Scheel. Computing absolute and essential spectra using continuation. *Physica D: Nonlinear Phenomena*, 229(2):166–183, May 2007.

[36] Qazi Ibadur Rahman and Gerhard Schmeisser. *Analytic Theory of Polynomials*. Clarendon Press, Oxford, 2002.

[37] Michael Reed and Barry Simon. *Methods of Modern Mathematical Physics IV: Analysis of Operators*, volume 4. Academic Press, 1978.

[38] L. Miguel Rodrigues and Kevin Zumbrun. Periodic-Coefficient Damping Estimates, and Stability of Large-Amplitude Roll Waves in Inclined Thin Film Flow. *SIAM Journal on Mathematical Analysis*, 48(1):268–280, January 2016.

[39] Jonathan A. Sherratt. Numerical continuation methods for studying periodic travelling wave (wavetrain) solutions of partial differential equations. *Applied Mathematics and Computation*, 218(9):4684–4694, January 2012.

[40] Jonathan A. Sherratt. Numerical continuation of boundaries in parameter space between stable and unstable periodic travelling wave (wavetrain) solutions of partial differential equations. *Advances in Computational Mathematics*, 39(1):175–192, July 2013.

[41] Jonathan A. Sherratt and Gabriel J. Lord. Nonlinear dynamics and pattern bifurcations in a model for vegetation stripes in semi-arid environments. *Theoretical Population Biology*, 71(1):1–11, February 2007.

[42] Olof Staffans. *Well-Posed Linear Systems*. Number 103 in Encyclopedia of Mathematics and its Applications. Cambridge University Press, Cambridge, 2005.

[43] Thomas H. Wolff. *Lectures on Harmonic Analysis*, volume 29 of *University Lecture Series*. American Mathematical Society, Providence, R.I, 2003.

[44] Kevin Zumbrun. Numerical error analysis for evans function computations: a numerical gap lemma, centered-coordinate methods, and the unreasonable effectiveness of continuous orthogonalization. *arXiv preprint arXiv:0904.0268*, 2009.